# Chemical Data for Flows and Feeder Dikes of the Yakima Basalt Subgroup, Columbia River Basalt Group, Washington, Oregon, and Idaho, and their Bearing on a Petrogenetic Model

U.S. GEOLOGICAL SURVEY BULLETIN 1821

U.S. DEPARTMENT OF THE INTERIOR

March 3, 1849

# AVAILABILITY OF BOOKS AND MAPS OF THE U.S. GEOLOGICAL SURVEY

Instructions on ordering publications of the U.S. Geological Survey, along with prices of the last offerings, are given in the current-year issues of the monthly catalog "New Publications of the U.S. Geological Survey." Prices of available U.S. Geological Survey publications released prior to the current year are listed in the most recent annual "Price and Availability List." Publications that are listed in various U.S. Geological Survey catalogs (**see back inside cover**) but not listed in the most recent annual "Price and Availability List" are no longer available.

Prices of reports released to the open files are given in the listing "U.S. Geological Survey Open-File Reports," updated monthly, which is for sale in microfiche from the U.S. Geological Survey, Books and Open-File Reports Section, Federal Center, Box 25425, Denver, CO 80225. Reports released through the NTIS may be obtained by writing to the National Technical Information Service, U.S. Department of Commerce, Springfield, VA 22161; please include NTIS report number with inquiry.

Order U.S. Geological Survey publications **by mail** or **over the counter** from the offices given below.

## BY MAIL

### Books

Professional Papers, Bulletins, Water-Supply Papers, Techniques of Water-Resources Investigations, Circulars, publications of general interest (such as leaflets, pamphlets, booklets), single copies of Earthquakes & Volcanoes, Preliminary Determination of Epicenters, and some miscellaneous reports, including some of the foregoing series that have gone out of print at the Superintendent of Documents, are obtainable by mail from

**U.S. Geological Survey, Books and Open-File Reports**
**Federal Center, Box 25425**
**Denver, CO 80225**

Subscriptions to periodicals (Earthquakes & Volcanoes and Preliminary Determination of Epicenters) can be obtained ONLY from the

**Superintendent of Documents**
**Government Printing Office**
**Washington, D.C. 20402**

(Check or money order must be payable to Superintendent of Documents.)

### Maps

For maps, address mail orders to

**U.S. Geological Survey, Map Distribution**
**Federal Center, Box 25286**
**Denver, CO 80225**

Residents of Alaska may order maps from

**Alaska Distribution Section, U.S. Geological Survey,**
**New Federal Building - Box 12**
**101 Twelfth Ave., Fairbanks, AK 99701**

## OVER THE COUNTER

### Books

Books of the U.S. Geological Survey are available over the counter at the following Geological Survey Public Inquiries Offices, all of which are authorized agents of the Superintendent of Documents:

- **WASHINGTON, D.C.**--Main Interior Bldg., 2600 corridor, 18th and C Sts., NW.
- **DENVER, Colorado**--Federal Bldg., Rm. 169, 1961 Stout St.
- **LOS ANGELES, California**--Federal Bldg., Rm. 7638, 300 N. Los Angeles St.
- **MENLO PARK, California**--Bldg. 3 (Stop 533), Rm. 3128, 345 Middlefield Rd.
- **RESTON, Virginia**--503 National Center, Rm. 1C402, 12201 Sunrise Valley Dr.
- **SALT LAKE CITY, Utah**--Federal Bldg., Rm. 8105, 125 South State St.
- **SAN FRANCISCO, California**--Customhouse, Rm. 504, 555 Battery St.
- **SPOKANE, Washington**--U.S. Courthouse, Rm. 678, West 920 Riverside Ave..
- **ANCHORAGE, Alaska**--Rm. 101, 4230 University Dr.
- **ANCHORAGE, Alaska**--Federal Bldg, Rm. E-146, 701 C St.

### Maps

Maps may be purchased over the counter at the U.S. Geological Survey offices where books are sold (all addresses in above list) and at the following Geological Survey offices:

- **ROLLA, Missouri**--1400 Independence Rd.
- **DENVER, Colorado**--Map Distribution, Bldg. 810, Federal Center
- **FAIRBANKS, Alaska**--New Federal Bldg., 101 Twelfth Ave.

# Chemical Data for Flows and Feeder Dikes of the Yakima Basalt Subgroup, Columbia River Basalt Group, Washington, Oregon, and Idaho, and their Bearing on a Petrogenetic Model

By THOMAS L. WRIGHT, MARGARET MANGAN, and
DONALD A. SWANSON

U.S. GEOLOGICAL SURVEY BULLETIN 1821

DEPARTMENT OF THE INTERIOR
DONALD PAUL HODEL, Secretary

U.S. GEOLOGICAL SURVEY
Dallas L. Peck, Director

March 3, 1849

UNITED STATES GOVERNMENT PRINTING OFFICE, WASHINGTON : 1989

---

For sale by the
Books and Open-File Reports Section
U.S. Geological Survey
Federal Center, Box 25425
Denver, CO 80225

**Library of Congress Cataloging-in-Publication Data**

Wright, Thomas L. (Thomas Llewellyn), 1935–
Chemical data for flows and feeder dikes of the
Yakima Basalt Subgroup, Columbia River Basalt Group,
Washington, Oregon, and Idaho, and their bearing on a
petrogenetic model.
(U.S. Geological Survey bulletin ; 1821)
Bibliography: p.
Supt. of Docs. no.: I 19.3:1821
1. Basalt—Northwest, Pacific—Analysis. 2. Petrogenesis—Northwest, Pacific. I. Mangan, Margaret T.
II. Swanson, Donald A. III. Title. IV. Series.
QE75.B9 no. 1821 557.3 s 89-600010
[QE462.B3] [552'.26'09795]

# CONTENTS

## FIGURES

## TABLES

# Chemical Data for Flows and Feeder Dikes of the Yakima Basalt Subgroup, Columbia River Basalt Group, Washington, Oregon, and Idaho, and their Bearing on a Petrogenetic Model

*By* Thomas L. Wright, Margaret Mangan, *and* Donald A. Swanson

## Abstract

Regional geologic mapping of the Yakima Basalt Subgroup of the Columbia River Basalt Group provides for a threefold division of the subgroup—from oldest to youngest, the Grande Ronde Basalt, Wanapum Basalt, and Saddle Mountains Basalt. Systems of feeder dikes and vents trending north to north-northwest have been identified for most units. Regional flow correlations, made on the basis of geologic mapping, major-oxide chemistry, and magnetic polarity, show that many flows have volumes of more than 500 km$^3$, traveled hundreds of kilometers from their vents, and had emplacement times of a few days to a few weeks.

Samples of the subgroup were extensively analyzed for major oxides, trace elements, and isotopes of Sr, εNd, Pb, and O. Chemical analyses allow recognition of geochemical units consisting of a flow or several related flows of near-uniform composition, some of which represent chemical types repeated throughout the section. Average compositions of geochemical units have been plotted and are used in drawing petrogenetic inferences. All regionally extensive flows are tholeiitic and have MgO contents in the range of 2.5–8.0 percent. Each formation is characterized by specific chemical compositions. Flows of the Grande Ronde Basalt are aphyric and have low MgO (3–6 percent), high $SiO_2$ (52–58 percent), and relatively low $TiO_2$ (1.5–2.5 percent) and FeO (9–13 percent) contents and a relatively low initial $^{87}Sr/^{86}Sr$ isotopic ratio (0.703–0.705). Most flows of the Wanapum Basalt have lower $SiO_2$ (49–52 percent) for the same range of MgO, much higher contents of $TiO_2$ (>3 percent) and FeO (13–15 percent), and somewhat higher initial $^{87}Sr/^{86}Sr$ (0.704–0.7055). Trace elements are similar overall in both formations despite the contrasts in major-oxide chemistry. Chondrite-normalized rare-earth patterns for both formations show enrichment in light rare earths, are slightly concave upward with small or no negative europium anomalies, and at differing degrees of absolute rare-earth content are parallel to slightly convergent toward the heavy rare earths.

The Saddle Mountains Basalt contains members spanning a wide range of major-oxide composition, including some whose major-oxide compositions match those of older units. With few exceptions, incompatible trace elements are enriched and compatible elements (particularly Sr and Sc) depleted relative to older formations, and values of the $^{87}Sr/^{86}Sr$ ratio are higher (>0.707). Chondrite-normalized rare-earth patterns for many of the ten members of the Saddle Mountains Basalt are steeper and show a more pronounced negative europium anomaly than those of the older formations. However, one member (the Umatilla Member) has a pronounced positive europium anomaly.

Trace-element variation, represented by interelement ratios or absolute abundances plotted against MgO content, is less coherent in the Yakima Basalt Subgroup than in oceanic basalts. Some major-oxide compositional trends suggest that crystal-liquid fractionation occurred, but several other lines of evidence, both geologic and geochemical, argue against low-pressure crustal storage and fractionation. This evidence includes the divergence of chemical trends for coexisting rock and glass from those relating one bulk rock composition to another, inconsistent incompatible trace-element enrichments, and the absence of major structural depressions such as grabens and calderas that should be associated with the virtually instantaneous eruption of the huge volumes represented by individual units. Major- and trace-element variation likewise is difficult to reconcile with any simple model of high-pressure fractionation, melting from a common source, or mixing of magma with crustal material, although some combination of these processes may have been important for some units.

Interpretation of the petrogenesis of the Yakima Basalt Subgroup requires consideration of such diverse topics as the tectonic history of the Pacific Northwest, generalized models of flood-basalt genesis, and the process of continental crustal underplating, in addition to the chemical and isotopic data. Recent geophysical studies and deep drill holes show that the Columbia River Basalt Group is underlain by upper Mesozoic and lower Cenozoic sedimentary rocks that define a large preexisting sedimentary basin. This depression may have been created as a back-arc basin when the older continental margin and associated subduction zone moved westward away from a once-continuous belt of plutonic rocks represented in the Pacific Northwest by the Idaho batholith. We postulate that large volumes of magma were generated in a mixed oceanic-continental source mantle and were emplaced as sill-like bodies at the base of the continental crust. These bodies were then progressively tapped during deep continental rifting and supplied magma to the surface via extensive linear vent systems. All of the magma is inferred to have equilibrated with clinopyroxene during either melting or storage. Recent experimental study of the Grande Ronde Basalt at pressures to 3 GPa suggests an origin by direct partial melting of a source related to mid-ocean ridge basalt and its source mantle, possibly at a depth of 70 km.

The earliest basalt of regional extent, the Grande Ronde Basalt, began to fill the basin with lava derived from fairly young oceanic crust and mantle contaminated with subducted oceanic sediment. Such magma was then repeatedly erupted after storage near the crust-mantle boundary and minor interaction with lower-crustal rocks during ascent. The Wanapum Basalt formed in much the same way, although from a part of the oceanic mantle that had undergone Fe-Ti-P metasomatism. The similarity of the major-oxide chemistry of the Saddle Mountains Basalt to that of older units suggests a source related in some way to that of the Grande Ronde and Wanapum Basalts. However, the different trace-element abundances and ratios require additional complexity, such as melting of a 2.5-Ga continental mantle having rather high incompatible element contents or melting of mantle that had undergone a second metasomatic event.

Eruption rates generally kept pace with continued basining during formation of the Yakima Basalt Subgroup. At times, the basin became filled and large-volume flows continued through the ancient Columbia River Gorge to the Pacific Ocean. At other times, continued subsidence of the central plateau, possibly combined with uplift of the eastern margin of the plateau, created a gentle westward-dipping slope. Volcanism waned around 14 Ma and finally stopped at about 6 Ma, though the weight of the basalt pile caused continued subsidence as isostatic equilibrium was reestablished.

## INTRODUCTION

The Columbia River Basalt Group forms the youngest known flood-basalt province; eruptions occurred over an 11-m.y. period (17–6 Ma) in the early to late Miocene (Watkins and Baksi, 1974; McKee and others, 1977, 1981; Hooper, 1982, fig. 2; Swanson and others, 1979a). The group contains more than 170,000 km$^3$ of tholeiitic basalt and covers an area of 160,000 km$^2$ to a maximum depth of at least 3 km, as inferred from surface exposures (fig. 1; Tolan and others, 1987), drill-hole data (Lingley and Walsh, 1986), and geophysical surveys (Stanley, 1984; Glover and others, 1985). The basalt is underlain by sedimentary rocks 4–5 km thick (Stanley, 1984; Glover and others, 1985), which in turn overlie crystalline basement that extends to the base of the crust, estimated to be 40 km deep (Catchings and others, 1984). Mapping of the province is complete; regional map compilations are by Swanson and others (1979b, 1980, 1981), Anderson and others (in press), and Hooper and Swanson (in press) and references therein. Wright and others (1973) summarized major-oxide chemistry of important units and used those data to define several chemical types. Trace-element data for selected units were published by Nathan and Fruchter (1974) and by the NASA-sponsored Basaltic Volcanism Study Project (1981). Subsequently, we have defined additional chemical types and analyzed trace elements for all chemical types defined by major oxides. Many of these data are contained in open-file reports (Wright and others, 1979, 1980, 1982); a summary is given by Swanson and Wright (1981). Isotopic data for Sr, εNd, Pb, and O are summarized by McDougall (1976), Nelson (1980; 1983), Carlson and others (1981), Carlson (1984a), and Church (1985).

The purposes of this paper are (1) to summarize the chemical composition of all units of the Yakima Basalt Subgroup (table 1) mapped by two of us (DAS and TLW) in Washington and northeastern Oregon and (2) to evaluate implications for the origin of the Yakima Basalt Subgroup from available geologic, petrographic, geochemical, and geophysical data. A definitive petrogenesis awaits quantitative modeling of chemical data using the results of experimental study of representative flow compositions. Such studies are currently underway by Eiichi Takahashi, and preliminary results are available (Takahashi, 1988). Ultimately, any quantitative petrogenetic model of the complex processes that gave rise to the basalt must be based on significantly improved understanding of the nature of the upper mantle and lower crust; such an understanding probably remains far in the future.

The descriptive sections of the main body of this paper give (1) summary tabulations and graphical representations of the major-oxide, trace-element, and isotope chemistry of the flows; (2) chemistry of feeder-dike systems for many units; and (3) a comparison of major-oxide chemistry of regionally extensive flows with that of glass selvedges from associated dikes or pillows. Discussion sections specify the critical observations that delimit possible conditions of magma generation, storage, and eruption and summarize the tectonic and magmatic evolution of the Yakima Basalt Subgroup. Tables 14–17 summarize chemical data for additional flows collected by us that either have been mapped in more detail by other workers or are interlayered with, but not considered by other workers to be a part of, the Columbia River Basalt Group. These flows include local flows in the Clearwater embayment of Idaho mapped by Camp (1981) and local flows in northeastern Oregon mapped by P.R. Hooper and W.T. Taubeneck (unpublished work). Both groups of flows are of Saddle Mountains age (table 14). With one exception, flows of the former group are considered to belong to the Yakima Basalt Subgroup. Flows of the latter group are, again with one exception, mapped separately by Hooper (1984) as the basalts of Powder River, which he excludes from the Columbia River Basalt Group.

## Acknowledgments

This paper is the product of a decade of work on the Columbia River Plateau. We acknowledge the Department of Energy and personnel of Rockwell International for providing part of the funding to support this research. Peter Hooper supplied many analyses through his laboratory at Washington State University; Brent Fabbi and Floyd Brown worked closely with the authors in providing a consistent body of data from U.S. Geological Survey laboratories. Kevin Black did a superb job in setting up and maintaining a complete data base for analytical data and sample locations. We appreciate comments on an early version of the manuscript made by P.R. Hooper, S. Reidel, K. Cox, and R. Wells, and we acknowledge Rick Carlson for many discussions of the petrogenetic interpretations based on his isotopic data. Eiichi Takahashi has shared the results of his ongoing experimental study and its implications for petrogenesis of the Columbia River Basalt Group. The present manuscript has benefited from thorough and incisive reviews by John Pallister and Rosalind Helz.

## STRATIGRAPHIC NOMENCLATURE AND GEOCHEMICAL UNITS

Swanson and others (1979a; table 1 and fig. 2) worked out a revised stratigraphy for the Columbia River Basalt Group (fig. 2). The Grande Ronde Basalt has no formally named members but is divided for purposes of mapping into four magnetostratigraphic units: from oldest to youngest, $R_1$, $N_1$, $R_2$, and $N_2$. The Wanapum Basalt has four formally named members: from oldest to youngest, the Eckler Mountain, Frenchman Springs, Roza, and Priest

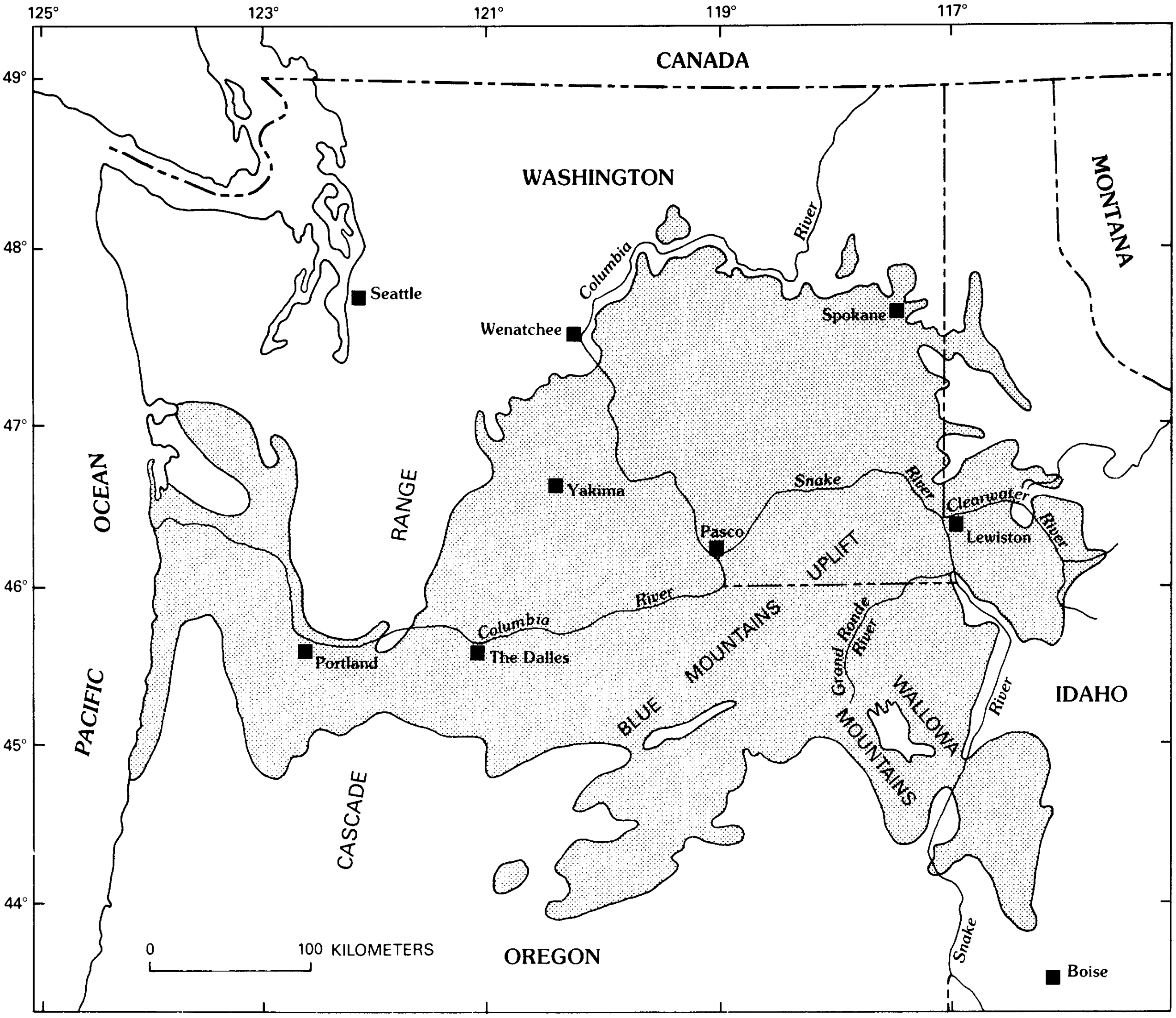

**Figure 1.** Index map of Columbia River Plateau. Outline of area covered by Columbia River Basalt Group (shaded) is modified from that given in Swanson and others (1979a) to include results of recent mapping west of Cascade Range (see Tolan and others, 1984, fig. 2). Compilation of mapping east of Cascade Range has resulted in slight modification of rest of boundary but not to an extent to affect material presented in this paper.

**Table 1.** Relation between stratigraphic position and chemistry, Yakima Subgroup, Columbia River Basalt Group

[MP, magnetic polarity as determined in the field using a fluxgate magnetometer; N, normal; R, reversed; T, transitional. Magnetic polarity units after Swanson and others (1979a). Geochemical units of the Grande Ronde Basalt are defined in Mangan and others (1985). Units marked with an asterisk (*) are defined from sections located in the western plateau]

| Formation<br>Member<br>Flow<br>(Informal Name) | Age (Ma) | MP | Geochemical unit |
|---|---|---|---|
| SADDLE MOUNTAINS BASALT | | | |
| Lower Monumental | 6 | N | LM |
| Ice Harbor | 8.5 | | |
| Basalt of Goose Island | | N | GOOSE |
| Basalt of Martindale | | | |
| Indian Memorial flow | | N | INDIAN |
| Martindale flow | | R | MARTIN |
| Basalt of Basin City | | N | BASIN |
| Buford | | N | BUFORD |
| Elephant Mountain | 10.5 | N,T | ELEPHANT |
| Wenaha flow (Walker, 1973) | | | |
| Pomona | 12.0 | R | POMONA |
| Basalt of Weippe (Camp, 1981) | | R | VC WEIPE |
| Esquatzel | | N | ESQUAT |
| | | N | RB ESQUAT |
| | | R | FS IC |
| Weissenfels Ridge | | | |
| Basalt of Slippery Creek | | N | SLIP |
| Basalt of Lewiston Orchards | | N | LEW ORCH |
| Sprague Lake flow | | | SPRAGUE |
| | | | SW SPRAG |
| Anatone flow (Price, 1974) | | | NEW |
| | | | SW NEW |
| Asotin | | N | ASOTIN |
| | | | VC ASOT |
| Huntzinger flow (Ward, 1976) | | N | SW HUNTZ |
| | | | HUNTZ |
| Basalt of Lapwai | | N | VC LAP |
| Eagle Lake flow | | N | EAGLE |
| Wilbur Creek | | N | WILBUR |
| Umatilla | | N | UMATILLA |
| | | | UM FRAC |
| Umatilla flow | | | PH UMTIL |
| Sopher Ridge flow | | | PH SOPHER |
| WANAPUM BASALT | | | |
| Priest Rapids | | R | PV |
| | | | LOLO INC |
| | | | ROSALIA |
| Powatka flow | | T,R | PH POWAT |
| Roza | | N2 | ROZA |
| Frenchman Springs | | N2 | FS ANOM |
| | | | FS INC |
| Eckler Mountain | | N2 | |
| Basalt of Shumaker Creek | | | SHUMAKER |
| | | | PH SHUM |
| Lookingglass flow | | | SW LOOK |
| Basalt of Dodge | | | DODGE |
| Basalt of Robinette Mountain | | | ROBIN |

| Formation--Continued<br>Magnetostratigraphic unit | Age (Ma) | MP | Geochemical unit |
|---|---|---|---|
| GRANDE RONDE BASALT | 16.5-14.4 | | |
| | | N | JOSEPH[1] |
| | | | GR INC |
| Magnetostratigraphic unit N2 | | N | 1 A |
| | | | 1A* |
| | | | 2 A |
| | | | UNC |
| | | | 3 A |
| | | | 3A* |
| | | | UNC |
| | | | 4 A |
| | | | 4A* |
| | | | UNC* |
| | | | 3B |
| | | | UNC |
| | | | 4B |
| | | | LH2 |
| | | | MG6 |
| | | | 2B |
| | | | 5 A |
| | | | 5A* |
| | | | UNC |
| | | | 2C |
| | | | 4C |
| | | | 5B |
| | | | 3C |
| | | | 3C* |
| Magnetostratigraphic unit N2 | | N | UNC |
| | | T | 5C |
| | | T | 5C* |
| Magnetostratigraphic unit R2 | | R | 3D |
| | | | 5D |
| | | | 5D* |
| | | | UNC |
| | | | 2D |
| | | | 2D* |
| | | | UNC |
| Magnetostratigraphic unit R2 | | R | AS16 |
| | | T | 2E |
| Magnetostratigraphic unit N1 | | N | UNC |
| | | | KB5 |
| | | | 3E |
| | | | UNC |
| | | | 3F |
| | | | 5E |
| | | | AS16 |
| | | | 3G |
| | | | 5F |
| | | | UNC |
| | | | AS16 |
| | | | 5G |
| | | | AS16 |
| | | | 5H |
| | | | AS16 |
| | | | UNC |
| Magnetostratigraphic unit N1 | | N | AS16 |
| Magnetostratigraphic unit R1 | | R | 2F |
| | | | 5I |
| | | | AS16 |
| IMNAHA (C-3) | 17-16 | R | |

---

[1] The Joseph volcanics unit of Kleck (1976) is composed of a series of glassy shield volcanoes sitting on top of the Grande Ronde Basalt in northeastern Oregon. Their chemistry suggests affinity with the Grande Ronde Basalt.

Rapids Members. Beeson and others (1985) have shown that there is no interbedding between these two formations, though such had been inferred by Swanson and others (1979a). Neither set of authors found evidence of a magnetic polarity reversal between Grande Ronde and Wanapum times. Accordingly, we believe that the Eckler Mountain and Frenchman Springs Members of the Wanapum Basalt fall in magnetostratigraphic unit $N_2$, as does the upper part of the Grande Ronde Basalt; the Roza Member is transitional from unit $N_2$ into unit $R_3$; and the Priest Rapids Member lies within unit $R_3$. The Saddle Mountains Basalt is divided into ten members (fig. 2), all of which are separated by erosional unconformities. The magnetostratigraphy is probably discontinuous; thus the polarity of each unit is designated in table 1 as N or R without a subscript.

Each member of the formations of the Yakima Basalt Subgroup (fig. 2) is composed of several flows, or sequences of flows, each of which has a distinctive major-oxide composition. The average chemistry of each flow sequence defines a geochemical unit of a certain chemical type[1], which is given an abbreviation related to its stratigraphic position (table 1). Some of the names of such units relate to locally mappable units defined since 1979 (see columns headed "flow" and "informal name" in table 1). Regional correlation of flows is based on geologic mapping, flow chemistry, and paleomagnetic measurements (compare Choiniere and Swanson, 1979; Hooper, 1981; Mangan and others, 1986). The stratigraphic nomenclature, chemical designation, radiometric age, and magnetic polarity of each unit in the Yakima Basalt Subgroup are given in table 1.

## GENERAL GEOLOGIC RELATIONS

The regional distribution of formations and members in the Yakima Basalt Subgroup was originally given by Swanson and others (1979a, plate 1); distribution maps for individual members have been updated by Anderson and others (in press), and the volumes of the formations that make up the Yakima Basalt Subgroup have been newly estimated by Tolan and others (1987). Flows of the Grande Ronde Basalt cover most of the Columbia Plateau. Products of individual eruptions range from plateau-covering basaltic floods to smaller flows of more local distribution (Mangan and others, 1985, 1986). Flow contacts in the Grande Ronde are generally tight; a few thin and discontinuous intercalations of sedimentary and tuffaceous deposits occur, principally near the margins of the Plateau. The regional extent of the Wanapum Basalt is nearly as great as that of the Grande Ronde Basalt. Both formations contain flows or sequences of flows with volumes in excess of 500 km$^3$; examples include the Roza Member, the Priest Rapids Member (LOLO geochemical unit); Grande Ronde Basalt, unit 4a*. Maximum thicknesses where flows were ponded are nearly 100 m, as estimated from surface exposures and drill holes.

A saprolite separates the Grande Ronde and Wanapum Basalts in the central part of the Columbia Plateau. The saprolite thickens toward the margins of the Plateau, where it may underlie or be replaced by sedimentary deposits (the Vantage Member of the Ellensburg Formation in the western Plateau and the Latah Formation in the eastern Plateau). The time interval during which the Grande Ronde Basalt was weathered was apparently not great, for no evidence

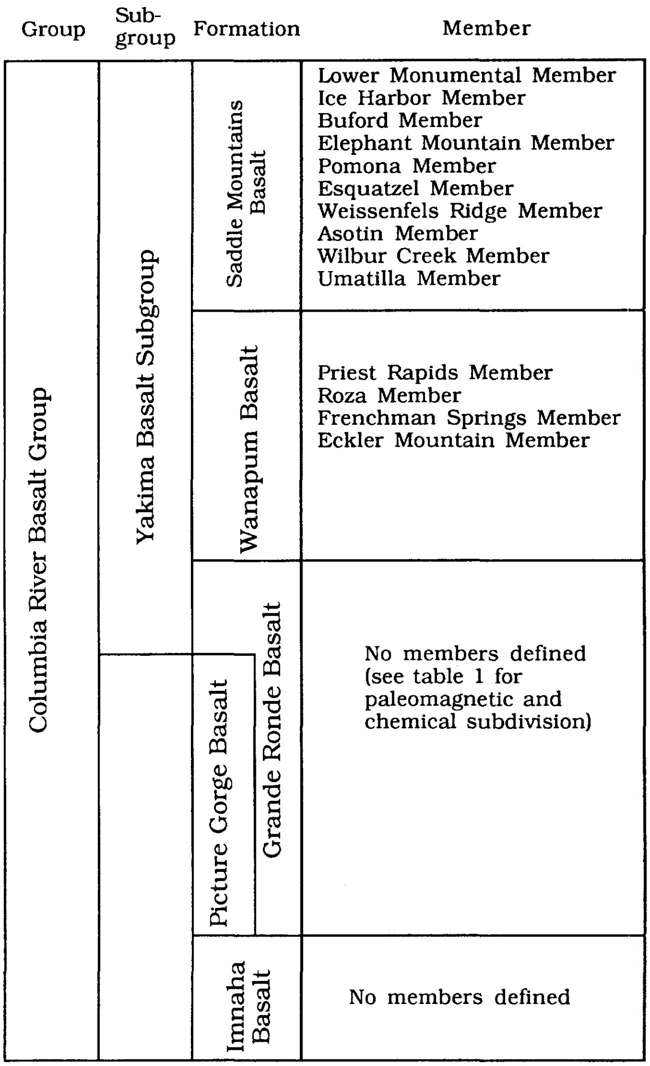

| Group | Sub-group | Formation | Member |
|---|---|---|---|
| Columbia River Basalt Group | Yakima Basalt Subgroup | Saddle Mountains Basalt | Lower Monumental Member<br>Ice Harbor Member<br>Buford Member<br>Elephant Mountain Member<br>Pomona Member<br>Esquatzel Member<br>Weissenfels Ridge Member<br>Asotin Member<br>Wilbur Creek Member<br>Umatilla Member |
| | | Wanapum Basalt | Priest Rapids Member<br>Roza Member<br>Frenchman Springs Member<br>Eckler Mountain Member |
| | | Grande Ronde Basalt | No members defined (see table 1 for paleomagnetic and chemical subdivision) |
| | | Picture Gorge Basalt | |
| | | Imnaha Basalt | No members defined |

**Figure 2.** Stratigraphy of the Columbia River Basalt Group, after Swanson and others (1979a).

---

[1] The term "geochemical unit" as used in this paper is similar to but not identical to the term "chemical type" used previously. The former term carries with it a specific stratigraphic as well as chemical meaning. The Grande Ronde Basalt is the only unit where chemical types, originally defined for one stratigraphically bound set of flows of similar chemistry are repeated throughout the stratigraphic section and thus are properly referred to as "chemical types," retaining the chemical definition while dropping the stratigraphic meaning; see, for example Mangan and others (1986).

for a polarity reversal has been recognized between Grande Ronde and Wanapum times.

The Saddle Mountains Basalt began to be erupted after an interval of erosion lasting perhaps as long as one million years. Saddle Mountains time extends from approximately 13 to 6 Ma, and significant time breaks separate the eruptions of each member of the Saddle Mountains (table 1). Many flows of the Saddle Mountains Basalt are preserved as remnants of valley-filling flows on the walls of present-day canyons and must originally have flowed down deep canyons cut into the Grande Ronde and Wanapum Basalts in the eastern part of the Plateau (Swanson and others, 1975a). Some individual flows are as voluminous as those in the Wanapum and Grande Ronde Basalts, and many traveled as far or farther because of channeling in river valleys. However, the Saddle Mountains Basalt covered less of the Plateau surface than did the earlier units.

## VENTS FOR FLOWS OF THE YAKIMA BASALT SUBGROUP

All flows were erupted from fissures and fed by dikes. Several outcrops are known in which a dike merges into the flow it fed (Swanson and others, 1975b). The location of a dike thus defines the trace of a vent fissure. Only rarely are the surface expressions of vents, such as cones and spatter ramparts, preserved (Bingham, 1970; Swanson and others, 1975b).

Dikes and vents for flows of each stratigraphically bound geochemical unit define one or more narrow linear vent systems (Swanson and others, 1975b), as long as 150 km, many of which are composed of echelon segments. Most or all vent systems trend NNW. (azimuth 310°–350°) and are located in central and eastern Washington, northeastern Oregon, and western Idaho (fig. 3), with most known dikes occurring in extreme southeastern Washington and northeastern Oregon (Taubeneck, 1970, 1978). Each linear vent system is near the eastern margin of the flows it fed, consistent with other indications that a gentle westward slope was formed and persisted during the time of eruption of the Yakima Basalt Subgroup. Maps showing the location of linear vent systems and the known extent of flows they fed are given in Swanson and others (1979a, plate 1) and in Anderson and others (1987). Locations and chemical analyses of individual dikes are given by Wright and others (1979, 1980). Locations of additional dikes and vents in Idaho are given by Camp (1981) and Swanson and others (1981).

Within the overall dike system (fig. 3) no regular progression of vent location through time has been recognized for the subgroup. Linear vent systems for the Grande Ronde Basalt occur throughout the entire area of the dike swarm. Linear vent systems for each member in the Wanapum Basalt occupy distinct regions, and there was an eastward migration of vents for the upper members of the Wanapum: those for the Frenchman Springs Member are near the western margin of the dike swarm, those for the Roza are in eastern Washington, and those for the Priest Rapids are in Idaho within the eastern part of the dike swarm. Sources for the Saddle Mountains Basalt are scattered across the entire area, from central Washington (Ice Harbor Member) through eastern Washington and Oregon (Elephant Mountain and Umatilla Members) to Idaho (Weissenfels Ridge Member), and show no systematic variation of vent location with time.

The following members of the Saddle Mountains Basalt have no identified source vents or dikes: Lower Monumental, Pomona, Esquatzel, Weissenfels Ridge (basalt of Slippery Creek), Asotin, and Wilbur Creek Members. Until recently, the basalt of Weippe (Camp, 1981) and its feeder dike were considered correlative with the Pomona Member. However, the paleomagnetic and isotopic signatures of the Weippe dike have been shown to differ from those of the mapped Pomona Member, although the major-oxide and trace-element chemistry are identical (P.R. Hooper, oral commun., 1986). In addition, no vent is known for the Lookingglass flow in the Eckler Mountain Member of the Wanapum Basalt. Four of these units traveled to or across the central area of the Columbia Plateau, and three of these (Pomona, Asotin, and Wilbur Creek Members) each have volumes that exceed 40 km$^3$. We made a careful search along the eastern margin of the outcrop area, after completion of the regional mapping, for dikes or vents that could have fed these units, but we found none. Therefore we conclude that the sources for these units are not presently exposed.

## CHEMICAL STUDY OF THE YAKIMA BASALT SUBGROUP

### Methods of Analysis

Major oxides were analyzed in the laboratories of the U.S. Geological Survey (USGS) in Reston, Virginia, (Rapid Rock) and Menlo Park, California, (X-ray fluorescence) and in the X-ray fluorescence laboratory at Washington State University (WSU) under the direction of P.R. Hooper (see Hooper, 1981). Electron microprobe analyses of natural sideromelane glass were obtained at the Smithsonian Institution in Washington, D.C. Trace-element determinations have been made by instrumental neutron activation analysis (INAA) for Ba, Co, Cr, Cs, Hf, Rb, Th, U, Zn, Zr, Sc, and the rare-earth elements La, Ce, Nd, Sm, Eu, Gd, Tb, Yb, and Lu; by X-ray fluorescence (XRF) for Ba, Rb, Sr, Zr, Nb, and Y; and by atomic absorption spectroscopy (AAS) for Cu and Ni. Ba, Rb, and Zr were therefore determined by both XRF and INAA. Analyses and methods used for major oxides and for trace-element data obtained by INAA are given by Wright and others (1979, 1980, 1982).

Analyses of trace elements by XRF were obtained from the USGS laboratory in Reston under the direction of Harry Rose; the analyst was Bob Johnson. Analyses by AAS were done by Jean Kane, also in the USGS laboratories in Reston.

The analytical errors of the various data, though difficult to estimate, are much less than the differences between defined geochemical units and therefore do not affect the discrimination of one such unit from another. Relative values for trace elements analyzed by two methods are in

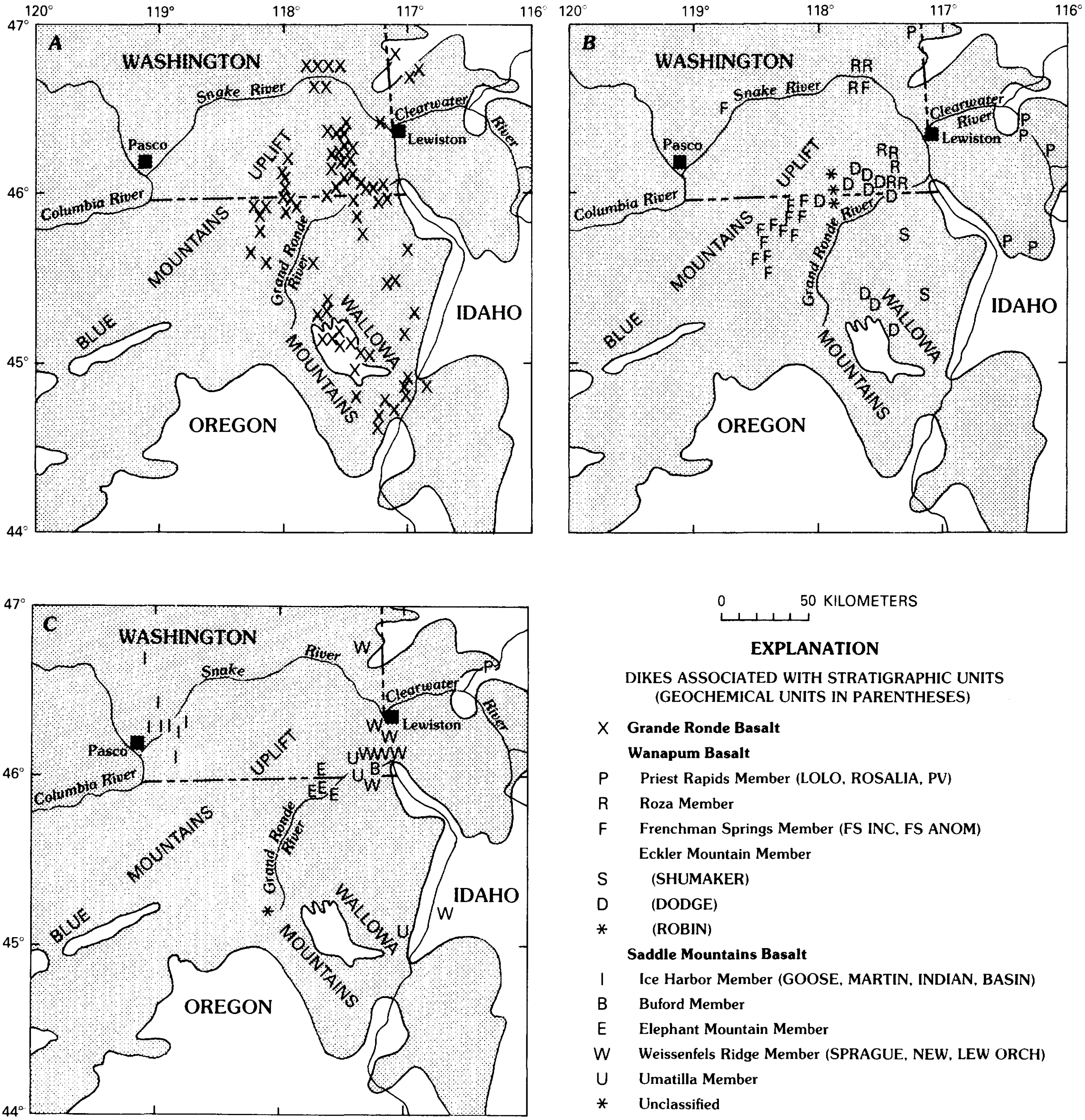

**Figure 3.** Location of linear vent systems for the Yakima Basalt Subgroup of the Columbia River Basalt Group. Area of Columbia River Basalt Group shaded. See table 1 for stratigraphic setting of units. *A*, Grande Ronde Basalt. *B*, Wanapum Basalt. *C*, Saddle Mountains Basalt.

**Table 2.** Average analytical differences among three laboratories

[XRF, U.S. Geological Survey, Menlo Park, X-ray fluorescence analyses; WSU, Washington State University, X-ray fluorescence analyses. Biases obtained by subtracting values obtained by reference laboratory, U.S. Geological Survey, Reston, rapid rock analyses. Biases calculated from analyses of selected samples done by at least two different laboratories, and from comparison of flow averages for major stratigraphic units calculated from analyses obtained from each laboratory in course of regional mapping. Biases vary somewhat as a function of bulk chemistry, although signs, + or -, are consistent. Analyses in tables in this paper have not been corrected]

| Oxide | Bias (XRF) | Bias (WSU) |
|---|---|---|
| $SiO_2$ | -0.74 | +0.33 |
| $Al_2O_3$ | 0.00 | -0.48 |
| 'FeO' | +0.35 | -0.30 |
| MgO | +0.01 | +0.16 |
| CaO | -0.08 | -0.17 |
| $K_2O$ | +0.07 | 0.00 |
| $TiO_2$ | +0.04 | +0.02 |
| $P_2O_5$ | +0.09 | +0.05 |
| MnO | n.a. | n.a. |

good agreement, although the precision and accuracy are probably greater for the XRF than for the INAA analyses. We have not specifically studied the chemical variation within single flows. An empirical measure of the variability within a geochemical unit is obtained from the variation shown by regional sampling of the same flow or stratigraphic unit, and this variability has been used to scale the plots (see below). Major-oxide analyses made in different laboratories show systematic differences (table 2), and only analyses from the USGS laboratories are used to discuss chemical differences and their interpretation. This is done for consistency and does not imply that these analyses are better than those from other laboratories.

## Presentation of Chemical Data

The chemical data on which the discussions and inferences in this paper are based are given in tabular form. Average whole-rock and glass compositions and trace-element ratios of geochemical units and whole-rock compositions of feeder dikes appear together with the main text (tables 3–12); chemical data on some additional analyzed flows (see table 14) are given in the appendix (tables 15–17); and the individual analyses from which the average compositions were derived are published separately as a U.S. Geological Survey Open-File Report (Wright, 1988).

The average major- and trace-element compositions of flows defining each geochemical unit are listed in stratigraphic order in tables 3–5. Each average represents at least two analyses. Data for samples used to compute the averages, including the range and standard deviation for each element, are summarized for the Grande Ronde Basalt in Mangan and others (1985) and for the Wanapum and Saddle Mountains Basalts in Wright (1988). The compositions of dikes for geochemical units that have well-defined linear vent systems are given in table 6; individual analyses are listed in Wright (1988). The averages calculated from WSU analyses are preceded by a two-letter abbreviation related to the original collectors of the sample: PH, Peter Hooper; VC, Victor Camp; WT, William Taubeneck; RB, Robert Bentley; SW, D.A. Swanson and T.L. Wright. Abbreviations for geochemical units are denoted similarly: SHUMAKER = USGS average, PH SHUM = WSU average for samples of the basalt of Shumaker Creek in table 1. Selected trace-element ratios for all formations are summarized in tables 7–9.

Selected data for all units of the Yakima Basalt Subgroup are also plotted in figures 4–6. Data are plotted by formation, with the Saddle Mountains Basalt divided into two sets of plots, one for flows whose major-oxide chemistry broadly resembles that of the Grande Ronde Basalt (relatively high $SiO_2$, low total iron as FeO, and low $TiO_2$), the other for flows whose major-oxide chemistry broadly resembles that of the upper part of the Wanapum Basalt (relatively low $SiO_2$, high total iron as FeO, and high $TiO_2$). Letter symbols given in tables 4 and 5 are related to stratigraphic position within the Saddle Mountains and Wanapum Basalts from top (A) toward bottom (Z). In the data for the Grande Ronde Basalt (table 3), symbols A–E refer to major geochemical units repeated throughout the section, 1 and 2 refer to two distinctively magnesian units of local extent, and X represents the remaining Grande Ronde flows (Mangan and others, 1985; 1986). An asterisk (*) in the name for a geochemical unit (for example, 1A*) is used to distinguish averages for units defined in the western plateau; the name used for the same unit in the eastern plateau has no asterisk (for example, 1A). The chemical data are plotted as follows:

*MgO variation diagrams* (fig. 4).—The chemistry of each unit is summarized on three plots showing, respectively, major oxides and compatible trace elements, incompatible trace elements, and selected trace-element ratios.

*Th (Thorium) variation diagrams* (fig. 5).—The same data (including MgO) are plotted against a well-determined incompatible element.

*Chondrite-normalized rrareearth-element (REE) data* (fig. 6).—Symbols differ from those used in tables 3–5 because of the plotting program used. The plots in figure 6 show only La, Ce, Sm, Eu, Tb, Yb, and Lu.

*Isotope data* (fig. 7).—Previously published data for isotopes of εNd, Pb, and O are plotted against $^{87}Sr/^{86}Sr$.

Except for plots of trace-element ratios, figures 4 and 5 are scaled so that the symbol size represents approximately two standard deviations in each oxide or element as estimated from statistical analysis of the geochemical units. This is necessarily somewhat subjective, as the standard deviation for a given element or oxide varies from one geochemical unit to another. Nonetheless they are sufficiently similar to interpret separation of symbols as a petrologically significant chemical difference. Symbol separation does not have the same meaning on plots of MgO or Th against element ratios, because of difficulty in estimating quantitatively the errors in the ratios.

The chemistry of natural glasses is tabulated separately (tables 10–12). Data from which the glass averages were calculated is given in Wright (1988). The major-oxide compositions of bulk rocks and associated quenched glasses are compared for selected units in figure 8.

The chemical characteristics that distinguish each unit in the Yakima Basalt Subgroup are summarized in table 13.

## Petrography

Petrographic data for most units of the Yakima Basalt Subgroup have been summarized by Wright and others (1973, table 3), although the unit names have been changed since (the names 'Upper', 'Middle', and 'Lower' Yakima Basalt of previous usage correspond, respectively, to what are now defined as the Saddle Mountains, Wanapum, and Grande Ronde Basalts). What follows is a brief recapitulation of the previously published data, with petrographic information added for units not identified in 1973.

*Grande Ronde Basalt.*—Rocks of this unit are mostly aphyric or sparsely microphyric with augite-plagioclase clots. Many flows have rare microphenocrysts of hypersthene. A few local flows are mappable on the basis of visible plagioclase phenocrysts but are not chemically distinctive.

*Wanapum Basalt.*—Rocks of this unit are commonly sparsely porphyritic with either single (as large as 1 cm) plagioclase phenocrysts (Roza Member; basalt of Dodge of the Eckler Mountain Member), large (1–3 cm) plagioclase clots (many flows of the Frenchman Springs Member; see also Beeson and others, 1985, table 1), or small (1–3 mm) olivine and plagioclase phenocrysts (Priest Rapids Member, LOLO geochemical unit). Some flows in the Frenchman Springs Member (see also Beeson and others, 1985) and a few flows in the basalt of Dodge are aphyric, as are the basalt of Robinette Mountain of the Eckler Mountain Member and other Wanapum flows not mentioned above. The basalt of Dodge is exceptionally coarse-grained (>1 mm) and is identifiable in the field, where it commonly weathers to a coarse grus.

*Saddle Mountains Basalt.*—Flows of the Pomona Member and the basalt of Martindale (of the Ice Harbor Member) are distiguished by an augite-plagioclase-olivine assemblage of phenocrysts and glomerocrysts. The basalt of Goose Island (of the Ice Harbor Member) is unique for the occurrence of microphenocrysts of ilmenite and titanmagnetite. The Esquatzel Member is distinguished by the presence of augite (as large as 5 mm) as the only phenocryst type. The rest of the Saddle Mountains Basalt flows are aphyric to sparsely porphyritic, with no phenocrysts large enough to be of use in mapping. Flows of the Asotin Member have a coarse subophitic texture that is distinctive on a weathered surface.

## Classification and Naming of Geochemical Units

The geochemical units (tables 1 and 3–6) were classified according to normative data using procedures recommended by Irvine and Baragar (1971) and by Wilkinson (1986). The total iron (FeO of tables 3–6) was partitioned to $Fe_2O_3$ and FeO in a ratio of 9:1 before calculating the norm. The Irvine and Baragar procedures yield more consistency in the naming of such units than do the Wilkinson procedures. With one exception, geochemical units in the Yakima Basalt Subgroup are classified as subalkaline tholeiitic basalt using their figure 4 (Ol′-Ne′-Q′), figure 5 (Cpx-Ol-Opx), figure 6 (normative plagioclase An content versus $Al_2O_3$), and figure 7A (normative plagioclase An content versus color index). The most fractionated chemistry in the Umatilla Member (UM FRAC geochemical unit of table 1) was classified as calc-alkaline tholeiitic andesite using their figures 6 and 7A. The single sample of magnesian Imnaha Basalt (table 15) was also classified as subalkaline tholeiitic basalt on their figures 4, 6, and 7A, although it was barely alkaline using figure 5. Classification of the basalts in terms of sodic or potassic affinity using their figure 8 (An-Ab′-Or) shows that all the samples of the Grande Ronde and Wanapum Basalts, and the single sample of the Imnaha Basalt, have average $K_2O$ contents. Some members of the Saddle Mountains Basalt (Pomona, Esquatzel, Asotin, Wilbur Creek, and Umatilla Members) have composition ranges that extend slightly into the field of K-rich basalts.

The basalts of Powder River (Hooper, 1984), whose compositions are given in table 15, were classified as a mixture of subalkaline and alkaline basalt using figures 4 and 5 of Irvine and Baragar (1971). Alkaline geochemical units include alkalic basalt (WT NEPH), hawaiite (WT SPRMT, WT SUGMT), and trachybasalt (WT WBRMT), using their figure 10 (normative plagioclase An content versus color index). WT JONES and WT ANDES were classified as calc-alkaline andesite using their figures 6 and 7A. Of the Idaho flows mapped by Victor Camp (table 15), only VC POT is classified as an alkaline basalt. The remaining geochemical units of Camp (1981), the PH EDEN unit in northeastern Oregon, and WT OBHTI and WT OBLTI units in the basalts of Powder River, are all classified as subalkaline tholeiitic basalt.

Classification using the procedures of Wilkinson (1986, table 1) resulted in all units containing a mixture of basalt and andesite varying from quartz- to olivine-tholeiitic affinity depending on MgO content. The most magnesian geochemical units in the Saddle Mountains Basalt (ASOTIN and VC ASOT) and Wanapum Basalt (ROBIN) are classified, because of their high content of $Al_2O_3$, as olivine subalkaline basalt. The UM FRAC geochemical unit is classified as a calc-alkaline tholeiitic dacite. The alkaline samples in the basalts of Powder River are classified as basanite (WT NEPH), high-Al transitional andesite (WT SUGMT and VC POT), and alkali andesite (WT SPRMT and WT WBRMT). WT ANDES and WT JONES are classified as calc-alkaline andesite and dacite, respectively. We prefer the simpler naming using the Irvine and Baragar (1971) procedures.

## Bulk Rock Chemistry: Observations

### Grande Ronde Basalt

The Grande Ronde Basalt (figures 4*A*–*C*, 5*A*–*B*) shows the most regular chemical variation of the three formations examined. All oxides and elements vary continuously over a limited range of MgO content (3–6 percent). Within this apparent continuum several different chemical subtypes, distinguished by small variations in MgO, $TiO_2$, and $P_2O_5$, have been defined (Mangan and Wright, 1984; Mangan and others, 1986). The most regular major-oxide variations are the covariance of CaO and MgO and a less strong covariance of $Al_2O_3$ and MgO. Among the compatible trace elements, Sc shows the most regular variation, a strong positive correlation with CaO. The Sc/CaO ratio rises as MgO decreases. The elements Co, Cr, Ni, Cu, and Sr also behave as compatible elements with decreasing MgO. The variation of Cu suggests the separation of a sulfide melt at or near the liquidus temperature of these basalts (see Skinner and Peck, 1969). One magnesian flow (LH 2 in table 3; symbol "1" in figs. 4*A*–*C* and 5*A*–*B*) has an anomalous chemistry marked by low $TiO_2$, FeO, Co, and Sc and high $SiO_2$ and Sr. This unit has a well-defined dike system (table 6; Mangan and others, 1986) and covers a limited area in the Snake River-Blue Mountains region. A few other symbols plot off the main trend for a single oxide or element but show no correlated anomalies for other analyzed elements. These represent single analyses and perhaps reflect analytical errors.

Incompatible trace elements and oxides show different degrees of enrichment with decreasing MgO (fig. 4*B*) or increasing Th (fig. 5*A*). The elements Cs and Rb behave most incompatibly (greatest enrichment), followed by $K_2O$ and Th. The elements Ba, La, and Hf are less enriched, followed by $TiO_2$, $P_2O_5$, Ta, Zr, and Nb. The least enrichment is shown by Yb, which remains nearly constant with decreasing MgO.

The spread of data for certain constituents is greater in samples of the Grande Ronde Basalt having MgO less than 3.5 percent. Particularly variable are $K_2O$ and Th, and a group of samples with high values for those elements plots above trends defined by the rest of the Grande Ronde Basalt samples (fig. 4*A*). This is expressed on the Th variation diagram (fig. 5*A*) by a change in slope separating the trend of samples with greater than 6 ppm Th from that defined by the rest of the data. Th continues to increase while the highly incompatible elements like Rb, Cs, and $K_2O$ may remain constant or decrease at higher values of Th.

Trace-element ratios (figs. 4*C*, 5*B*) are highly variable, in part owing to the error amplification inherent in calculating ratios. The only ratios that remain fairly constant over a wide range of MgO and Th contents are K/Rb and Hf/Ta. The compatible nature of Sr is strikingly demonstrated by the steep positive slopes of K/Sr and Rb/Sr. The ratio Hf/Th shows a regular decrease with increasing Th or decreasing MgO, emphasizing the compatible behavior of Hf relative to Th.

The Grande Ronde Basalt also shows regular and similar chondrite-normalized rare-earth patterns (fig. 6*A*). Samples with the lowest MgO contents have the highest REE contents; all patterns are enriched in light rare earths and slightly concave upward. A small negative Eu anomaly, expressed as the ratio of analyzed Eu to Eu measured by linear extrapolation between Sm and Tb, is common. This Eu anomaly ranges from 0.94 to 0.77 and is not correlated with either MgO or the La/Yb ratio. The ratio La/Yb is 4.0–5.5 for chondrite-normalized La contents of 55 to 95 and increases with increasing Th (fig. 5*B*) or decreasing MgO (fig. 4*C*).

The data for the Joseph volcanic unit of Kleck (1976) plot within the range of the low-MgO compositions in the Grande Ronde Basalt (table 15; symbol # in figs. 4*A*–*C*, 5*A*–*B*, 6*A*). This chemistry and the stratigraphic position of the Joseph volcanic unit indicate that it is the latest outpouring of the Grande Ronde Basalt and formed a line of small shields.

The Sr-isotope data for the Grande Ronde Basalt are tightly clustered near $^{87}Sr/^{86}Sr = 0.7050$ (fig. 7*A*); the total range is 0.7043–0.7055, including samples of McDougall (1976) for which Sr is the only isotopic system analyzed. McDougall (1976, tables 4 and 6) demonstrated a consistent difference within the Grande Ronde Basalt between samples collected in southeastern Washington and adjacent Oregon, within the area of many feeder dikes, and samples from central Washington. We now know that all of the latter samples were from flows that were also erupted from eastern vents (Mangan and others, 1986) but are from the uppermost magnetostratigraphic unit ($N_2$), whereas the eastern samples are from older units ($R_2$ and $N_1$). Hooper (1984, fig. 2) generalized the relations between $^{87}Sr/^{86}Sr$ and magnetostratigraphy to draw a smooth trend showing increasing $^{87}Sr/^{86}Sr$ with decreasing age, from the Imnaha Basalt through the Grande Ronde Basalt to the top of the Wanapum Basalt. We interpret the same data to indicate a discontinuous jump near the $R_2$–$N_2$ unit boundary, with little Sr-isotopic distinction among the regionally correlated older flows. Within parts of units $R_2$ and $N_2$ $^{87}Sr/^{86}Sr$

increases with increasing age. The other isotopes also vary over fairly narrow ranges. Neodymium isotopic data, expressed as the difference from a chondritic value (εNd) generally show an inverse correlation with $^{87}Sr/^{86}Sr$. On a plot of eNd against $^{87}Sr/^{86}Sr$ (see fig. 7*A*; Carlson, 1984a, fig. 3) the samples of the Grande Ronde Basalt define a linear pattern with little scatter.

### Wanapum Basalt

The Wanapum Basalt can be divided into two broad chemical groupings, which are also stratigraphically separate. The oldest stratigraphic unit (Eckler Mountain Member) is confined to the southeastern part of the province, where the flows occupy elongate outcrop belts parallel to known linear vent systems (Swanson and others, 1975b, 1979a). Except for $P_2O_5$, major oxides of the Eckler Mountain Member plot near or on the extrapolated trends for the Grande Ronde Basalt on variation diagrams using either MgO or Th as a base (compare figs. 4*D–F* and 5*C–D* with figs. 4*A–C* and 5*A–B* (symbols G, H, I, and J)); one unit, the basalt of Dodge, is identical in major-oxide chemistry to some magnesian flows of the Grande Ronde Basalt. The upper stratigraphic units of the Wanapum Basalt (the Frenchman Springs, Roza, and Priest Rapids Members; symbols A–F) contain the same range of MgO (3–6 percent) as the Grande Ronde Basalt but have distinctly higher FeO, $TiO_2$, and $P_2O_5$ and lower $SiO_2$ contents.

The Wanapum, like the Grande Ronde, shows a strong covariance of CaO with MgO and Sc and an increasing Sc/CaO ratio with decreasing MgO. Other chemical variations are less regular; for example, $TiO_2$ and $P_2O_5$ are poorly correlated.

Trace elements for all members of the Wanapum Basalt plot close to trends defined for the Grande Ronde Basalt, although several incompatible elements (Hf, Nb, Ta, Zr, Y, and the REE) and Ni are systematically enriched in the Wanapum at the same MgO content (compare fig. 4*E* with fig. 4*B*). The chondrite-normalized rare-earth patterns (fig. 6*B*) for the Wanapum have shapes similar to those for the Grande Ronde and also show an overall increase in REE abundance with decreasing MgO; the total REE content is generally higher in all but the DODGE and ROBIN geochemical units. Slightly negative Eu anomalies, as defined above, are present and range from 0.93 to 0.99. The La/Yb ratio is similar in all units, except the DODGE and ROBIN geochemical units, and ranges between 4 and 5 (figs. 4*F*, 5*D*). However, the variation of La/Yb ratio with MgO or Th is the opposite of that in the Grande Ronde: the ratio decreases with decreasing MgO or increasing Th in the Wanapum Basalt. The basalt of Robinette Mountain has the flattest REE pattern of any unit in either the Grande Ronde or Wanapum Basalt, with a La/Yb ratio of only 2.4.

Isotopic data for the Wanapum Basalt overlap on all plots with those for the Grande Ronde Basalt (compare fig. 7*B* with fig. 7*A*). Both units show a positive correlation of $^{87}Sr/^{86}Sr$ with $^{208}Pb/^{204}Pb$ and a negative correlation with $^{206}Pb/^{204}Pb$ and εNd; $^{207}Pb/^{204}Pb$ is constant at about 15.6, and $\delta^{18}O$, which varies between +5 and +7, does not correlate with variations in other isotopes.

### Saddle Mountains Basalt

The Saddle Mountains Basalt (figs. 4*G–L*, 5*E–H*) has a much wider range of chemical composition than either the Grande Ronde or Wanapum Basalt, yet it retains a strong positive correlation of CaO with MgO. Many members of the Saddle Mountains Basalt have major-oxide compositions similar to those of older units. We have divided the plots into those geochemical units broadly similar to ones in the Grande Ronde Basalt or the Eckler Mountain Member of the Wanapum Basalt (that is, relatively high $SiO_2$ coupled with low $TiO_2$ and total iron) and those geochemical units broadly similar to the upper units of Wanapum Basalt (that is, relatively low $SiO_2$ coupled with high $TiO_2$ and total iron). Examples of the former are BUFORD, POMONA, VC WEIPE, ASOTIN, SW HUNTZ, HUNTZ, VC LAP, and WILBUR; examples of the latter are LM, ELEPHANT, LEW ORCH, SPRAGUE, SW SPRAG, NEW, and SW NEW. However, the trace elements in all the geochemical units are quite distinct and serve to distinguish the Saddle Mountains Basalt from older units. Most incompatible elements, with the notable exception of Cs, are highly enriched, and some compatible elements (for example, Sc and Sr) are depleted, in the Saddle Mountains Basalt relative to their levels in older units.

Comparison of the Saddle Mountains Basalt with older units (Wanapum Basalt and Grande Ronde Basalt) is most easily made on an element-by-element basis at the same MgO content (fig. 4). Results of such comparison are shown in the following table (elements marginal between two categories are shown intermediate between two columns):

| | Co | Cr | Sr | Zn | Sc | Cu | Ni | Ba | Cs | Hf | Nb | Rb | Ta | Th | U | Y | Zr | La | Yb |
|---|---|---|---|---|---|---|---|---|---|---|---|---|---|---|---|---|---|---|---|
| **Saddle Mountains Basalt relative to Grande Ronde Basalt** | | | | | | | | | | | | | | | | | | | |
| Enriched | x | – | – | – | – | – | x | x | – | x | x | – | x | x | – | x | x | x | – |
| Similar | – | x | – | x | – | x | – | x | – | – | – | x | – | – | x | – | – | – | x |
| Depleted | – | – | x | – | x | – | – | – | x | – | – | – | – | – | – | – | – | – | – |
| **Saddle Mountains Basalt relative to Wanapum Basalt** | | | | | | | | | | | | | | | | | | | |
| Enriched | x | – | – | – | – | – | – | – | – | x | x | – | x | x | – | – | x | x | x |
| Similar | – | x | – | – | x | x | x | x | x | – | – | x | – | – | x | x | – | – | x |
| Depleted | – | – | x | x | x | – | – | – | – | – | – | x | – | – | – | – | – | – | – |

The Th variation diagrams (fig. 5*E*, 5*G*) for the Saddle Mountains Basalt show different trends for all incompatible elements relative to those for the Grande Ronde or Wanapum Basalt (fig. 5*A*, 5*C*). Chondrite-normalized rare earth patterns (fig. 6*C*) are also steeper for a given MgO content than those of the Grande Ronde or Wanapum, and the La/Yb ratio reaches values greater than 7 (compare fig. 4*H*, 4*K* with fig. 4*B*, 4*E*). Negative europium anomalies are more pronounced in the Saddle Mountains Basalt than in older units of similar major-oxide chemistry, particularly in flows with high total REE content. Some units of the Saddle Mountains Basalt show unique chemical characteristics, including extreme values for certain elements. Flows of the Ice Harbor Member have higher Sc, Hf, Nb, Ta, Zr, and REE and lower Th and Ni than other units in the Saddle Mountains Basalt. The Ice Harbor Member is richer in REE (fig. 6*C*) than many other Saddle Mountains Basalt units, but its La/Yb ratios of 5–6 (fig. 4*L*) are not especially high. The basalt of Goose Island (symbol B in fig. 4*J*–*K*) has an extreme composition marked by high total iron and $P_2O_5$, far exceeding the range normally found in basalt. This unit also has abnormally high enrichment of Hf, Y, Nb, Ta, and REE. Significantly, Eu anomalies are absent from all geochemical units in the Ice Harbor Member, even the iron-rich GOOSE composition.

The Esquatzel Member has exceptionally high values of Rb and Th, and the Umatilla Member has exceptionally high values of Ba, Rb, Th, and Eu. The Umatilla is the only unit within the Yakima Basalt Subgroup that has a pronounced positive Eu anomaly.

Isotope data for the Saddle Mountains Basalt show that mean data for all isotope systems fall close to the trends defined by the older units extrapolated to higher values of $^{87}Sr/^{86}Sr$. For many units of the Saddle Mountains Basalt, values of $^{87}Sr/^{86}Sr$ cluster around 0.7076. The samples forming this cluster show wider scatter in Pb isotope ratios than the Wanapum or Grande Ronde Basalt. Overall, the Saddle Mountains Basalt has higher values of $^{208}Pb/^{204}Pb$ and $^{207}Pb/^{204}Pb$ than the Grande Ronde and Wanapum Basalts. It also has generally lower values of $^{206}Pb/^{204}Pb$, although the Elephant Mountain, Lower Monumental, and Esquatzel Members have values that equal or exceed those of the Grande Ronde-Wanapum sequence. Values of $\varepsilon$Nd and $\delta^{18}O$ are fairly constant. Data for the following members of the Saddle Mountains Basalt plot at even higher values of $^{87}Sr/^{86}Sr$, with wide and generally uncorrelated scatter in the other isotopes: Lower Monumental, Esquatzel Asotin (Huntzinger flow only), Wilbur Creek, and Umatilla.

Data for additional analyzed flows are given in the appendix (tables 14–17), summarized in a manner similar to that of tables 1, 3–9, and 13.

### Comparison of Chemistry of Dikes and Flows

Major-oxide analyses of feeder dikes have been previously published (Wright and others, 1979, 1980, 1982). Limited trace-element data were obtained for representative dikes of several geochemical units (table 6). Most dikes are uniquely identifiable from both trace elements and major oxides and correlated with specific flows or several flows of similar chemistry. Although one study (Ross, 1983) has shown individual dikes to be chemically inhomogeneous, and another (Taubeneck, 1970) identified inclusions of country rock in many dikes, the data of table 6 show general agreement between analyses of dikes and the average chemistry of flows they fed. Exceptions are (1) the Grande Ronde Basalt, where ambiguity exists for dikes whose chemistry matches that of flows occuring at several different stratigraphic levels and (2) dikes that apparently did not reach the surface to feed a flow (for example, Fairview Bar dike of Ross, 1983; analyses 78-365 and 78-366 in table 2 of Wright and others, 1980). MgO variation diagrams (not shown) indicate no systematic differences in either MgO or other elements between flows and related dikes; all differences in composition are within the range of variation shown by the flows (Mangan and others, 1985; Wright, 1988) and the dikes (Wright, 1988).

## Glass Chemistry: Observations

Fresh sideromelane is common as selvedges on dikes, on partially palagonitized vent spatter, in water-quenched pillows, and in hyaloclastic debris. Glass is also infrequently preserved on chilled flow bases or unoxidized pahoehoe flow tops. We systematically collected fresh glass and prepared grain mounts for analysis by electron microprobe at the Smithsonian Institution (see Wright and others, 1979, 1980, 1982 for analyses and description of method). Uncorrected analyses are given in Wright (1988), grouped by stratigraphic unit and geochemical unit. For glass-rock pairs, the $Na_2O$ content (and, rarely, $K_2O$ content) of the glass is almost always lower than that of the bulk rock, a relation not possible in normal basaltic crystallization. We ascribe this anomalous relation either to hydration and leaching during the first stage of palagonitization or to loss of sodium during electron bombardment (Rutherford and others, 1985). In rare instances $K_2O$, $Na_2O$, or both may have been added to the glass. Helz (1978) did not find a similar discrepancy in her study of the Ice Harbor Member, perhaps because she worked only with polished thin sections and analyzed only the freshest glass.

We adjusted the $Na_2O$ content of glass for each geochemical unit according to preliminary petrologic mixing calculations, which match the bulk rock with phenocrysts plus glass using a representative set of phenocryst compositions (R.T. Helz, unpublished data). In practice we added less than 0.5 percent $Na_2O$ to each glass average to bring the $Na_2O$ in the glass to about 0.1–0.2 percent higher than that of the corresponding rock. The adjusted data, normalized to 100 percent, and the corresponding rock chemistry are tabulated in tables 10–12 and plotted in figure 8. These glass-rock pairs demonstrate chemical trends expected from phenocryst-related, low-pressure crystallization.

The glass-rock trends of figure 8 differ systematically from the trends defined by the bulk composition of rocks in the same formation, defined by the trends of figure 4. This is particularly evident on plots of MgO against CaO and $Al_2O_3$ for the Grande Ronde Basalt (fig. 8*A*). A similar observation can be made for the Wanapum (fig. 8*B*) and the Saddle Mountains (fig. 8*C*) Basalts, although the bulk-rock trends are not as closely defined as for the Grande Ronde Basalt.

## DISCUSSION: IMPLICATIONS FOR THE ORIGIN OF THE YAKIMA BASALT SUBGROUP

In this section we use information of many kinds to address the fundamental questions of the melting, storage, and mechanics of eruption of the flood basalts of the Yakima Basalt Subgroup. These include the development of a basin to hold the basalt, evolution of a tectonic setting in which rapid eruption of large volumes of basalt could be realized, and the nature of source regions and storage areas consistent with the eruptive history, chemistry, and petrology of the basalts. We draw on information gained from the following: field mapping, stratigraphic study and age dating, geochemical study of the Yakima Basalt Subgroup, and tectonic history of the Pacific Northwest.

### Emplacement of Flows

Geologic mapping combined with the chemical data presented in this paper provide insights into the nature of the eruptions that produced the Yakima Basalt Subgroup. Most eruptions were in the eastern part of the province (fig. 3) and fed flows that moved westward down a gentle paleoslope estimated to have been about 1:1,000. Although ongoing subsidence beneath the central Columbia Plateau near Pasco (fig. 1) temporarily reversed the slope in the western part of the province, the largest flows, which have volumes exceeding 500 $km^3$, traveled across the Pasco Basin and ponded against the opposed slope of the rising Cascade Range. Smaller eruptions produced flows of local extent that traveled only a few kilometers from their source. Some of these flows (for example, the basalts of Dodge and Robinette Mountain of the Eckler Mountain Member; the Ice Harbor Member) were confined to shallow grabens parallel to their vent systems. Emplacement of the voluminous flows was virtually instantaneous, as evidenced by (1) flat upper flow surfaces, which, together with columnar jointing, indicate ponding of a fluid, and (2) similar crystallinity of dike selvedges and basaltic pillows in the same unit separated by 100 km or more (see Shaw and Swanson, 1970; unpub. data of C.A. Hodges for internal dikes in the Roza Member of the Wanapum Basalt—see Hodges, 1978; data of Mangan and others, 1985, 1986, p. 1317 for the Grande Ronde Basalt). Shaw and Swanson (1970) estimated eruption rates as high as 1 $km^3/d$ per kilometer of fissure length for the Roza Member. Our mapping and the studies of Swanson and others (1975b) and Mangan and others (1986) are consistent with this figure for the Roza and demonstrate similar relations for large flows of the Grande Ronde Basalt and flows of the Priest Rapids Member of the Wanapum Basalt. We do not know the source dikes for many of the Saddle Mountains units, but we assume from the widespread distribution of the flows that eruption rates were similar to those of the older units.

Eruption rates for the localized flows were probably less than those for the plateau-covering units but still high, as indicated by the absence of thickening of units toward their vents. The viscosities of the flows, calculated from their chemistry (Shaw, 1972), are comparable to or higher than those calculated for basalts of Kilauea, known to form shields or to build up the rift zones in the vicinity of their source vents. Therefore the rates of eruption for all but the least voluminous flows are inferred to be higher for the Yakima Basalt Subgroup, in order to produce ponded flows even at distances of only a few kilometers.

Swanson and others (1975b) emphasized that, although instantaneous eruption rates (discharges) were very high, the average rate at which magma was generated to supply the flows of the Yakima Basalt Subgroup need not have been particularly high. This supply rate for the period of maximum activity (obtained by dividing the total volume of the Grande Ronde and Wanapum Basalts by the length of time during which eruptions occurred) is about 0.075 $km^3/yr$, close to the magma supply rate of 0.1 $km^3/yr$ currently estimated for Kilauea (Swanson, 1972). If the supply rate is equated with the melting rate in the mantle, then magma that fed the most voluminous individual flows in the Yakima Basalt Subgroup required 5,000–20,000 yr to accumulate before eruption.

### Magma Storage Before Eruption

The most voluminous flows in the Yakima Basalt Subgroup have volumes comparable to those of large eruptions of ash-flow tuff, yet no evidence exists for surface deformation in the form of calderas associated with vent areas. Evidence is also lacking for the existence of discrete volcanic centers or of rhyolites, both of which are associated with basaltic provinces known to have crustal magma reservoirs (for example, Iceland and the Snake River Plain). Deformation broadly contemporaneous with volcanism took place in the western part of the Columbia Plateau (compressional folding; Reidel, 1984), the central part (shallow basining), and the eastern part (formation of complex faulted basins; Hooper and Camp, 1981).

Evidence is not convincing, however, that this deformation is directly or specifically connected with large eruptions. Therefore the observations favor magma storage at deep crustal or subcrustal depths.

In general the chemical variations within the Yakima Basalt Subgroup do not fit simple phenocryst-related fractionation in shallow reservoirs (that is, total pressure ≤200 MPa, depth ≤6 km). Stratigraphically adjacent units do not show a simple chemical relation to one another, in terms of either bulk-rock chemistry or glass-rock trends. Aphyric and porphyritic flows within the same stratigraphic unit (for example, the Frenchman Springs Member or the basalt of Dodge of the Eckler Mountain Member) are chemically identical, a relation that seems to deny the possibility of crystal accumulation. Incompatible-element enrichments vary greatly with either decreasing MgO or increasing Th, inconsistent with low-pressure crystallization of olivine, pyroxene, and plagioclase. In general, Cs, Rb, $K_2O$, and Th show enrichment of as much as twice that shown by Hf, Zr, La, Ta, and $P_2O_5$ for a given decrease in MgO (fig. 4). All these observations contrast with those from basalt erupted in ocean-ridge and oceanic-island settings, where abundant evidence exists of shallow crystal fractionation and accumulation superimposed on chemical variation related to deeper processes.

One reviewer of this paper (J. Pallister) pointed out that the chemical data plot near the low-pressure cotectic in the simplified basalt system and suggested that this is evidence for crustal storage. However, this relation does not prove crustal storage; most basalts with fairly low MgO will plot near the low-pressure cotectic in the simplified basalt system, irrespective of their origin.

The chemical variations thus are not consistent with simple crystal fractionation at low pressure. They do not, however, prove the complete absence of crustal storage, because more complex models of crystallization combined with assimilation or replenishment of melt might satisfactorily explain the chemical data. For example, Helz (1978, 1980) has shown that some of the basalt in the Ice Harbor Member experienced intracrustal storage (pressure 350 MPa, depth 10 km). Of the large-volume flows, the Pomona Member is the only one that might have undergone crustal storage, because its phenocryst assemblage is similar to that of the basalt of Martindale of the Ice Harbor Member studied by Helz (1978).

Finally, there is evidence for sulfur saturation of magma in storage. Compatible behavior of sulfophile elements, particularly Cu, implies the existence at near-liquidus temperatures of an immiscible sulfide liquid in much magma of the Yakima Basalt Subgroup (see also Skinner and Peck, 1969). The former existence of such liquid has been confirmed by the identification of spherical blebs of crystalline sulfides found during electron microprobe traverses across dike selvedges (R.T. Helz, unpub. data).

## Nature of the Source Mantle

### Inferences Based on Geochemical Data

The following geochemical observations need to be explained in any satisfactory model of magma generation for the Yakima Basalt Subgroup. In themselves they also provide some limitations on the chemistry and mineralogy of the source mantle.

1. MgO and CaO are correlated with a slope of about 1.2 for all formations in the Yakima Basalt Subgroup. This correlation holds independent of other chemical variations (fig. 4). Helz (1978, p. 211) pointed out that this ratio matches that in clinopyroxene over a considerable range of pressure and is also typical of melt increments derived from partial melting of clinopyroxene-rich sources. That Sc also varies with CaO is consistent with clinopyroxene fractionation. Therefore we propose, following Helz (1978), that the magma of the Yakima Basalt Subgroup equilibrated with clinopyroxene at some stage in its history.
2. Chondrite-normalized REE patterns are enriched in light rare earths and are concave upward. The La/Yb ratio is relatively low (4–5.5) and fairly uniform in the Grande Ronde Basalt, most of the Wanapum Basalt, and many members of the Saddle Mountains Basalt. The shape of the rare-earth patterns and, as with the CaO/MgO ratio, the similarity of all rare-earth patterns independent of other chemical variations are consistent with equilibration with clinopyroxene either as a melting residue or during storage. The absence of high values of the La/Yb ratio and of significant negative europium anomalies disallow the presence of garnet or plagioclase as significant residual or fractionating phases, assuming that the source and storage regions were not subjected to unusually high oxygen fugacities.
3. Each formation boundary involves significant chemical changes that reflect changes in the melting regime.
    a. Grande Ronde-Wanapum.

       The Frenchman Springs, Roza, and Priest Rapids Members represent a major shift to magma with less $SiO_2$, more FeO and $TiO_2$, and higher content of incompatible elements when compared at the same MgO content. The shift in major-oxide chemistry occurred over a short time interval (within one magnetic polarity epoch). The Eckler Mountain Member is a transition unit; it shows slight trace-element enrichment but retains a chemistry characterized by high $SiO_2$ and low FeO and $TiO_2$, similar to that of the underlying Grande Ronde Basalt.

       Isotopic ratios remain the same across the Grande Ronde-Wanapum boundary. Values of $^{87}Sr/^{86}Sr$ (fig. 7) are 0.7043–0.7055 for the Grande

Ronde Basalt and 0.7049–0.7055 for the Wanapum. The aggregate volume of the Wanapum Basalt is about 7 percent that of the Grande Ronde Basalt (Tolan and others, 1987). The length of time during which eruptions occurred is too poorly known, within the limitation of present K-Ar ages, to prove that the supply rate changed across this boundary. The overall magma production rate may have begun to decrease in Wanapum time (see Hooper, 1982, fig. 2), whereas the discharge during individual eruptions of plateau-covering flows remained about the same as in Grande Ronde time.

b. Wanapum-Saddle Mountains.

A major time break separates the last Wanapum and first Saddle Mountains eruptions, a break sufficiently long to allow the cutting of canyons in the older formations. The magma production rate decreased markedly as the time between eruptions increased, and large-volume flows of the Saddle Mountains Basalt were transported westward through deep canyons and shallow valleys cut in older formations.

A major chemical break also coincides with the Wanapum-Saddle Mountains boundary. The $^{87}Sr/^{86}Sr$ ratio jumps to over 0.707 for several Saddle Mountains units of otherwise diverse major-oxide and trace-element chemistry and widely separated vent systems. Some units have extremely high $^{87}Sr/^{86}Sr$, as high as 0.715. Major-oxide chemistry of many units is similar to that of the Wanapum or Grande Ronde Basalt. Most trace elements are enriched, particularly P, Zr, Hf, Ta, Y, and Nb; K, Cs, and Rb are not as enriched and may in some cases be depleted relative to earlier geochemical units having similar major-oxide chemistry.

The chemical variations in the Yakima Basalt Subgroup cannot all be explained within a common mantle source. Rather, we postulate that the chemical changes seen at formation boundaries indicate significant changes in the mantle source for the magma.

4. Tectonic classification of geochemical units.

Rocks of the Yakima Basalt Subgroup are inconsistently classified on the many published diagrams that use major-oxide or trace-element chemistry to infer tectonic setting. We classified the rocks using the following sources:

a. Pearce and Cann (1973, figs. 3 and 4): Zr-Ti/100-Y; Zr-Ti/100-Sr/2; categories are calc-alkaline basalt (CAB), low-potassium tholeiite (LKT), within-plate basalt (WPB), and ocean-floor basalt (OFB).
b. Pearce and others (1977, fig. 1): MgO-FeO*-$Al_2O_3$; categories are ocean island (OI), ocean-ridge and floor (ORF), continental (C), orogenic (O), and spreading-center island (SCI).
c. Wood (1980, fig. 1): Th-Hf/3-Ta; categories are N-type MORB (NOF), E-type MORB including tholeiitic within-plate basalt (EOF-WPT), alkaline within-plate (AWPT), and destructive plate-margin (DPM).

Results of the classification are shown in the following table: (–, units that plot outside of the classification boundaries):

| Formation<br>Member | Classification | | | |
|---|---|---|---|---|
| | a (fig. 3) | a (fig. 4) | b | c |
| Grande Ronde Basalt | Mostly WPB, some CAB,OFB | Mostly OFB,CAB | C | All DPM |
| Wanapum Basalt | | | | |
| Priest Rapids | WPB | OFB | C | DPM |
| Roza | WPB | OFB | C | DPM |
| Frenchman Springs | WPB | OFB | C | DPM |
| Eckler Mountain | CAB,WPB,OFB | OFB,LKT-CAB | C,ORF(ROBIN) | DPM,WPT (ROBIN) |
| Saddle Mountains Basalt | | | | |
| Lower Monumental | WPB | OFB | C | – |
| Ice Harbor | CAB(GOOSE),WPB | (GOOSE),OFB | OIB | WPT |
| Buford | WPB-CAB | OFB | C | DPM |
| Elephant Mountain | WPB | OFB | C | DPM |
| Pomona | WPB | OFB | OIB-ORF | DPM |
| Esquatzel | WPB | OFB | C | DPM |
| Weissenfels Ridge | WPB-OFB | OFB | OIB,C,ORF | WPT |
| Asotin | WPB-OFB | OFB | OIB-ORF | DPM |
| Wilbur Creek | CAB | CAB | C | DPM |
| Umatilla | – | – | SCI | DPM |

The most consistent discrimination is that on the basis of major oxides using classification b (Pearce and others, 1977), which identifies most of the basalt units as belonging to a continental setting. The classification of Wood (1980) is apparently the least consistent with the known tectonic setting, for most of the units are classified as basalt associated with a destructive plate margin. This inconsistency was also noted by Prestvik and Goles (1985). These tabulations demonstrate the difficulty in blindly using chemistry to infer tectonic setting. However, the apparent failure of the classifications may be not so much a negation of the method as an indication of the mixed nature of the source regions for the Yakima Basalt Subgroup. The tectonic history of the area presently occupied by the Yakima Basalt Subgroup is complex, and the problems of classification may be related to chemical signatures inherited from a source region composed of continental, oceanic, and subducted components.

#### Inferences Based on the Tectonic History

The source region for the Yakima Basalt Subgroup may be further delimited by consideration of the following:

1. History of plate interactions at the western edge of the North American continent.

   Hamilton and Myers (1966) suggested that the Idaho batholith and the Sierra Nevada batholith were once a continuous coastal plutonic belt, later disrupted by Tertiary extension, that formed a major basin in back of the zone of continued subduction, now represented by the Cascade Range. Consistent with this is the oceanic character of pre-Tertiary rocks exposed beneath the eastern margin of the Columbia Plateau (Vallier, 1977). Additional evidence for the existence of a back-arc basin in Tertiary time is summarized by Eaton (1984 and references cited there). The north-northwest-trending zone of linear vent systems for the Yakima Basalt Subgroup is on the northward extension of the Northern Nevada rift in the Basin and Range province to the south (Zoback and Thompson, 1978). Eaton (1984, p. 292) suggests that at the beginning of plateau volcanism about 17 Ma, shallow crustal faulting in the Basin and Range to the south gave way to wholesale lithospheric rifting to the north.

   The fact that most of the presently exposed dikes of the Yakima Basalt Subgroup lie west of the pre-Tertiary continental margin implies that oceanic crust and mantle are likely to have formed a significant part of the source region for the lava. Westward migration of the continental margin provided in addition a continental component of mantle and crust to the sources for the Yakima Basalt Subgroup, particularly for the Saddle Mountains Basalt.

2. The record of paleomagnetic rotations in the Tertiary rocks of the Pacific Northwest.

   The paleomagnetic history records block rotations in front of the back-arc basin (Simpson and Cox, 1977; Beck, 1980; Beck and Plumley, 1980; Magill and Cox, 1981; a recent summary is by Fox and Beck, 1985). These may have contributed to the complex distribution of oceanic crust and mantle in the source area for the basalt (see also Heller and Ryberg, 1983). The tectonic history therefore is consistent with the existence of a complexly heterogeneous source region for the Yakima Basalt Subgroup.

3. The present mantle structure beneath the Columbia Plateau.

   The mantle structure has been recently reevaluated using a variety of geophysical methods. The depth to the Moho has been determined to be 40 km using seismic refraction methods (Catchings and others, 1984; Catchings and Mooney, 1988), an increase from the earlier value of 30 km obtained by Hill (1972). The higher value agrees with analysis of teleseismic *P*-wave arrivals (Michaelson and Weaver, 1986, fig. 10). Michaelson and Weaver's data also identify an east-dipping high-velocity zone extending well into the mantle at least as far east as the central plateau; they interpret this zone as the subducting Juan de Fuca plate. Catchings and Mooney (1988) consider the deep crustal and upper mantle structure beneath the central Columbia Plateau to be complex and atypical of normal deep continental crust.

We conclude that the complex chemical variation within the Yakima Basalt Subgroup is related to the presence of the following types of material in the source region: depleted oceanic mantle, subducted oceanic crust, original continental mantle, and old continental crust.

## SUMMARY AND SYNTHESIS: MAGMA GENERATION, STORAGE, AND ERUPTION OF THE YAKIMA BASALT SUBGROUP

### Previous Hypotheses

Discussion of the origin of the Yakima Basalt Subgroup requires an explanation for (1) the extremely high extrusion rates and large flow volumes characterizing the eruptions of flood basalt and (2) the chemical variation and petrographic character of the flows making up the Yakima Basalt Subgroup.

The earliest paper to discuss the distinctive character of flood basalt eruptions was by Shaw and Swanson (1970), who demonstrated the necessity for individual lava flows to be erupted at rates several orders of magnitude higher than those historically observed in active volcanic areas. They did not, however, address the ultimate cause of such high eruption rates. Swanson and others (1975b) showed that the magma supply rate during Grande Ronde Basalt time (the time of maximum activity) was actually not excessive compared to that of other basaltic provinces characterized by lower discharge rates for individual eruptions. This finding indicates that the distinctive origin of flood basalts is related to the mechanics of storage and extrusion rather than to unusual conditions accompanying melting. Cox (1980) provided a general model for the origin of flood basalts that involved emplacement of thick sills at the crust-mantle boundary and occasional release of magma to the surface through deep crustal fractures; in this model the magma is erupted at high rates because of the high differential pressure that results when the lower lithosphere is fractured.

The earliest statement regarding the petrogenesis of the basalts was made by Waters (1961, p. 583), who concluded that the different units of the then-named Columbia River Basalt were "products from separate magmatic hearths, and not differentiates of a hypothetical uniform magma." Many years later, McDougall (1976) postulated that the basalt was produced by partial melting of the upper mantle following diapiric upwelling of a peridotite having low to moderate water content. He further postulated that the basalt underwent extensive olivine fractionation and some crustal contamination at low pressures before eruption in an extensional environment analagous to that of a back-arc basin. Thompson (1977; see also Thompson and others, 1983) also postulated formation of the basalt in a back-arc basin and pointed out that subducted oceanic crust could not be ruled out in considering the petrogenesis. Helz (1978) was the first worker to develop a comprehensive model for the origin of the Ice Harbor Member (of the Saddle Mountains Basalt). She postulated that the four types of basalt in the member represented separate partial melting events in a mantle source dominated by clinopyroxene. The immediate source regions for two of the basalt types (basalt of Basin City and basalt of Goose Island) were at pressures greater than 1 GPa, and the mechanism of magma release was considered to be deep continental rifting. The other two units (basalt of Martindale and basalt of Indian Memorial) underwent brief storage at crustal levels (pressures of 300–400 MPa) before erupting to the surface. This model was extended to discuss the origin of the entire Yakima Basalt Subgroup (Helz and Wright, 1982, 1987), particularly regarding the need for a pyroxene-rich source. A metasomatic event was postulated to have preceded the first eruption of the Saddle Mountains Basalt. Helz (1978, p. 215) also made a detailed criticism of the model of Thompson (1977) and showed that many of Thompson's assumptions did not fit the field evidence or chemical data.

Cox (1980), in his general model for flood-basalt genesis, postulated a peridotite source, a picritic primary magma, and extensive fractionation of olivine, augite, and plagioclase to produce the observed flood-basalt sequences around the world. He did not specifically infer the origin of the Columbia River Basalt, but his model agrees with the earlier specific model of McDougall (1976).

Duncan (1982) proposed that eruptions of the Columbia River Basalt Group were triggered by a hot spot that is presently located beneath Yellowstone and which he inferred to have previously formed an oceanic volcanic lineament in early Tertiary time. Duncan related late Eocene and Oligocene volcanism in the Coast Range, Miocene volcanism on the Columbia Plateau, and the basalt of the Snake River Plain and Yellowstone to westward migration of the North American plate over this hot spot.

Reidel (1983) accepted the idea that a pyroxene-rich mantle produced melts of the Grande Ronde Basalt that were stored and partly crystallized in deep crustal storage areas. He explained the chemical character of the Grande Ronde Basalt by discontinuous mixing of freshly melted magma with previously stored magma undergoing fractionation of plagioclase, augite, and olivine.

Hooper (1984) postulated large (>700 km$^3$) storage reservoirs near the crust-mantle boundary as a source for the more voluminous units of the Columbia River Basalt Group. He accepted Cox's (1980) idea that primary magma was melted from a peridotite source and that subsequent fractionation of olivine, augite, and plagioclase yielded the fundamental chemical character of the basalt. Hooper also recognized the need for crustal assimilation in an open replenished magma system and for a metasomatic component to explain some of the chemical variation.

Carlson and others (1981) and Carlson (1984a, b) have provided a comprehensive model for the origin of the Columbia River Basalt Group through analyses of four isotopic series: Sr, Nd, Pb, and O. Carlson's work builds on earlier studies by McDougall (1976), DePaolo and Wasserburg (1979), Nelson (1983), and Church (1985). Carlson's model combines initial mantle heterogeneity with fractionation and crustal contamination to explain the isotopic data. He interprets the chemistry of the Yakima Basalt Subgroup in terms of interaction of at least four end members: (C1) mantle depleted in incompatible-elements, (C2) mantle contaminated by subducted oceanic sediment, (C3) metasomatically enriched subcontinental lithosphere, and (C4) upper crust.

Isotopic values for these end members are tabulated below (Carlson, 1984a, table 4) and plotted in figure 7 using symbols 1, 2, 3, and 4, respectively.

| | C1 | C2 | C3 | C4 |
|---|---|---|---|---|
| $^{87}Sr/^{86}Sr$ | 0.7035 | 0.7038 | 0.7076 | 0.715 |
| εNd | +6.5 | +4.5 | –6.0 | –30.0 |
| $^{206}Pb/^{204}Pb$ | 18.77 | 19.09 | 18.66 | 17.0 |
| $^{207}Pb/^{204}Pb$ | 15.51 | 15.65 | 15.65 | 15.52 |
| $^{208}Pb/^{204}Pb$ | 38.28 | 28.73 | 39.44 | 38.5 |
| $\delta^{18}O$ | +5.6 | +6.1 | +5.8 | +14.0 |

We consider Carlson's model to provide a good framework within which to examine the Yakima Basalt Subgroup, but we recognize the difficulties in reconciling quantitatively the isotopic data with the major-oxide and trace-element chemistry.

## Synthesis

We favor a model emphasizing the following points:

1. Following Cox (1980) we postulate storage of Yakima Basalt Subgroup melt in large sill-like reservoirs at the base of the crust (about 40 km deep and at 1.2 GPa pressure). If these storage reservoirs were located directly beneath the longest linear vent systems, and if their volumes were made equal to that of a representative large-volume flow, minimum dimensions of the stored magma body would be 150 by 15 by 0.5 km. The 40-km depth would provide the energy for eruption to the surface when the crust was disrupted by deep continental rifting; draining of such deep sills during flood-basalt eruptions would not be likely to produce significant surface deformation. At the estimated magma supply rate of 0.075 km$^3$/yr (Swanson and others, 1975b), such reservoirs would take 10,000–20,000 yr to accumulate magma for the largest eruptions. Presumably, smaller eruptions would tap reservoirs that were at an earlier stage of development after only a few hundreds or thousands of years of magma accumulation. These estimates are minimum values because we do not know what percentage of magma in storage actually was erupted.
2. Little evidence exists for fractionation of olivine, augite, and plagioclase, as postulated in the Cox (1980) and Hooper (1984) models. Helz's (1978) experimental results on the Ice Harbor Member show olivine to be barely on the liquidus at high pressure for compositions more magnesian and less silicic than most of the large-volume flows. The basalt flows are characterized by small negative europium anomalies that are not, however, correlated with MgO content, degree of incompatible-element enrichment, total rare-earth content, or other possible indicators of fractionation or degree of melting. Thus we do not interpret the presence of the europium anomalies as caused by extensive plagioclase fractionation. The shape of rare-earth patterns, their near parallelism in all units of the Yakima Basalt Subgroup, and the CaO-MgO coherence are also consistent with the evidence against extensive plagioclase fractionation and argue for melt in equilibrium with clinopyroxene and probably derived from a pyroxene-rich source. Possibly, however, picritic melt was produced initially, and ultramafic cumulate contributed to the process of underplating the lithosphere (see below) after ponding of less mafic magma at the base of the lithosphere. This hypothesis requires a significantly higher magma production rate than that estimated from the eruption rates given above.

   Our inference that the magma was primary melt from a pyroxene-rich mantle is made on the basis of the extremely large volume of olivine-rich primary magma that would be required to produce such large volumes of uniform magma, as well as on the absence of any olivine-controlled (picritic) flows in the Yakima Basalt Subgroup. This inference has received support from high-pressure experiments conducted by E. Takahashi, who postulates (Takahashi, 1988) that the chemical trends in the Grande Ronde Basalt are consistent with a high and varying degree of partial melting from a source chemically similar to midocean-ridge basalt at a pressure of 2.25 GPa corresponding to a depth of 70 km. These data are consistent with the model presented by Helz and Wright (1987).
3. Continental crustal underplating (Lachenbruch and Sass, 1978; Furlong and Fountain, 1986) is attractive as a mechanism to explain both the seismic velocity structure and the presence of large bodies of melt stored at the base of the lithosphere. Whether magma is released as flood basalt may depend critically on the tectonics of shallower regions. Lachenbruch and Sass (1978) show that rapid extension, as in the Basin and Range province in Nevada, results in emplacement of large quantities of basaltic magma within the lithosphere; this magma serves as a heat source for crustal melting and production of large-volume silicic melts. Slower extension, as across the Columbia Plateau, may allow deep crustal rifting to directly tap the basaltic magma emplaced at the base of the lithosphere, with little crustal interaction during transport to the surface.

The chemical and isotopic variations within each formation of the Yakima Basalt Subgroup are a function of small-scale source heterogeneity, as well as of differences in rate and degree of partial melting and interaction with continental crust; the latter processes are important only for certain units. The isotopic evidence for source heterogeneity and crustal interaction are neatly summarized by Carlson and others (1981) and Carlson (1984a). Major and abrupt changes in chemical composition at the top of the Eckler Mountain Member and the top of the Wanapum Basalt must, however, be ascribed to fundamental changes in the source composition, most likely owing to some form of metasomatism, as first suggested by Helz and Wright (1982) and amplified later (Helz and Wright, 1987).

Some units underwent a brief period of crustal storage, as for example the basalt of Martindale of the Ice Harbor Member (Helz, 1978, 1980). Of the large-volume units, the Pomona Member is the only one whose petrography indicates a period of crustal storage. Other members of the Saddle Mountains Basalt, such as the Lower Mounumental (source unknown but at least as far east as western Idaho), the Esquatzel (source unknown), and the Umatilla (source in southeasternmost Washington), must have had specific interaction, either melt-rock or rock-rock, with (Precambrian?) continental crust in order to explain their anomalous isotopic signatures.

Once eruption was initiated, most flows must have developed their present phenocryst assemblage near the surface or after ponding. Possibly some units were superheated on eruption, depending on the phase relations and on the rate of heat loss during transport to the surface. The presence of phenocrysts in dikes that fed porphyritic flows implies formation of those phenocrysts before eruption. However, even scattered large plagioclase phenocysts show no evidence of either concentration or flow orientation, so we infer that they could have formed in a turbulent environment just before eruption or after ponding.

Some flows have an unusual posteruption history. Hooper (1985) and Reidel and Fecht (1987) make compelling cases for the mixing of two independently generated magmas before and during eruption to the surface or after ponding or both. We have also determined that at least one thick flow of the Grande Ronde Basalt shows evidence of contemporaneous eruption and mixing in a single cooling unit of lava of mixed chemistry. The flows of the Roza Member show peculiar structures similar to ring dikes (Hodges, 1978). We have determined that the glassy selvages on these dikes have the same chemical composition as that of both the fresh sideromelane at Roza vents and the unpalagonitized pillow selvages where the Roza went into water far from its source. Hodges infers that these dikes originated from within the basalt, and we infer that they may have formed over areas where magma was being fed directly into an already ponded flow.

The structural evolution of the plateau was marked throughout the flood-basalt eruptions by uplift of the Rocky Mountains to the east and the Cascades to the west and subsidence of the area between. Eruptions of the Yakima Basalt Subgroup may have indirectly accelerated basining and other structural adjustments in the Columbia Plateau. The Grande Ronde and Wanapum flows having the largest volumes temporarily masked the deformation and formed a fairly flat surface of ponded basalt. The ancestral Columbia River system was antecedent to the Cascades and carried many of these flows beyond the Plateau to or near the Pacific Ocean (Tolan and others, 1984). The longer time intervals between eruptions of the Saddle Mountains Basalt allowed a more mature drainage to develop. By the beginning of Saddle Mountains time, the ancestral Snake-Clearwater system and most of its major tributaries had formed on the Plateau (Swanson and others, 1975a; Fecht and others, 1986; Waitt and Swanson, 1987). Flows of the Saddle Mountains Basalt were channeled, and some moved great distances, ponding against the rising Cascades. The Pomona Member is the only one that traversed both the ancestral Snake-Clearwater and Columbia River drainages, reaching the coast and pouring into the Pacifc Ocean (Tolan and others, 1984). The eruptions came to a gradual end; the last three events, of decreasing size, are dated at 10.5 Ma (Elephant Mountain Member), 8.5 Ma (Ice Harbor Member), and 6.0 Ma (Lower Monumental Member). Subsidence continued in the Pasco Basin through at least the Pliocene, until isostatic equilibrium was reestablished.

## REFERENCES CITED

Anderson, J.L., Beeson, M.H., Bentley, R.D., Fecht, K.R., Hooper, P.R., Niem, A.R., Reidel, S.P., Swanson, D.A., Tolan, T.L., and Wright, T.L., 1987, Distribution maps of stratigraphic units of the Columbia River Basalt Group, *in* Schuster, J.E., ed.: Selected papers on the geology of Washington: Washington Division of Geology and Earth Resources Bulletin 77, p. 183–195.

Basaltic Volcanism Study Project, 1981, Basaltic volcanism on the terrestrial planets: Elmsford, New York, Pergamon Press, 1286 p.

Beck, M.E., Jr., 1980, Paleomagnetic record of plate-margin tectonic processes along the western edge of North America: Journal of Geophysical Research, v. 85, p. 7115–7131.

Beck, M.E., Jr., and Plumley, P.W., 1980, Paleomagnetism of intrusive rocks in the Coast Range of Oregon: microplate rotations in middle Tertiary time: Geology, v. 8, p. 573–577.

Beeson, M.H., Fecht, K.R., Reidel, S.P., and Tolan, T.L., 1985, Regional correlations within the Frenchman Springs Member of the Columbia River Basalt Group: new insights into the middle Miocene tectonics of northwestern Oregon: Oregon Geology, v. 47, p. 87–96.

Bingham, J.W., 1970, Several probable source vents for the Roza and Priest Rapids type basalt in Whitman and Adams Counties, Washington, *in* Gilmour, E.H., and Stradling, Dale., eds., Proceedings of the Second Columbia River Basalt Symposium: Cheney, Eastern Washington State College Press, p. 171–172.

Camp, V.E., 1981, Geologic studies of the Columbia Plateau: Part II. Upper Miocene basalt distribution reflecting source locations, tectonism, and drainage history of the Clearwater embayment, Idaho: Geological Society of America Bulletin, v. 92, pt. I, p. 669–678.

Carlson, R.W., 1984a, Isotopic constraints on Columbia River flood basalt genesis and the nature of the subcontinental mantle: Geochimica et Cosmochimica Acta, v. 48, p. 2357–2372.

———1984b, Tectonic influence on magma composition of Cenozoic basalts from the Columbia River Plateau and Northwestern Great Basin, U.S.A., *in* Explosive volcanism: inception, evolution, and hazards: National Research Council Studies in Geophysics: Washington, D.C., National Academy Press, p. 23–33.

Carlson, R.W., Lugmair, G.W., and MacDougall, J.D., 1981, Columbia River volcanism: The question of mantle heterogeneity or crustal contamination: Geochimica et Cosmochimica Acta, v. 45, p. 2483–2499.

Catchings, R.D., and Mooney, W.D., 1988, Crustal Structure of the Columbia Plateau: evidence for Continental Rifting: Journal of Geophysical Research, v. 93, p. 459–474.

Catchings, R.D., Mooney, W.D., and Holbrook, W.S., 1984, Crustal structure of southeastern Washington from seismic refraction [abs.]: Eos, American Geophysical Union Transactions, v. 65, p. 988.

Choiniere, S.R., and Swanson, D.A., 1979, Magnetostratigraphy and correlation of Miocene basalts of the northern Oregon coast and Columbia Plateau, southeast Washington: American Journal of Science, v. 279, p. 755–777.

Church, S.E., 1985, Genetic interpretation of lead-isotopic data from the Columbia River Basalt Group, Oregon, Washington, and Idaho: Geological Society of America Bulletin, v. 96, p. 676–690.

Cox, K.G., 1980, A model for flood basalt volcanism: Journal of Petrology, v. 21, p. 629–650.

DePaolo, D.J., and Wasserburg, G.J., 1979, Neodymium isotopes in flood basalts from the Siberian Platform and inferences about their mantle sources: National Acadamy of Science Proceedings, v. 76, p. 3056–3060.

Duncan, R.A., 1982, A captured island chain in the coast range of Oregon and Washington: Journal of Geophysical Research, v. 87, p. 10,827–10,837.

Eaton, G.P., 1984, The Miocene Great Basin of western North America as an extending back-arc region: Tectonophysics, v. 102, p. 275–295.

Fecht, K.R., Reidel, S.R., and Tallman, A.M., 1986, Paleodrainage of the Columbia River system on the Columbia Plateau of Washington State—a summary: Rockwell Hanford Company, Richland, Washington, Document RHO–BWI–SA–318, 55 p.

Fox, K.F., Jr., and Beck, M.E., Jr., 1985, Paleomagnetic results for Eocene volcanic rocks from northeastern Washington and the Tertiary tectonics of the Pacific northwest: Tectonics, v. 4, p. 323–341.

Furlong, K.P., and Fountain, D.M., 1986, Continental crustal underplating: thermal considerations and seismic-petrologic consequences: Journal of Geophysical Research, v. 91, p. 8285–8294.

Glover, D.W., Malone, S.D., and Rohay, A.C., 1985, Crustal structure of the Columbia Basin, Washington, from borehole and refraction data [abs.]: Eos, American Geophysical Union Transactions, v. 66, p. 1361.

Hamilton, W.E., and Myers, W.B., 1966, Cenozoic tectonics of the western United States: Review of Geophysics, v. 4, p. 509–549.

Haskin, L.A., Haskin, M.A., Frey, F.A., and Wildman, T.R., 1968, Relative and absolute terrestrial abundances of the rare earths, *in* Ahrens, L.H., ed., Origin and distribution of the elements: New York, Pergamon Press, p. 889–912.

Heller, P.L., and Ryberg, P.T., 1983, Sedimentary record of subduction to forearc transition in the rotated Eocene basin of western Oregon: Geology, v. 11, p. 380–383.

Helz, R.T., 1978, The petrogenesis of the Ice Harbor Member, Columbia Plateau, Washington—a chemical and experimental study: University Park, Pennsylvania, Pennsylvania State University, Ph.D. dissertation, 284 p.

———1980, Chemical and experimental study of the Ice Harbor member of the Yakima Basalt Subgroup: evidence for intracrustal storage and contamination [abs.]: Eos, American Geophysical Union Transactions, v. 61, p. 68.

Helz, R.T., and Wright, T.L., 1982, Inferred petrology of the source of the Yakima Basalt subgroup: Abstracts submitted to the IAVCEI/IAGC scientific Assembly on the Generation of Major Basalt Types, Reykjavik, Iceland August 15–22, 1982 [unpag.].

———1987, A model for the origin of the Yakima Basalt Subgroup, NW USA [abs.]: Geological Society of America Abstracts with Programs, v. 19, no. 6, p. 388.

Hill, D.P., 1972, Crustal and upper mantle structure of the Columbia Plateau from long range seismic-refraction measurements: Geological Society of America Bulletin, v. 83, p. 1639–1648.

Hodges, C.A., 1978, Basaltic ring structures of the Columbia Plateau: Geological Society of America Bulletin, v. 89, p. 1281–1289.

Hooper, P.R., 1981, The role of magnetic polarity and chemical analyses in establishing the stratigraphy, tectonic evolution and petrogenesis of the Columbia River Basalt, *in* Subbarao, K.V., and Sukheswala, R.N., eds., Deccan volcanism and related basalt provinces in other parts of the world: Geological Society of India, Memoir 3, p. 362–376.

———1982, The Columbia River basalts: Science, v. 215, p. 1463–1468.

———1984, Physical and chemical constraints on the evolution of the Columbia River basalt: Geology, v. 12, p. 495–499.

———1985, A case of simple magma mixing in the Columbia River Basalt Group: The Wilbur Creek, Lapwai, and Asotin flows, Saddle Mountains Formation: Contributions to Mineralogy and Petrology, v. 91, p. 66–73.

Hooper, P.R., and Camp, V.C., 1981, Deformation of the southeast part of the Columbia River Plateau: Geology, v. 9., p. 323–328.

Hooper, P.R., and Swanson, D.A., in press, Columbia River Basalt Group and associated volcanic rocks in the Blue Mountain region, *in* Walker, G.W., ed., Cenozoic geology of the Blue Mountains region: U.S. Geological Survey Professional Paper 1437.

Irvine, T.N., and Baragar, W.R.A., 1971, A guide to the chemical classification of the common volcanic rocks: Canadian Journal of Earth Sciences, v. 8, p. 523–548.

Kleck, W.D., 1976, Chemistry, petrography, and stratigraphy of the Columbia River Group in the Imnaha Valley region, eastern Oregon and western Idaho: Pullman, Washington State University, Ph.D. dissertation, 203 p.

Lachenbruch, A.H., and Sass, J.H., 1978, Models of an extending lithosphere and heat flow in the Basin and Range province, *in* Smith, R.B., and Eaton, G.P., eds., Cenozoic tectonics and regional geophysics of the western Cordillera: Geological Society of America Memoir 152, p. 209–250.

Lingley, W.S., Jr., and Walsh, T.J., 1986, Issues related to petroleum drilling near the proposed high-level nuclear waste repository at Hanford: Washington Geologic Newsletter, v.

14, p. 10–19.

Magill, James, and Cox, Allan, 1981, Post-Oligocene tectonic rotation of the Oregon western Cascade Range and the Klamath Mountains: Geology, v. 9, p. 127–131.

Mangan, M.T., and Wright, T.L., 1984, Regional correlation of Grande Ronde Basalt flows, Columbia River Basalt Group [abs.]: Eos, American Geophysical Union Transactions, v. 65, p. 1153.

Mangan, M.T., Wright, T.L., Swanson, D.A., and Byerly, G.R., 1985, Major oxide, trace element, and glass chemistry pertinent to regional correlation of Grande Ronde Basalt flows, Columbia River Basalt Group, Washington: U.S. Geological Survey Open-File Report 85-747, 74 p.

———1986, Regional correlation of Grande Ronde Basalt flows, Columbia River Basalt Group, Washington, Oregon, and Idaho: Geological Society of America Bulletin, v. 97, p. 1300–1318.

McDougall, Ian, 1976, Geochemistry and origin of basalt of the Columbia River Group, Oregon and Washington: Geological Society of America Bulletin, v. 87, p. 777–792.

McKee, E.H., Hooper, P.R., and Kleck, W.D., 1981, Age of Imnaha Basalt—oldest basalt flows of the Columbia River Basalt Group, northwest United States: Isochron/West, no. 31, p. 31–33.

McKee, E.H., Swanson, D.A., and Wright, T.L., 1977, Duration and volume of Columbia River Basalt volcanism, Washington, Oregon, and Idaho [abs.]: Geological Society of America Abstracts with Programs, v. 9, p. 463–464.

Michaelson, C.A., and Weaver, C.S., 1986, Upper mantle structure from teleseismic *P*-wave arrivals in Washington and northern Oregon: Journal of Geophysical Research, v. 91, p. 209–250.

Nathan, Simon., and Fruchter, J.S., 1974, Geochemical and paleomagnetic stratigraphy of the Picture Gorge and Yakima Basalts (Columbia River Group) in central Oregon: Geological Society of America Bulletin, v. 85, p. 63–76.

Nelson, D.O., 1980, Strontium isotope and trace element geochemistry of the Saddle Mountains and Grande Ronde Basalts of the Columbia River Group: Corvallis, Oregon State University, Ph.D. dissertation, 224 p.

———1983, Implications of oxygen-isotope data and trace-element modeling for a large-scale mixing model for the Columbia River Basalt: Geology, v. 11, p. 248–251.

Pearce, J.A., and Cann, J.R., 1973, Tectonic setting of basic volcanic rocks determined using trace-element analysis: Earth and Planetary Science Letters, v. 19, p. 290–300.

Pearce, J.A., Gorman, B.E., and Birkett, T.C., 1977, The relationship between major element chemistry and tectonic environment of basic and intermediate volcanic rocks: Earth and Planetary Science Letters, v. 36, p. 121–132.

Prestvik, Tore, and Goles, G.G., 1985, Comments on petrogenesis and the tectonic setting of Columbia River basalts: Earth and Planetary Science Letters, v. 72, p. 65–73.

Price, S.M., 1974, A geochemical classification of dikes of the Grande Ronde Swarm, Columbia River Basalt: Atlantic Richfield Hanford Co., U.S. Atomic Energy Commission Report ARH–SA-202, 29 p.

Reidel, S.P., 1983, Stratigraphy and petrogenesis of the Grande Ronde Basalt from the deep canyon country of Washington, Oregon, and Idaho: Geological Society of America Bulletin, v. 94, p. 519–542.

———1984, The Saddle Mountains: the evolution of an anticline in the Yakima fold belt: American Journal of Science, v. 272, p. 870–893.

Reidel, S.P., and Fecht, K.R., 1987, The Huntzinger flow: evidence of surface mixing of the Columbia River Basalt and its petrogenetic implications: Geological Society of America Bulletin, v. 98, p. 664–677.

Ross, M.E., 1983, Chemical and mineralogic variations within four dikes of the Columbia River Basalt Group, southeastern Columbia Plateau: Geological Society of America Bulletin, v. 94, p. 1117–1126.

Rutherford, M.J., Sigirdsson, Haralder, Cary, Steven, and Davis, Andrew, 1985, The May 18, 1980, eruption of Mount St. Helens: 1. Melt composition and experimental phase equilibria: Journal of Geophysical Research, v. 90, p. 2929–2947.

Shaw, H.R., 1972, Viscosities of magmatic silicate liquids: an empirical method of prediction: American Journal of Science, v. 272, p. 870–893.

Shaw, H.R., and Swanson, D.A., 1970, Eruption and flow rates of flood basalts, *in* Gilmour, E.H., and Stradling, Dale., eds., Proceedings of the Second Columbia River Basalt Symposium: Cheney, Washington, Eastern Washington State College Press, p. 271–299.

Simpson, R.W., and Cox, Allan, 1977, Paleomagnetic evidence for tectonic rotation of the Oregon Coast Range: Geology, v. 5, p. 585–589.

Skinner, B.J., and Peck, D.L., 1969, An immiscible sulfide melt from Hawaii *in* Wilson, H.D.B., ed., Magmatic ore deposits: Economic Geology Monograph 4, p. 310–322.

Stanley, W.D., 1984, Tectonic study of Cascade Range and Columbia Plateau in Washington State based upon magnetotelluric soundings: Journal of Geophysical Research, v. 89, p. 4447–4460.

Swanson, D.A., 1972, Magma supply rate at Kilauea volcano, 1952–1971: Science, v. 175, p. 169–170.

Swanson, D.A., Anderson, J.L., Bentley, R.D., Byerly, G.R., Camp, V.E., Gardner, J.N., and Wright, T.L., 1979b, Reconnaissance geologic map of the Columbia River Basalt Group in eastern Washington and northern Idaho: U.S. Geological Survey Open-File Report 79-1363, 26 p., 12 map sheets, scale 1:250,000.

Swanson, D.A., Anderson, J.L., Camp, V.E., Hooper, P.R., Taubeneck, W.H., and Wright, T.L., 1981, Reconnaissance geologic map of the columbia River Basalt Group, northern Oregon and western Idaho: U.S. Geological Survey Open-file report 81-797, 33 p., 5 map sheets, scale 1:250,000.

Swanson, D.A., and Wright, T.L., 1981, The regional approach to studying the Columbia River Basalt, *in* Subbarao, K.V., and Sukheswala, R.N., eds., Deccan volcanism and related basalt provinces in other parts of the world: Geological Society of India, Memoir 3, p. 58–80.

Swanson, D.A., Wright, T.L., Camp, V.E., Gardner, J.N., Helz, R.T., Price, S.M., Reidel, S.P., and Ross, M.E., 1980, Reconnaissance geologic map of the Columbia River Basalt Group, Pullman and Walla Walla quadrangle, southeast Washington and adjacent Idaho: U.S. Geological Survey Miscellaneous Investigations Map I–1139, scale 1:250,000.

Swanson, D.A., Wright, T.L., and Clem, Richard, 1975a, Intracanyon flows of Yakima Basalt along the Snake River, southeast Washington [abs]: Geological Society of America Abstracts with Programs, v. 7, no. 5, p. 645.

Swanson, D.A., Wright, T.L., and Helz, R.T., 1975b, Linear vent systems and estimated rates of magma production and eruption for the Yakima Basalt on the Columbia River Plateau: American Journal of Science, v. 275, p. 877–905.

Swanson, D.A., Wright, T.L., Hooper, P.R., and Bentley, R.D., 1979a, Revisions in stratigraphic nomenclature of the Columbia River Basalt Group: U.S. Geological Survey Bulletin 1457–G, p. G1–G59.

Takahashi, Eiichi, 1988, High-pressure melting study on Columbia River basalts [abs.]: Eos, Transactions, American Geophysical Union, v. 69, p. 524.

Taubeneck, W.H., 1970, Dikes of Columbia River Basalt in northeastern Oregon, western Idaho, and southeastern Washington, *in* Gilmour, E.H., and Stradling, Dale, eds., Proceedings of the Second Columbia River Basalt Symposium: Cheney, Washington, Eastern Washington State College Press, p. 73–96.

———1978, Two new sources for Columbia River Basalt in western Idaho—The Slate Creek and Greer Dike Swarms [abs.]: Geological Society of America Abstracts with Programs, v. 10, p. 239–240.

———1980, Diatremes in Columbia River Basalt near the crest of the west escarpment of the Grande Ronde Graben, northeast Oregon [abs.]: Geological Society of America Abstracts with Programs, v. 12, no. 3, p. 155.

Thompson, R.N., 1977, Columbia/Snake River-Yellowstone magmatism in the context of western U.S.A. Cenozoic geodynamics: Tectonophysics, v. 39, p. 621–636.

Thompson, R.N., Morrison, M.A., Dickin, A.P., and Hendry, G.L., 1983, Continental flood basalts ... arachnids rule OK?, *in* Hawkesworth, C.J., and Norry, M.J., eds., Continental basalts and mantle xenoliths: Nantwich, England, Shiva Publishing Limited, p. 158–185.

Tolan, T.L., Beeson, M.H., and Vogt, B.F., 1984, Exploring the Neogene history of the Columbia River: Discussion and geologic field trip guide to the Columbia River Gorge. Part 1, Discussion: Oregon Geology, v. 46, no. 8, p. 87–97.

Tolan, T.L., Reidel, S.P., Beeson, M.H., Anderson, J.L., Fecht, K.R., and Swanson, D.A., 1987, Revisions to the areal extent and volume of the Columbia River Basalt Group (CRBG) [abs.]: Geological Society of America Abstracts with Programs, v. 19, no. 6, p. 458.

Vallier, T.L., 1977, The Permian and Triassic Seven Devils Group, western Idaho and northeastern Oregon: U.S. Geological Survey Bulletin 1437, 58 p.

Waitt, R.B., Jr., and Swanson, D.B., 1987, Geomorphic evolution of the Columbia Plain and River, p. 403–416 *in* Baker, V.R., Greeley, Ronald, Komar, P.D., Swanson, D.A., and Waitt, R.B., Jr., ch. 11 *in* Graf, W.L., ed, Geomorphic systems of North America: Boulder, Colorado, Geological Society of America, Centennial Special Volume 2, 643 p.

Walker, G.W., 1973, Contrasting compositions of the youngest Columbia River Basalt flows in Union and Wallowa Counties, northeastern Oregon: Geological Society of America Bulletin, v. 84, p. 425–430.

Ward, A.W., Jr., 1976, Petrology and chemistry of the Huntzinger flow, Columbia River Basalt, Washington: Atlantic Richfield Hanford Co., U.S. Atomic Energy Commission Report ARH–SA–272, 134 p.

Waters, A.C., 1961, Stratigraphic and lithologic variations in the Columbia River Basalt: American Journal of Science, v. 259, p. 583–611.

Watkins, N.D., and Baksi, A.K., 1974, Magnetostratigraphy and oroclinal folding of the Columbia River, Steens, and Owyhee Basalts in Oregon, Washington, and Idaho: American Journal of Science, v. 274, p. 148–189.

Wilkinson, J.F.G., 1986, Classification and average chemical composition of common basalts and andesites: Journal of Petrology, v. 27, p. 31–62.

Wood, D.A., 1980, The application of a Th-Hf-Ta diagram to establishing the nature of crustal contamination of basaltic lava of the British Tertiary province: Earth and Planetary Science Letters, v. 50, p. 11–30.

Wright, T.L., 1988, Chemical analyses of rocks and glasses used to compute average compositions for geochemical units in the Yakima Basalt Subgroup, Columbia River Basalt Group, Idaho, Oregon, and Washington: U.S. Geological Survey Open-File Report 88-263, 71 p.

Wright, T.L., Black, K.N., Swanson, D.A., and O'Hearn, Tim, 1980, Columbia River Basalt: 1978–1979 sample data and chemical analyses: U.S. Geological Survey Open-File Report 80-921, 99 p.

———1982, Columbia River Basalt: 1980–1981 sample data and chemical analyses: U.S. Geological Survey Open-File Report 82-532, 51 p.

Wright, T.L., Grolier, M.J., and Swanson, D.A., 1973, Chemical variation related to stratigraphy of the Columbia River Basalt: Geological Society of America Bulletin, v. 84, p. 371–386.

Wright, T.L., Swanson, D.A., Helz, R.T., and Byerly, G.R., 1979, Major oxide, trace element, and glass chemistry of Columbia River basalt samples collected between 1971 and 1977: U.S. Geological Survey Open-File Report 79-711, 160 p.

Zoback, M.L., and Thompson, G.A., 1978, Basin and Range rifting in northern Nevada: clues from a mid-Miocene rift and its subsequent offsets: Geology, v. 6, p. 111–116.

# TABLES 3–17; FIGURES 4–9

**Table 3.** Average chemical composition of geochemical units in the Grande Ronde Basalt

[Geochemical units listed in approximate stratigraphic order, see table 1; chemical types A-E are major types repeated throughout section, 1 and 2 are distinctively magnesian units of local extent, and X refers to all other Grande Ronde flows. Trace elements followed by X are analyzed by X-ray fluorescence; all others analyzed by instrumental neutron activation. n.a., not analyzed. Data from which these average compositions were calculated are given in Mangan and others (1985)]

| Geochemical unit-------- | 1A | 1A* | 3A | 3A | 3A | 3A | UNC | 4A | 4A | 4A* | 3B | LH2 | MG6 |
|---|---|---|---|---|---|---|---|---|---|---|---|---|---|
| Chemical type- | A | A | C | C | C | C | X | D | D | D | C | 1 | 2 |
| Major oxides (weight percent) | | | | | | | | | | | | | |
| $SiO_2$ | 54.58 | 54.53 | 53.53 | 53.65 | 54.09 | 53.71 | 54.52 | 54.52 | 53.83 | 53.99 | 53.66 | 53.80 | 51.52 |
| $Al_2O_3$ | 14.51 | 14.32 | 14.52 | 14.30 | 14.42 | 14.34 | 14.51 | 14.30 | 13.89 | 14.14 | 14.71 | 15.19 | 14.98 |
| FeO | 10.93 | 11.08 | 11.34 | 11.31 | 11.17 | 11.34 | 10.20 | 12.10 | 11.62 | 11.72 | 11.21 | 9.40 | 11.83 |
| MgO | 4.53 | 4.83 | 5.19 | 5.23 | 4.95 | 5.24 | 5.14 | 4.52 | 4.83 | 4.84 | 5.13 | 6.12 | 5.96 |
| CaO | 8.53 | 8.43 | 9.09 | 9.01 | 8.80 | 8.95 | 8.95 | 7.81 | 8.84 | 8.53 | 8.83 | 10.09 | 9.71 |
| $Na_2O$ | 2.84 | 3.04 | 2.81 | 2.84 | 2.81 | 2.91 | 2.89 | 2.83 | 2.88 | 3.00 | 2.77 | 2.88 | 2.76 |
| $K_2O$ | 1.42 | 1.32 | 1.02 | 1.04 | 1.18 | 1.10 | 1.13 | 0.97 | 1.32 | 1.22 | 1.31 | 0.69 | 0.60 |
| $TiO_2$ | 1.80 | 1.73 | 1.74 | 1.83 | 1.81 | 1.75 | 1.91 | 2.05 | 1.97 | 1.86 | 1.72 | 1.13 | 1.70 |
| $P_2O_5$ | 0.36 | 0.28 | 0.26 | 0.29 | 0.32 | 0.23 | 0.32 | 0.33 | 0.32 | 0.27 | 0.27 | 0.26 | 0.32 |
| MnO | 0.18 | 0.18 | 0.21 | 0.18 | 0.19 | 0.19 | 0.17 | 0.19 | 0.21 | 0.19 | 0.20 | 0.16 | 0.18 |
| Total | 99.68 | 99.74 | 99.71 | 99.68 | 99.74 | 99.76 | 99.74 | 99.62 | 99.71 | 99.76 | 99.81 | 99.72 | 99.56 |
| Trace elements (parts per million) | | | | | | | | | | | | | |
| Ba | 579 | 502 | 464 | 458 | 537 | 472 | 507 | 450 | 494 | 439 | 518 | 367 | 407 |
| BaX | 577 | 537 | 465 | 469 | 491 | 454 | 487 | 433 | 512 | 439 | 500 | n.a. | 0 |
| Co | 37.30 | 33.60 | 38.80 | 38.50 | 40.0 | 38.60 | 40.80 | 39.80 | 38.60 | 38.10 | 39.50 | 34 | 40.10 |
| Cr | 43.40 | 39.10 | 52.40 | 49.90 | 60 | 54.90 | 51 | 31 | 25.30 | 23.80 | 48.90 | 84.50 | 99.80 |
| Cs | 0.90 | 0.85 | 0.70 | 0.50 | 1.10 | 0.65 | 0.92 | 0.39 | 0.80 | 0.50 | 0.70 | n.a. | 0.43 |
| Hf | 4.14 | 3.70 | 3.70 | 4.05 | 3.97 | 3.85 | 4.03 | 3.81 | 4.10 | 3.90 | 3.80 | 2.77 | 3.20 |
| NbX | 11 | 13 | 11 | 13 | 16 | 11.50 | 12 | 12 | 15 | 14 | 12 | n.a. | 0 |
| Rb | 30.60 | 29.50 | 26.50 | 29 | 30 | 30.50 | 35.50 | 27 | 33 | 27 | 35.20 | 17.20 | 26.50 |
| RbX | 32.70 | 34.50 | 28 | 23 | 26 | 29.50 | 32 | 24 | 31 | 29 | 31 | 26 | 0 |
| SrX | 334 | 325 | 333 | 315 | 363 | 335 | 322 | 321 | 337 | 338 | 328 | 486 | 0 |
| Ta | 0.75 | 0.72 | 0.70 | 0.67 | 0.76 | 0.73 | 0.74 | 0.71 | 0.78 | 0.72 | 0.69 | 0.43 | 0.62 |
| Th | 4.19 | 3.60 | 3.20 | 3.60 | 3.66 | 3.40 | 3.53 | 3.22 | 3.79 | 3.60 | 3.63 | 1.85 | 2.38 |
| U | 1.10 | 1.05 | 0.80 | 0.88 | n.a. | 0.75 | 1.20 | n.a. | n.a. | 0.80 | 0.80 | n.a. | 0.90 |
| YX | 33.30 | 31 | 31 | 31 | 40 | 32 | 30 | 30 | 33 | 32 | 30 | 23 | 0 |
| Zn | 132 | 114 | 113 | 122 | 138 | 118 | 127 | 120 | 130 | 112 | 142 | 122 | 123 |
| Zr | 163 | 160 | 115 | 207 | n.a. | 135 | 150 | 213 | 144 | 76 | 200 | n.a. | 147 |
| ZrX | 170 | 167 | 158 | 157 | 175 | 158 | 164 | 157 | 173 | 164 | 161 | 119 | 0 |
| Sc | 34.50 | 31 | 36.30 | 37.20 | 36.70 | 37.80 | 37 | 36.10 | 36.80 | 35.20 | 37.10 | 36.80 | 38.30 |
| La | 22.10 | 18.50 | 18 | 19.40 | 20.80 | 19.50 | 19.90 | 18.10 | 20.40 | 19 | 20.10 | 15.60 | 16 |
| Ce | 43.20 | 38.50 | 35.50 | 38.80 | 43.10 | 38 | 38.80 | 36.30 | 39.90 | 37 | 40.20 | 30.90 | 32.30 |
| Nd | 26.60 | 24 | 20.50 | 23 | 23.70 | 22.50 | 24.50 | 28 | 27 | 23 | 23.50 | 18.40 | 21.30 |
| Sm | 6 | 5.30 | 5.10 | 5.40 | 6 | 5.60 | 5.60 | 5.70 | 5.90 | 5.20 | 5.60 | 4.30 | 3.80 |
| Eu | 1.61 | 1.57 | 1.58 | 1.59 | 1.81 | 1.64 | 1.62 | 1.42 | 1.66 | 1.57 | 1.69 | 1.25 | 1.44 |
| Gd | 5.30 | 5.30 | 6.20 | 6.30 | n.a. | 4.60 | 6.10 | 5.40 | 6.10 | 4.80 | 5.90 | n.a. | 4.80 |
| Tb | 0.96 | 0.84 | 0.84 | 0.95 | 1.10 | 0.90 | 0.98 | 0.90 | 0.85 | 0.82 | 1 | 0.77 | 0.78 |
| Yb | 3.13 | 2.90 | 3.15 | 3.30 | 3.12 | 3.25 | 3.17 | 3.03 | 3.20 | 3.10 | 3.12 | 1.93 | 2.90 |
| Lu | 0.52 | 0.43 | 0.47 | 0.47 | 0.56 | 0.48 | 0.49 | 0.51 | 0.52 | 0.46 | 0.51 | 0.41 | 0.41 |
| Cu | 31.30 | 29.50 | 36 | 34 | n.a. | 34 | 36 | 36 | 28 | 28 | 33 | n.a. | 0 |
| Ni | 15.70 | 10.50 | 18 | 14 | n.a. | 15.50 | 16 | 17 | 16 | 8 | 14 | n.a. | 0 |
| Normalized major-oxide contents (weight percent) | | | | | | | | | | | | | |
| $SiO_2$ | 54.76 | 54.67 | 53.69 | 53.82 | 54.23 | 53.84 | 54.66 | 54.73 | 53.99 | 54.12 | 53.76 | 53.95 | 51.75 |
| $Al_2O_3$ | 14.56 | 14.36 | 14.56 | 14.35 | 14.46 | 14.37 | 14.55 | 14.35 | 13.93 | 14.17 | 14.74 | 15.23 | 15.05 |
| FeO | 10.97 | 11.11 | 11.37 | 11.35 | 11.20 | 11.37 | 10.23 | 12.15 | 11.65 | 11.75 | 11.23 | 9.43 | 11.88 |
| MgO | 4.54 | 4.84 | 5.21 | 5.25 | 4.96 | 5.25 | 5.15 | 4.54 | 4.84 | 4.85 | 5.14 | 6.14 | 5.99 |
| CaO | 8.56 | 8.45 | 9.12 | 9.04 | 8.82 | 8.97 | 8.97 | 7.84 | 8.87 | 8.55 | 8.85 | 10.12 | 9.75 |
| $Na_2O$ | 2.85 | 3.05 | 2.82 | 2.85 | 2.82 | 2.92 | 2.90 | 2.84 | 2.89 | 3.01 | 2.78 | 2.89 | 2.77 |
| $K_2O$ | 1.42 | 1.32 | 1.02 | 1.04 | 1.18 | 1.10 | 1.13 | 0.97 | 1.32 | 1.22 | 1.31 | 0.69 | 0.60 |
| $TiO_2$ | 1.81 | 1.73 | 1.75 | 1.84 | 1.81 | 1.75 | 1.91 | 2.06 | 1.98 | 1.86 | 1.72 | 1.13 | 1.71 |
| $P_2O_5$ | 0.36 | 0.28 | 0.26 | 0.29 | 0.32 | 0.23 | 0.32 | 0.33 | 0.32 | 0.27 | 0.27 | 0.26 | 0.32 |
| MnO | 0.18 | 0.18 | 0.21 | 0.18 | 0.19 | 0.19 | 0.17 | 0.19 | 0.21 | 0.19 | 0.20 | 0.16 | 0.18 |
| Total | 100.00 | 100.00 | 100.00 | 100.00 | 100.00 | 100.00 | 100.00 | 100.00 | 100.00 | 100.00 | 100.00 | 100.00 | 100.00 |

**Table 3.** Average chemical composition of geochemical units in the Grande Ronde Basalt—*Continued*

| Geochemical unit-------- | 2B | 5A | 5A | 5A | 5A | 5A* | 2C | 2C | 5B | 3C | 3C | 3C* | |
|---|---|---|---|---|---|---|---|---|---|---|---|---|---|
| Chemical type - | 2 | B | E | E | E | E | E | B | B | E | C | C | C |
| Major oxides (weight percent) | | | | | | | | | | | | | |
| $SiO_2$ | 52.44 | 56.69 | 55.59 | 56.04 | 55.99 | 55.94 | 56.46 | 54.80 | 55.42 | 56.24 | 54.35 | 53.29 | 53.75 |
| $Al_2O_3$ | 14.67 | 13.56 | 13.77 | 14.06 | 13.91 | 13.46 | 13.98 | 13.35 | 13.80 | 14.13 | 14.33 | 14.56 | 14.54 |
| FeO | 11.45 | 11.01 | 11.95 | 11.16 | 11.62 | 11.63 | 11.17 | 12.90 | 12.13 | 10.92 | 10.87 | 10.89 | 11.27 |
| MgO | 5.51 | 3.43 | 3.74 | 3.67 | 3.72 | 3.70 | 3.62 | 3.61 | 3.41 | 3.73 | 4.62 | 5.44 | 5.12 |
| CaO | 9.76 | 7.07 | 7.20 | 7.24 | 6.95 | 7.31 | 7.09 | 6.93 | 7.01 | 7.15 | 9.04 | 9.70 | 8.68 |
| $Na_2O$ | 2.92 | 3.00 | 2.91 | 3.02 | 3.23 | 2.90 | 3.31 | 3.36 | 3.15 | 3.02 | 2.94 | 2.82 | 3.08 |
| $K_2O$ | 0.75 | 2.16 | 1.81 | 2.03 | 1.70 | 1.94 | 1.75 | 1.69 | 1.99 | 2.20 | 1.38 | 1.01 | 1.13 |
| $TiO_2$ | 1.56 | 2.28 | 1.96 | 1.95 | 1.97 | 2.12 | 1.92 | 2.38 | 2.27 | 1.88 | 1.76 | 1.64 | 1.72 |
| $P_2O_5$ | 0.29 | 0.41 | 0.34 | 0.34 | 0.35 | 0.31 | 0.28 | 0.42 | 0.38 | 0.32 | 0.31 | 0.24 | 0.27 |
| MnO | 0.18 | 0.20 | 0.19 | 0.19 | 0.18 | 0.20 | 0.18 | 0.20 | 0.20 | 0.18 | 0.20 | 0.19 | 0.18 |
| Total | 99.53 | 99.81 | 99.46 | 99.70 | 99.62 | 99.51 | 99.76 | 99.64 | 99.76 | 99.77 | 99.80 | 99.78 | 99.74 |
| Trace elements (parts per million) | | | | | | | | | | | | | |
| Ba | 432 | 843 | 733 | 759 | 713 | 777 | 679 | 736 | 746 | 707 | 533 | 413 | 485 |
| BaX | 393 | n.a. | 689 | 767 | 705 | 782 | 704 | 702 | n.a. | 715 | 410 | 414 | 474 |
| Co | 38.4 | 35.1 | 37.3 | 37.3 | 37.7 | 35.9 | 35.2 | 36.8 | 36.1 | 33.7 | 43.9 | 39.5 | 38.8 |
| Cr | 110 | 6.1 | 6.9 | 11.6 | 10.0 | 8.5 | 9.4 | 3.5 | n.a. | 10.8 | 56.2 | 129.6 | 52.7 |
| Cs | 0.89 | 1.39 | 1.62 | 1.37 | 0.81 | 1.60 | 0.94 | 0.85 | 1.37 | 1.33 | 0.86 | 0.68 | 0.66 |
| Hf | 3.12 | 4.90 | 4.96 | 4.88 | 4.90 | 4.97 | 4.75 | 5.00 | 4.80 | 4.61 | 3.83 | 3.38 | 3.58 |
| NbX | 13 | n.a. | 14 | 13 | 15 | 11 | 16 | 15 | n.a. | 14 | 24 | 12 | 14.3 |
| Rb | 19.1 | 56.4 | 57.0 | 53.1 | 51.8 | 53.0 | 51.3 | 48.7 | 46.5 | 56.0 | 30.7 | 22.7 | 28.7 |
| RbX | 26.0 | n.a. | 54.70 | 49.0 | 48.0 | 57.0 | 53.7 | 51.3 | n.a. | 53.0 | 36.0 | 25.5 | 30.0 |
| SrX | 381 | n.a. | 341 | 339 | 324 | 336 | 333 | 336 | n.a. | 319 | 345 | 317 | 354 |
| Ta | 0.62 | 0.64 | 0.93 | 0.99 | 0.93 | 0.90 | 0.90 | 0.95 | 0.86 | 0.87 | 0.79 | 0.64 | 0.72 |
| Th | 2.26 | 5.91 | 6.40 | 6.15 | 6.58 | 6.30 | 6.27 | 5.73 | 5.62 | 6.10 | 3.66 | 3.10 | 3.16 |
| U | 0.69 | n.a. | 1.59 | 1.70 | 1.56 | 1.80 | 1.59 | 1.43 | n.a. | 1.70 | n.a. | 0.82 | 0.79 |
| YX | 30.7 | n.a. | 34.0 | 34.0 | 35.0 | 34.0 | 35.0 | 39.3 | n.a. | 34.0 | 28.0 | 29.5 | 32.0 |
| Zn | 125 | 134 | 130 | 138 | 138 | 132 | 136 | 142 | 133 | 131 | 130 | 128 | 125 |
| Zr | 179 | n.a. | 194 | 144 | n.a. | 243 | 189 | 200 | n.a. | 214 | n.a. | 116 | 165 |
| ZrX | 131 | n.a. | 199 | 190 | 190 | 201 | 189 | 196 | n.a. | 184 | 160 | 137 | 148 |
| Sc | 37.5 | 32.4 | 31.3 | 31.8 | 32.1 | 31.8 | 30.7 | 33.1 | 32.8 | 29.9 | 36.4 | 37.9 | 36.0 |
| La | 17.3 | 30.0 | 28.0 | 26.9 | 27.0 | 26.7 | 27.6 | 27.8 | 28.1 | 25.8 | 19.8 | 16.8 | 18.7 |
| Ce | 34.2 | 58.5 | 53.7 | 53.7 | 54.2 | 51.0 | 52.0 | 53.8 | 55.2 | 48.9 | 40.2 | 33.7 | 37.0 |
| Nd | 22.3 | 36.9 | 31.8 | 30.5 | 28.3 | 28.0 | 30.0 | 31.0 | 29.9 | 31.0 | 23.0 | 19.0 | 22.3 |
| Sm | 5.1 | 7.5 | 6.8 | 6.7 | 6.8 | 6.3 | 6.5 | 7.1 | 7.0 | 6.3 | 5.8 | 4.9 | 5.5 |
| Eu | 1.55 | 2.20 | 1.83 | 1.89 | 1.99 | 1.80 | 1.84 | 1.98 | 2.19 | 1.69 | 1.76 | 1.51 | 1.58 |
| Gd | 4.6 | n.a. | 7.3 | 6.6 | 8.4 | 6.6 | 6.5 | 7.1 | n.a. | 7.9 | n.a. | 4.5 | 20.4 |
| Tb | 0.88 | 1.29 | 1.18 | 1 | 1.13 | 1.18 | 0.99 | 1.25 | 1.07 | 0.88 | 0.99 | 0.88 | 0.85 |
| Yb | 2.69 | 3.78 | 3.53 | 3.09 | 3.17 | 3.48 | 3.41 | 3.63 | 3.54 | 3.31 | 2.73 | 2.67 | 3.10 |
| Lu | 0.44 | 0.64 | 0.51 | 0.52 | 0.54 | 0.53 | 0.50 | 0.55 | 0.56 | 0.50 | 0.51 | 0.45 | 0.45 |
| Cu | 49.5 | n.a. | 13.8 | 15.0 | 13.0 | 17.0 | n.a. | 13.0 | n.a. | n.a. | n.a. | n.a. | n.a. |
| Ni | 20.0 | n.a. | 6.4 | 6.2 | 6.5 | 7.0 | n.a. | 5.2 | n.a. | n.a. | n.a. | n.a. | n.a. |
| Normalized major-oxide contents (weight percent) | | | | | | | | | | | | | |
| SiO2 | 52.69 | 56.80 | 55.89 | 56.21 | 56.20 | 56.22 | 56.60 | 55.00 | 55.55 | 56.37 | 54.46 | 53.41 | 53.89 |
| $Al_2O_3$ | 14.74 | 13.59 | 13.84 | 14.10 | 13.96 | 13.53 | 14.01 | 13.40 | 13.83 | 14.16 | 14.36 | 14.59 | 14.58 |
| FeO | 11.50 | 11.03 | 12.01 | 11.19 | 11.66 | 11.69 | 11.20 | 12.95 | 12.16 | 10.95 | 10.89 | 10.91 | 11.30 |
| MgO | 5.54 | 3.44 | 3.76 | 3.68 | 3.73 | 3.72 | 3.63 | 3.62 | 3.42 | 3.74 | 4.63 | 5.45 | 5.13 |
| CaO | 9.81 | 7.08 | 7.24 | 7.26 | 6.98 | 7.35 | 7.11 | 6.96 | 7.03 | 7.17 | 9.06 | 9.72 | 8.70 |
| $Na_2O$ | 2.93 | 3.01 | 2.93 | 3.03 | 3.24 | 2.91 | 3.32 | 3.37 | 3.16 | 3.03 | 2.95 | 2.83 | 3.09 |
| $K_2O$ | 0.75 | 2.16 | 1.82 | 2.04 | 1.71 | 1.95 | 1.75 | 1.70 | 1.99 | 2.21 | 1.38 | 1.01 | 1.13 |
| $TiO_2$ | 1.57 | 2.28 | 1.97 | 1.96 | 1.98 | 2.13 | 1.92 | 2.39 | 2.28 | 1.88 | 1.76 | 1.64 | 1.72 |
| $P_2O_5$ | 0.29 | 0.41 | 0.34 | 0.34 | 0.35 | 0.31 | 0.28 | 0.42 | 0.38 | 0.32 | 0.31 | 0.24 | 0.27 |
| MnO | 0.18 | 0.20 | 0.19 | 0.19 | 0.18 | 0.20 | 0.18 | 0.20 | 0.20 | 0.18 | 0.20 | 0.19 | 0.18 |
| Total | 100.00 | 100.00 | 100.00 | 100.00 | 100.00 | 100.00 | 100.00 | 100.00 | 100.00 | 100.00 | 100.00 | 100.00 | 100.00 |

**Table 3.** Average chemical composition of geochemical units in the Grande Ronde Basalt—*Continued*

| Geochemical unit-------- | 3D | 5D | 5D | UNC | 2D | 2D | 2D | 2D | 2D | 2D | 2D | 2D | 2D* |
|---|---|---|---|---|---|---|---|---|---|---|---|---|---|
| Chemical type - | C | E | E | X | B | B | B | B | B | B | B | B | B |
| | | | | | Major oxides (weight percent) | | | | | | | | |
| $SiO_2$ | 53.43 | 54.90 | 55.17 | 54.97 | 54.45 | 54.65 | 54.22 | 54.71 | 56.07 | 54.01 | 55.44 | 55.56 | 55.39 |
| $Al_2O_3$ | 14.60 | 14.04 | 14.01 | 13.46 | 13.93 | 14.18 | 14.12 | 14.09 | 13.61 | 13.93 | 13.85 | 13.75 | 13.95 |
| FeO | 11.22 | 11.98 | 11.52 | 12.33 | 12.43 | 12.04 | 12.81 | 12.03 | 11.66 | 12.68 | 11.95 | 11.82 | 11.92 |
| MgO | 5.25 | 4.16 | 4.37 | 3.81 | 3.89 | 3.79 | 3.66 | 3.55 | 3.23 | 3.80 | 3.46 | 3.50 | 3.54 |
| CaO | 9.10 | 7.79 | 7.74 | 7.45 | 7.60 | 7.48 | 7.03 | 7.29 | 6.78 | 7.24 | 6.97 | 7.09 | 7.09 |
| $Na_2O$ | 2.89 | 2.82 | 3.09 | 3.03 | 3.10 | 3.18 | 3.27 | 2.95 | 2.99 | 3.16 | 3.11 | 3.19 | 3.15 |
| $K_2O$ | 1.11 | 1.66 | 1.54 | 1.73 | 1.65 | 1.73 | 1.68 | 2.10 | 2.39 | 1.84 | 2.01 | 2.01 | 1.87 |
| $TiO_2$ | 1.72 | 1.96 | 1.87 | 2.30 | 2.13 | 2.12 | 2.25 | 2.43 | 2.31 | 2.46 | 2.33 | 2.22 | 2.31 |
| $P_2O_5$ | 0.26 | 0.29 | 0.28 | 0.50 | 0.39 | 0.37 | 0.43 | 0.44 | 0.52 | 0.44 | 0.46 | 0.43 | 0.37 |
| MnO | 0.19 | 0.18 | 0.19 | 0.20 | 0.21 | 0.19 | 0.20 | 0.20 | 0.22 | 0.20 | 0.21 | 0.20 | 0.18 |
| Total | 99.77 | 99.78 | 99.78 | 99.78 | 99.78 | 99.73 | 99.67 | 99.79 | 99.78 | 99.76 | 99.79 | 99.77 | 99.77 |
| | | | | | Trace elements (parts per million) | | | | | | | | |
| Ba | 495 | 644 | 632 | 727 | 692 | 630 | 693 | 701 | 824 | 714 | 802 | 730 | 685 |
| BaX | 485 | n.a. | n.a. | n.a. | 645 | 649 | 683 | n.a. | 827 | 706 | 619 | 715 | 746 |
| Co | 41.1 | 41.5 | 41.9 | 41.1 | 43.4 | 38.0 | 38.6 | 40.2 | 38.4 | 38.7 | 37.1 | 34.6 | 35.9 |
| Cr | 100.0 | 19.1 | 22.3 | 9.2 | 14.0 | 8.3 | 10.3 | 13.5 | 9.4 | 14.5 | 11.7 | 12.5 | 7.9 |
| Cs | 0.71 | 1.29 | 0.82 | 1.08 | 1.12 | 0.65 | 1.01 | 1.28 | 1.54 | 1.14 | 1.50 | 1.32 | 1.38 |
| Hf | 3.72 | 4.30 | 4.17 | 4.79 | 4.82 | 4.48 | 4.67 | 5.14 | 4.91 | 4.99 | 5.27 | 4.74 | 4.88 |
| NbX | 13.3 | n.a. | n.a. | n.a. | 16.0 | 13.0 | 10.0 | n.a. | 12.0 | 12.0 | 14.0 | 13.0 | 14.0 |
| Rb | 27.7 | 41.0 | 41.3 | 39.5 | 37.5 | 50.0 | 36.4 | 57.5 | 69.2 | 46.3 | 48.6 | 45.4 | 55.0 |
| RbX | 36.3 | n.a. | n.a. | n.a. | 48.0 | 41.0 | 29.0 | n.a. | 66.0 | 46.0 | 54.0 | 51.0 | 52.0 |
| SrX | 308 | n.a. | n.a. | n.a. | 313 | 312 | 322 | n.a. | 321 | 312 | 340 | 359 | 324 |
| Ta | 0.74 | 0.9 | 0.95 | 0.99 | 0.85 | 0.91 | 0.95 | 1.02 | 0.91 | 0.88 | 0.95 | 0.90 | 0.92 |
| Th | 3.46 | 4.82 | 4.99 | 5.33 | 4.58 | 5.0 | 4.96 | 5.33 | 7.34 | 5.16 | 5.96 | 6.38 | 6.50 |
| U | 1.02 | n.a. | n.a. | n.a. | n.a. | 1.27 | 1.44 | n.a. | n.a. | 1.18 | n.a. | 1.78 | 1.63 |
| YX | 33.3 | n.a. | n.a. | n.a. | 40.0 | 32.0 | 32.0 | n.a. | 34.0 | 33.0 | 33.0 | 37.0 | 35.0 |
| Zn | 131 | 141 | 128 | 150 | 151 | 149 | 139 | 147 | 137 | 147 | 147 | 140 | 145 |
| Zr | 120 | n.a. | n.a. | n.a. | n.a. | 159 | 151 | n.a. | n.a. | 198 | n.a. | 178 | 157 |
| ZrX | 164 | n.a. | n.a. | n.a. | 194 | 176 | 183 | n.a. | 198 | 194 | 231 | 183 | 191 |
| Sc | 37.1 | 34.2 | 33.0 | 33.5 | 35.8 | 32.6 | 32.6 | 33.4 | 29.3 | 32.5 | 31.0 | 31.0 | 30.5 |
| La | 18.3 | 22.9 | 21.6 | 26.2 | 25.1 | 24.0 | 25.9 | 27.6 | 28.9 | 26.0 | 28.7 | 27.6 | 27.9 |
| Ce | 37.5 | 44.8 | 42.6 | 54.0 | 51.3 | 46.2 | 53.1 | 58.7 | 57.5 | 54.6 | 58.5 | 54.2 | 56.0 |
| Nd | 20.5 | 26.2 | 21.8 | 29.8 | 30.3 | 27.0 | 28.8 | 32.7 | 37.1 | 31.7 | 33.5 | 29.9 | 28.0 |
| Sm | 5.3 | 6.0 | 5.9 | 7.3 | 7.1 | 6.5 | 7.0 | 7.8 | 8.0 | 7.3 | 7.8 | 7.3 | 7.3 |
| Eu | 1.66 | 1.90 | 1.77 | 2.13 | 2.11 | 1.83 | 2.05 | 2.34 | 2.08 | 2.02 | 2.19 | 2.06 | 1.92 |
| Gd | 5.0 | n.a. | n.a. | n.a. | n.a. | 6.6 | 6.6 | n.a. | n.a. | 7.0 | n.a. | 7.0 | 6.2 |
| Tb | 0.96 | 1.17 | 1.04 | 1.07 | 1.42 | 0.93 | 1.05 | 1.35 | 1.22 | 1.21 | 1.2 | 1.08 | 1.20 |
| Yb | 2.72 | 2.96 | 2.79 | 3.37 | 3.41 | 3.54 | 3.56 | 3.65 | 3.40 | 3.54 | 3.67 | 3.13 | 3.40 |
| Lu | 0.50 | 0.54 | 0.50 | 0.63 | 0.62 | 0.53 | 0.58 | 0.61 | 0.55 | 0.59 | 0.63 | 0.55 | 0.52 |
| Cu | 41.0 | n.a. | n.a. | n.a. | 62.0 | n.a. | n.a. | n.a. | 18.0 | n.a. | n.a. | n.a. | n.a. |
| Ni | 16.0 | n.a. | n.a. | n.a. | 17.0 | n.a. | n.a. | n.a. | 6.0 | n.a. | n.a. | n.a. | n.a. |
| | | | | | Normalized major-oxide contents (weight percent) | | | | | | | | |
| $SiO_2$ | 53.55 | 55.02 | 55.29 | 55.09 | 54.57 | 54.80 | 54.40 | 54.83 | 56.19 | 54.14 | 55.56 | 55.69 | 55.52 |
| $Al_2O_3$ | 14.63 | 14.07 | 14.04 | 13.49 | 13.96 | 14.22 | 14.17 | 14.12 | 13.64 | 13.96 | 13.88 | 13.78 | 13.98 |
| FeO | 11.25 | 12.01 | 11.55 | 12.36 | 12.46 | 12.07 | 12.85 | 12.06 | 11.69 | 12.71 | 11.98 | 11.85 | 11.95 |
| MgO | 5.26 | 4.17 | 4.38 | 3.82 | 3.90 | 3.80 | 3.67 | 3.56 | 3.24 | 3.81 | 3.47 | 3.51 | 3.55 |
| CaO | 9.12 | 7.81 | 7.76 | 7.47 | 7.62 | 7.50 | 7.05 | 7.31 | 6.79 | 7.26 | 6.98 | 7.11 | 7.11 |
| $Na_2O$ | 2.90 | 2.83 | 3.10 | 3.04 | 3.11 | 3.19 | 3.28 | 2.96 | 3.00 | 3.17 | 3.12 | 3.20 | 3.16 |
| $K_2O$ | 1.11 | 1.66 | 1.54 | 1.73 | 1.65 | 1.73 | 1.69 | 2.10 | 2.40 | 1.84 | 2.01 | 2.01 | 1.87 |
| $TiO_2$ | 1.72 | 1.96 | 1.87 | 2.31 | 2.13 | 2.13 | 2.26 | 2.44 | 2.32 | 2.47 | 2.33 | 2.23 | 2.32 |
| $P_2O_5$ | 0.26 | 0.29 | 0.28 | 0.50 | 0.39 | 0.37 | 0.43 | 0.44 | 0.52 | 0.44 | 0.46 | 0.43 | 0.37 |
| MnO | 0.19 | 0.18 | 0.19 | 0.20 | 0.21 | 0.19 | 0.20 | 0.20 | 0.22 | 0.20 | 0.21 | 0.20 | 0.18 |
| Total | 100.00 | 100.00 | 100.00 | 100.00 | 100.00 | 100.00 | 100.00 | 100.00 | 100.00 | 100.00 | 100.00 | 100.00 | 100.00 |

**Table 3.** Average chemical composition of geochemical units in the Grande Ronde Basalt—*Continued*

| Geochemical unit-------- | 2D* | 2D* | 2D | 2D | UNC | AS16 | AS16 | AS16 | AS16 | KB5 | KB5 | 3E | 3E |
|---|---|---|---|---|---|---|---|---|---|---|---|---|---|
| Chemical type - | B | B | B | B | X | 4 | 4 | 4 | 4 | 3 | 3 | C | C |
| Major oxides (weight percent) | | | | | | | | | | | | | |
| $SiO_2$ | 55.25 | 55.08 | 55.81 | 56.27 | 56.04 | 54.15 | 54.09 | 53.83 | 54.56 | 53.66 | 53.56 | 54.67 | 53.96 |
| $Al_2O_3$ | 13.93 | 13.89 | 14.20 | 14.12 | 14.10 | 13.70 | 14.27 | 14.08 | 13.71 | 13.77 | 14.17 | 14.13 | 14.42 |
| FeO | 12.02 | 12.24 | 11.76 | 11.43 | 10.26 | 12.26 | 11.95 | 12.44 | 12.03 | 12.86 | 12.64 | 11.26 | 11.17 |
| MgO | 3.60 | 3.50 | 3.40 | 3.50 | 3.76 | 4.59 | 4.48 | 4.40 | 4.49 | 4.13 | 4.16 | 5.05 | 5.16 |
| CaO | 7.11 | 6.99 | 6.95 | 6.44 | 7.59 | 8.19 | 8.26 | 7.99 | 8.01 | 7.82 | 7.79 | 8.14 | 8.79 |
| $Na_2O$ | 3.28 | 3.39 | 3.01 | 3.32 | 3.07 | 2.96 | 2.90 | 3.09 | 3.19 | 3.15 | 3.11 | 3.28 | 3.07 |
| $K_2O$ | 1.76 | 1.82 | 1.91 | 1.91 | 2.04 | 1.43 | 1.34 | 1.33 | 1.19 | 1.50 | 1.52 | 1.16 | 1.15 |
| $TiO_2$ | 2.24 | 2.30 | 2.16 | 2.23 | 2.14 | 2.00 | 2.00 | 2.09 | 2.06 | 2.24 | 2.21 | 1.71 | 1.66 |
| $P_2O_5$ | 0.35 | 0.37 | 0.39 | 0.41 | 0.43 | 0.32 | 0.30 | 0.33 | 0.35 | 0.43 | 0.41 | 0.25 | 0.24 |
| MnO | 0.18 | 0.19 | 0.18 | 0.17 | 0.21 | 0.20 | 0.19 | 0.20 | 0.21 | 0.22 | 0.21 | 0.16 | 0.19 |
| Total | 99.72 | 99.77 | 99.77 | 99.80 | 99.64 | 99.80 | 99.78 | 99.78 | 99.80 | 99.78 | 99.78 | 99.81 | 99.81 |
| Trace elements (parts per million) | | | | | | | | | | | | | |
| Ba | 689 | 755 | 730 | 722 | 844 | 491 | 504 | 609 | 549 | 585 | 530 | 427 | 480 |
| BaX | 700 | 710 | n.a. | 614 | 873 | n.a. | n.a. | n.a. | n.a. | 597 | n.a. | n.a. | 346 |
| Co | 35.3 | 33.3 | 36.3 | 40.7 | 35.7 | 42.2 | 42.7 | 41.9 | 42.4 | 39.6 | 40.7 | 39.6 | 39.8 |
| Cr | 10.7 | 7.9 | 11.8 | 17.3 | 10.6 | 23.4 | 19.8 | 19.3 | 21.9 | 22.5 | 22.6 | 25.5 | 24.2 |
| Cs | 1.40 | 1.50 | 1.37 | 1.10 | 1.34 | 1.80 | 1.13 | 0.94 | n.a. | 1.12 | 1.18 | 0.95 | 0.97 |
| Hf | 4.71 | 5.20 | 4.93 | 4.77 | 4.86 | 3.94 | 3.98 | 4.08 | 4.14 | 4.27 | 4.14 | 3.65 | 3.59 |
| NbX | 14.5 | 16.0 | n.a. | 13.0 | 14.0 | n.a. | n.a. | n.a. | n.a. | 12.0 | n.a. | n.a. | 11.0 |
| Rb | 49.0 | 51.0 | 41.2 | 38.2 | 61.0 | 28.9 | 33.8 | 43.9 | 23.5 | 30.8 | 39.5 | n.a. | 25.8 |
| RbX | 53.5 | 49.0 | n.a. | 50.0 | 57.0 | n.a. | n.a. | n.a. | n.a. | 40.5 | n.a. | n.a. | 30.0 |
| SrX | 332 | 337 | n.a. | 380 | 330 | n.a. | n.a. | n.a. | n.a. | 342 | n.a. | n.a. | 298 |
| Ta | 0.84 | 0.96 | 0.90 | 0.84 | 0.88 | 0.68 | 0.73 | 0.67 | 0.74 | 0.83 | 0.83 | 0.62 | 0.72 |
| Th | 6.05 | 5.80 | 6.80 | 6.71 | 6.50 | 3.84 | 3.77 | 3.96 | 3.73 | 3.95 | 4.33 | 3.84 | 3.48 |
| U | 1.50 | 1.45 | n.a. | n.a. | 1.50 | n.a. | n.a. | n.a. | n.a. | n.a. | n.a. | n.a. | n.a. |
| YX | 36.0 | 39.0 | n.a. | 38.0 | 35.0 | n.a. | n.a. | n.a. | n.a. | 36.0 | n.a. | n.a. | 31.0 |
| Zn | 137 | 146 | 146 | 137 | 138 | 136 | 138 | 143 | 145 | 146 | 146 | 122 | 129 |
| Zr | 179 | 195 | n.a. | n.a. | 125 | n.a. | n.a. | n.a. | n.a. | n.a. | n.a. | n.a. | n.a. |
| ZrX | 190 | 207 | n.a. | 201 | 191 | n.a. | n.a. | n.a. | n.a. | 177 | n.a. | n.a. | 145 |
| Sc | 31.3 | 30.8 | 31.9 | 31.3 | 30.2 | 35.0 | 36.0 | 35.7 | 35.2 | 35.9 | 36.5 | 34.2 | 34.6 |
| La | 26.3 | 27.9 | 27.7 | 27.3 | 27.6 | 18.6 | 18.7 | 19.1 | 19.1 | 21.3 | 20.6 | 16.5 | 16.7 |
| Ce | 50.3 | 56.0 | 58.1 | 55.8 | 54.0 | 38.9 | 38.8 | 41.7 | 39.1 | 44.6 | 43.0 | 34.2 | 36.5 |
| Nd | 27.5 | 31.0 | 32.5 | 32.1 | 30.0 | 23.0 | 23.9 | 26.8 | 23.2 | 26.6 | 25.8 | 21.3 | 20.50 |
| Sm | 6.6 | 7.3 | 7.6 | 7.3 | 7.0 | 6.2 | 6.1 | 6.2 | 6.1 | 6.6 | 6.8 | 5.4 | 5.3 |
| Eu | 1.86 | 2.09 | 2.17 | 2.15 | 1.94 | 1.71 | 1.77 | 1.90 | 1.75 | 1.99 | 1.99 | 1.65 | 1.66 |
| Gd | 6.3 | 8.2 | n.a. | n.a. | 6.0 | n.a. | n.a. | n.a. | n.a. | n.a. | n.a. | n.a. | n.a. |
| Tb | 1.00 | 1.08 | 1.23 | 1.21 | 1.02 | 1.07 | 1.18 | 1.25 | 1.00 | 1.19 | 1.10 | 1.14 | 0.85 |
| Yb | 3.42 | 3.94 | 3.58 | 3.1 | 3.47 | 2.83 | 3.10 | 3.29 | 2.94 | 3.35 | 3.52 | 2.59 | 2.41 |
| Lu | 0.52 | 0.59 | 0.55 | 0.53 | 0.51 | 0.51 | 0.53 | 0.54 | 0.55 | 0.58 | 0.59 | 0.44 | 0.48 |
| Cu | n.a. | n.a. | n.a. | n.a. | n.a. | n.a. | n.a. | n.a. | n.a. | 27.0 | n.a. | n.a. | n.a. |
| Ni | n.a. | n.a. | n.a. | n.a. | n.a. | n.a. | n.a. | n.a. | n.a. | 10.5 | n.a. | n.a. | n.a. |
| Normalized major-oxide contents (weight percent) | | | | | | | | | | | | | |
| $SiO_2$ | 55.41 | 55.21 | 55.94 | 56.38 | 56.24 | 54.26 | 54.21 | 53.95 | 54.67 | 53.78 | 53.68 | 54.77 | 54.06 |
| $Al_2O_3$ | 13.97 | 13.92 | 14.23 | 14.15 | 14.15 | 13.73 | 14.30 | 14.11 | 13.74 | 13.80 | 14.20 | 14.16 | 14.45 |
| FeO | 12.05 | 12.27 | 11.79 | 11.45 | 10.30 | 12.28 | 11.98 | 12.47 | 12.05 | 12.89 | 12.67 | 11.28 | 11.19 |
| MgO | 3.61 | 3.51 | 3.41 | 3.51 | 3.77 | 4.60 | 4.49 | 4.41 | 4.50 | 4.14 | 4.17 | 5.06 | 5.17 |
| CaO | 7.13 | 7.01 | 6.97 | 6.45 | 7.62 | 8.21 | 8.28 | 8.01 | 8.03 | 7.84 | 7.81 | 8.16 | 8.81 |
| $Na_2O$ | 3.29 | 3.40 | 3.02 | 3.33 | 3.08 | 2.97 | 2.91 | 3.10 | 3.20 | 3.16 | 3.12 | 3.29 | 3.08 |
| $K_2O$ | 1.76 | 1.82 | 1.91 | 1.91 | 2.05 | 1.43 | 1.34 | 1.33 | 1.19 | 1.50 | 1.52 | 1.16 | 1.15 |
| $TiO_2$ | 2.25 | 2.31 | 2.16 | 2.23 | 2.15 | 2.00 | 2.00 | 2.09 | 2.06 | 2.24 | 2.21 | 1.71 | 1.66 |
| $P_2O_5$ | 0.35 | 0.37 | 0.39 | 0.41 | 0.43 | 0.32 | 0.30 | 0.33 | 0.35 | 0.43 | 0.41 | 0.25 | 0.24 |
| MnO | 0.18 | 0.19 | 0.18 | 0.17 | 0.21 | 0.20 | 0.19 | 0.20 | 0.21 | 0.22 | 0.21 | 0.16 | 0.19 |
| Total | 100.00 | 100.00 | 100.00 | 100.00 | 100.00 | 100.00 | 100.00 | 100.00 | 100.00 | 100.00 | 100.00 | 100.00 | 100.00 |

**Table 3.** Average chemical composition of geochemical units in the Grande Ronde Basalt—*Continued*

| Geochemical unit-------- | AS16 | 3F | 5E | AS16 | AS16 | AS16 | AS16 | 3G | 3G | 5F | 5F | AS16 | AS16 |
|---|---|---|---|---|---|---|---|---|---|---|---|---|---|
| Chemical type - | 4 | C | E | 4 | 4 | 4 | 4 | C | C | E | E | 4 | 4 |
| Major oxides (weight percent) | | | | | | | | | | | | | |
| $SiO_2$ | 53.90 | 54.21 | 54.46 | 54.39 | 54.30 | 53.97 | 54.43 | 55.01 | 54.41 | 55.68 | 55.40 | 54.35 | 54.47 |
| $Al_2O_3$ | 13.97 | 14.59 | 14.43 | 14.41 | 14.05 | 14.03 | 14.17 | 14.87 | 14.50 | 14.38 | 13.81 | 13.93 | 14.27 |
| FeO | 12.52 | 11.01 | 11.53 | 11.64 | 12.15 | 12.43 | 12.62 | 10.11 | 11.21 | 11.01 | 12.02 | 12.48 | 11.83 |
| MgO | 4.27 | 4.99 | 4.49 | 4.23 | 3.94 | 4.43 | 4.07 | 4.72 | 4.79 | 3.93 | 3.77 | 4.05 | 4.29 |
| CaO | 7.89 | 8.84 | 8.14 | 8.13 | 7.77 | 7.71 | 7.27 | 8.59 | 8.53 | 7.56 | 7.22 | 7.51 | 7.93 |
| $Na_2O$ | 3.13 | 2.94 | 2.99 | 3.12 | 3.08 | 3.26 | 3.22 | 3.12 | 2.94 | 3.22 | 3.43 | 3.51 | 3.30 |
| $K_2O$ | 1.54 | 1.12 | 1.45 | 1.39 | 1.72 | 1.38 | 1.40 | 1.19 | 1.25 | 1.57 | 1.57 | 1.43 | 1.29 |
| $TiO_2$ | 1.95 | 1.67 | 1.79 | 1.94 | 2.18 | 2.01 | 2.05 | 1.73 | 1.70 | 1.95 | 2.04 | 1.98 | 1.93 |
| $P_2O_5$ | 0.41 | 0.25 | 0.30 | 0.34 | 0.40 | 0.39 | 0.34 | 0.29 | 0.26 | 0.30 | 0.34 | 0.33 | 0.27 |
| MnO | 0.21 | 0.18 | 0.20 | 0.20 | 0.20 | 0.19 | 0.20 | 0.19 | 0.19 | 0.19 | 0.18 | 0.22 | 0.20 |
| Total | 99.79 | 99.80 | 99.78 | 99.79 | 99.79 | 99.80 | 99.77 | 99.82 | 99.78 | 99.79 | 99.78 | 99.79 | 99.78 |
| Trace elements (parts per million) | | | | | | | | | | | | | |
| Ba | 574 | 497 | 542 | 550 | 566 | 607 | 636 | 611 | 479 | 676 | 547 | 543 | 543 |
| BaX | n.a. | 528 | n.a. | n.a. | 614 | n.a. | n.a. | n.a. | n.a. | 647 | n.a. | 564 | n.a. |
| Co | 38.7 | 39.1 | 40.0 | 38.4 | 38.7 | 39.3 | 39.5 | 36.4 | 38.9 | 39.5 | 38.5 | 39.5 | 38.4 |
| Cr | 16.3 | 22.9 | 17.2 | 16.3 | 21.6 | 14.5 | 13.7 | 24.0 | 30.6 | 10.0 | 5.3 | 13.8 | 13.5 |
| Cs | 1.01 | 1.00 | 1.08 | 0.90 | 1.35 | 0.90 | 1.18 | 0.85 | 1.08 | 1.19 | 0.80 | 1.41 | 0.70 |
| Hf | 4.22 | 3.61 | 4.10 | 4.00 | 4.15 | 4.23 | 4.45 | 3.89 | 3.76 | 4.74 | 4.95 | 4.25 | 4.22 |
| NbX | n.a. | 8.0 | n.a. | n.a. | 12.0 | n.a. | n.a. | n.a. | n.a. | 12.0 | n.a. | 13.0 | n.a. |
| Rb | 30.1 | 26.8 | 35.4 | 33.9 | 36.6 | 37.6 | 56.4 | 23.1 | 39.8 | 37.7 | 47.9 | 40.5 | 21.4 |
| RbX | n.a. | 29.0 | n.a. | n.a. | 41.0 | n.a. | n.a. | n.a. | n.a. | 38.0 | n.a. | 39.0 | n.a. |
| SrX | n.a. | 346 | n.a. | n.a. | 333 | n.a. | n.a. | n.a. | n.a. | 324 | n.a. | 306 | n.a. |
| Ta | 0.74 | 0.68 | 0.69 | 0.83 | 0.70 | 0.72 | 0.81 | 0.71 | 0.64 | 0.84 | 0.82 | 0.64 | 0.78 |
| Th | 3.82 | 3.58 | 3.72 | 4.19 | 4.59 | 4.22 | 4.49 | 3.95 | 3.49 | 4.53 | 3.96 | 3.78 | 3.87 |
| U | 0.0 | n.a. | n.a. | n.a. | n.a. | n.a. | n.a. | n.a. | n.a. | n.a. | n.a. | n.a. | n.a. |
| YX | 0.0 | 35.0 | n.a. | n.a. | 33.0 | n.a. | n.a. | n.a. | n.a. | 35.0 | n.a. | 33.0 | n.a. |
| Zn | 152 | 132 | 135 | 134 | 144 | 137 | 140 | 142 | 132 | 147 | 134 | 127 | 146.00 |
| Zr | 0 | n.a. | n.a. | n.a. | n.a. | n.a. | n.a. | n.a. | n.a. | n.a. | n.a. | n.a. | n.a. |
| ZrX | n.a. | 154 | n.a. | n.a. | 179 | n.a. | n.a. | n.a. | n.a. | 197 | n.a. | 178 | n.a. |
| Sc | 36.5 | 35.2 | 35.8 | 34.9 | 35.5 | 35.5 | 34.5 | 35.6 | 34.7 | 33.2 | 32.6 | 32.8 | 32.8 |
| La | 21.1 | 17.4 | 19.5 | 20.7 | 22.2 | 20.2 | 21.3 | 19.0 | 18.1 | 21.3 | 22.3 | 20.1 | 19.2 |
| Ce | 44.6 | 36.8 | 40.8 | 42.5 | 46.2 | 41.2 | 44.8 | 40.3 | 36.8 | 45.8 | 45.9 | 42.0 | 39.3 |
| Nd | 26.3 | 20.7 | 24.1 | 24.9 | 25.5 | 21.2 | 26.8 | 24.1 | 21.2 | 25.9 | 26.0 | 24.2 | 22.1 |
| Sm | 6.6 | 5.4 | 6.1 | 5.9 | 6.2 | 5.8 | 6.9 | 5.7 | 5.3 | 6.7 | 6.5 | 6.0 | 5.8 |
| Eu | 2.00 | 1.64 | 1.84 | 1.82 | 1.97 | 1.88 | 2.04 | 1.74 | 1.68 | 2.06 | 1.99 | 1.91 | 1.75 |
| Gd | n.a. | n.a. | n.a. | n.a. | n.a. | n.a. | n.a. | n.a. | n.a. | n.a. | n.a. | n.a. | n.a. |
| Tb | 1.03 | 0.96 | 1.04 | 0.97 | 1.02 | 1.02 | 1.17 | 0.98 | 0.94 | 1.12 | 1.08 | 1.19 | 1.24 |
| Yb | 3.26 | 2.51 | 3.15 | 2.99 | 2.95 | 3.03 | 3.25 | 2.84 | 2.63 | 3.23 | 3.19 | 3.02 | 2.92 |
| Lu | 0.62 | 0.48 | 0.54 | 0.52 | 0.53 | 0.59 | 0.58 | 0.54 | 0.49 | 0.57 | 0.57 | 0.57 | 0.50 |
| Cu | n.a. | 37.0 | n.a. | n.a. | 25.0 | n.a. | n.a. | n.a. | n.a. | 32.5 | n.a. | 52.0 | n.a. |
| Ni | n.a. | 16.0 | n.a. | n.a. | 10.0 | n.a. | n.a. | n.a. | n.a. | 12.0 | n.a. | 10.0 | n.a. |
| Normalized major-oxide contents (weight percent) | | | | | | | | | | | | | |
| $SiO_2$ | 54.01 | 54.32 | 54.58 | 54.50 | 54.41 | 54.08 | 54.56 | 55.11 | 54.53 | 55.80 | 55.52 | 54.46 | 54.59 |
| $Al_2O_3$ | 14.00 | 14.62 | 14.46 | 14.44 | 14.08 | 14.06 | 14.20 | 14.90 | 14.53 | 14.41 | 13.84 | 13.96 | 14.30 |
| FeO | 12.55 | 11.03 | 11.56 | 11.66 | 12.18 | 12.45 | 12.65 | 10.13 | 11.23 | 11.03 | 12.05 | 12.51 | 11.86 |
| MgO | 4.28 | 5.00 | 4.50 | 4.24 | 3.95 | 4.44 | 4.08 | 4.73 | 4.80 | 3.94 | 3.78 | 4.06 | 4.30 |
| CaO | 7.91 | 8.86 | 8.16 | 8.15 | 7.79 | 7.73 | 7.29 | 8.61 | 8.55 | 7.58 | 7.24 | 7.53 | 7.95 |
| $Na_2O$ | 3.14 | 2.95 | 3.00 | 3.13 | 3.09 | 3.27 | 3.23 | 3.13 | 2.95 | 3.23 | 3.44 | 3.52 | 3.31 |
| $K_2O$ | 1.54 | 1.12 | 1.45 | 1.39 | 1.72 | 1.38 | 1.40 | 1.19 | 1.25 | 1.57 | 1.57 | 1.43 | 1.29 |
| $TiO_2$ | 1.95 | 1.67 | 1.79 | 1.94 | 2.18 | 2.01 | 2.05 | 1.73 | 1.70 | 1.95 | 2.04 | 1.98 | 1.93 |
| $P_2O_5$ | 0.41 | 0.25 | 0.30 | 0.34 | 0.40 | 0.39 | 0.34 | 0.29 | 0.26 | 0.30 | 0.34 | 0.33 | 0.27 |
| MnO | 0.21 | 0.18 | 0.20 | 0.20 | 0.20 | 0.19 | 0.20 | 0.19 | 0.19 | 0.19 | 0.18 | 0.22 | 0.20 |
| Total | 100.00 | 100.00 | 100.00 | 100.00 | 100.00 | 100.00 | 100.00 | 100.00 | 100.00 | 100.00 | 100.00 | 100.00 | 100.00 |

**Table 3.** Average chemical composition of geochemical units in the Grande Ronde Basalt—*Continued*

| Geochemical unit-------- | AS16 | AS16 | 5H | AS16 | UNC | AS16 | AS16 | 2F | 2F | 5I | AS16 |
|---|---|---|---|---|---|---|---|---|---|---|---|
| Chemical type - | 4 | 4 | E | 4 | X | 4 | 4 | B | B | E | 4 |
| Major oxides (weight percent) | | | | | | | | | | | |
| $SiO_2$ | 54.15 | 53.75 | 55.24 | 54.54 | 56.66 | 56.60 | 54.60 | 54.74 | 54.68 | 55.82 | 54.21 |
| $Al_2O_3$ | 14.00 | 14.55 | 14.21 | 14.54 | 13.88 | 13.52 | 14.67 | 13.61 | 13.58 | 14.02 | 13.75 |
| FeO | 12.46 | 12.61 | 11.50 | 11.60 | 11.67 | 11.87 | 11.61 | 12.86 | 12.81 | 11.33 | 12.13 |
| MgO | 4.07 | 4.40 | 4.00 | 4.24 | 3.12 | 3.32 | 4.20 | 3.82 | 3.62 | 3.96 | 4.39 |
| CaO | 7.88 | 7.98 | 7.66 | 7.83 | 6.65 | 6.88 | 7.71 | 7.29 | 7.13 | 7.49 | 8.34 |
| $Na_2O$ | 3.04 | 2.88 | 3.03 | 3.13 | 3.18 | 3.09 | 3.09 | 3.17 | 3.46 | 3.09 | 2.85 |
| $K_2O$ | 1.57 | 1.06 | 1.67 | 1.52 | 1.99 | 1.94 | 1.44 | 1.54 | 1.58 | 1.61 | 1.44 |
| $TiO_2$ | 2.07 | 2.11 | 1.99 | 1.93 | 2.14 | 2.09 | 1.99 | 2.16 | 2.27 | 2.00 | 2.15 |
| $P_2O_5$ | 0.36 | 0.26 | 0.29 | 0.29 | 0.32 | 0.30 | 0.32 | 0.37 | 0.44 | 0.31 | 0.34 |
| MnO | 0.20 | 0.18 | 0.19 | 0.19 | 0.18 | 0.19 | 0.18 | 0.23 | 0.20 | 0.19 | 0.20 |
| Total | 99.80 | 99.78 | 99.78 | 99.81 | 99.79 | 99.80 | 99.81 | 99.79 | 99.77 | 99.82 | 99.80 |
| Trace elements (parts per million) | | | | | | | | | | | |
| Ba | 536 | 496 | 642 | 639 | 710 | 641 | 597 | 557 | 644 | 574 | 534 |
| BaX | n.a. | n.a. | n.a. | n.a. | 634 | 681 | n.a. | 583 | n.a. | n.a. | n.a. |
| Co | 37.9 | 39.5 | 40.3 | 38.3 | 37.0 | 36.5 | 38.5 | 38.5 | 38.8 | 39.0 | 40.5 |
| Cr | 10.9 | 13.0 | 12.3 | 14.6 | 9.0 | 10.2 | 16.7 | 17.2 | 14.5 | 11.3 | 35.3 |
| Cs | 1.31 | 1.12 | 1.30 | 1.20 | 1.86 | 1.44 | 1.46 | 0.80 | 1.22 | 1.33 | 1.57 |
| Hf | 4.55 | 4.67 | 4.62 | 4.43 | 5.22 | 5.05 | 4.80 | 4.94 | 5.33 | 4.82 | 4.64 |
| NbX | n.a. | n.a. | n.a. | n.a. | 15.5 | 15.0 | n.a. | 16.0 | n.a. | n.a. | n.a. |
| Rb | 47.8 | 25.5 | 52.4 | 30.8 | 53.0 | 49.2 | 34.9 | 50.1 | 39.6 | 47.2 | 40.4 |
| RbX | n.a. | n.a. | n.a. | n.a. | 64.0 | 54.0 | n.a. | 42.0 | n.a. | n.a. | n.a. |
| SrX | n.a. | n.a. | n.a. | n.a. | 337 | 327 | n.a. | 305 | n.a. | n.a. | n.a. |
| Ta | 0.69 | 0.93 | 0.90 | 0.83 | 0.95 | 0.90 | 0.77 | 0.85 | 0.81 | 0.87 | 0.88 |
| Th | 3.83 | 4.73 | 4.71 | 4.39 | 5.81 | 5.54 | 4.87 | 4.30 | 4.49 | 5.26 | 3.79 |
| U | 0.0 | n.a. | n.a. | n.a. | n.a. | n.a. | n.a. | n.a. | n.a. | n.a. | n.a. |
| YX | n.a. | n.a. | n.a. | n.a. | 40.0 | 35.0 | n.a. | 39.0 | n.a. | n.a. | n.a. |
| Zn | 132 | 137 | 128 | 146 | 145 | 135 | 147 | 137 | 143 | 117 | 125 |
| Zr | n.a. | n.a. | n.a. | n.a. | n.a. | n.a. | n.a. | n.a. | n.a. | n.a. | n.a. |
| ZrX | n.a. | n.a. | n.a. | n.a. | 217 | 206 | n.a. | 200 | n.a. | n.a. | n.a. |
| Sc | 33.7 | 33.3 | 32.7 | 34.0 | 30.1 | 30.6 | 31.5 | 33.1 | 33.2 | 31.0 | 34.1 |
| La | 21.1 | 21.1 | 21.7 | 20.3 | 24.8 | 23.3 | 23.1 | 22.1 | 23.7 | 22.2 | 21.2 |
| Ce | 44.5 | 44.0 | 45.5 | 41.9 | 52.4 | 48.6 | 48.7 | 47.4 | 51.6 | 46.5 | 46.1 |
| Nd | 26.9 | 26.5 | 27.7 | 25.3 | 31.6 | 29.0 | 27.4 | 30.6 | 34.7 | 26.6 | 26.7 |
| Sm | 6.4 | 6.7 | 6.6 | 6.4 | 7.2 | 6.7 | 7.0 | 6.9 | 7.5 | 6.4 | 6.7 |
| Eu | 1.97 | 1.96 | 1.87 | 1.91 | 1.98 | 2.00 | 1.95 | 2.11 | 2.26 | 1.87 | 1.96 |
| Gd | n.a. | n.a. | n.a. | n.a. | n.a. | n.a. | n.a. | n.a. | n.a. | n.a. | n.a. |
| Tb | 1.01 | 0.98 | 1.16 | 1.03 | 1.16 | 1.15 | 1.11 | 1.21 | 1.23 | 1.00 | 1.17 |
| Yb | 3.06 | 3.04 | 3.09 | 3.19 | 3.39 | 3.19 | 3.07 | 3.45 | 3.84 | 2.87 | 3.40 |
| Lu | 0.58 | 0.56 | 0.52 | 0.57 | 0.59 | 0.56 | 0.54 | 0.57 | 0.63 | 0.51 | 0.55 |
| Cu | n.a. | n.a. | n.a. | n.a. | 19.0 | 21.0 | n.a. | 42.0 | n.a. | n.a. | n.a. |
| Ni | n.a. | n.a. | n.a. | n.a. | 10.0 | 10.0 | n.a. | 14.0 | n.a. | n.a. | n.a. |
| Normalized major-oxide contents (weight percent) | | | | | | | | | | | |
| $SiO_2$ | 54.26 | 53.87 | 55.36 | 54.64 | 56.78 | 56.71 | 54.70 | 54.86 | 54.81 | 55.92 | 54.32 |
| $Al_2O_3$ | 14.03 | 14.58 | 14.24 | 14.57 | 13.91 | 13.55 | 14.70 | 13.64 | 13.61 | 14.05 | 13.78 |
| FeO | 12.48 | 12.64 | 11.53 | 11.62 | 11.69 | 11.89 | 11.63 | 12.89 | 12.84 | 11.35 | 12.15 |
| MgO | 4.08 | 4.41 | 4.01 | 4.25 | 3.13 | 3.33 | 4.21 | 3.83 | 3.63 | 3.97 | 4.40 |
| CaO | 7.90 | 8.00 | 7.68 | 7.84 | 6.66 | 6.89 | 7.72 | 7.31 | 7.15 | 7.50 | 8.36 |
| $Na_2O$ | 3.05 | 2.89 | 3.04 | 3.14 | 3.19 | 3.10 | 3.10 | 3.18 | 3.47 | 3.10 | 2.86 |
| $K_2O$ | 1.57 | 1.06 | 1.67 | 1.52 | 1.99 | 1.94 | 1.44 | 1.54 | 1.58 | 1.61 | 1.44 |
| $TiO_2$ | 2.07 | 2.11 | 1.99 | 1.93 | 2.14 | 2.09 | 1.99 | 2.16 | 2.28 | 2.00 | 2.15 |
| $P_2O_5$ | 0.36 | 0.26 | 0.29 | 0.29 | 0.32 | 0.30 | 0.32 | 0.37 | 0.44 | 0.31 | 0.34 |
| MnO | 0.20 | 0.18 | 0.19 | 0.19 | 0.18 | 0.19 | 0.18 | 0.23 | 0.20 | 0.19 | 0.20 |
| Total | 100.00 | 100.00 | 100.00 | 100.00 | 100.00 | 100.00 | 100.00 | 100.00 | 100.00 | 100.00 | 100.00 |

**Table 4.** Average chemical composition of geochemical units in the Wanapum Basalt

[Chemical types listed in approximate stratigraphic order, see table 1. Trace elements followed by X analyzed by X-ray fluorescence; all others analyzed by instrumental neutron activation. n.a., not analyzed; Data from which these average compositions are calculated are given in Wright (1988)]

| Geochemical unit-------- | PV | LOLO INC | ROSALIA | PH POWAT | ROZA | FS ANOM | FS INC | SHUMAKER | PH SHUM | SW LOOK | DODGE | ROBIN |
|---|---|---|---|---|---|---|---|---|---|---|---|---|
| Chemical type- | A | B | C | D | E | F | F | G | G | H | I | J |
| | | | | | Major oxides (weight percent) | | | | | | | |
| $SiO_2$ | 51.27 | 49.98 | 49.78 | 53.82 | 50.74 | 52.68 | 51.51 | 54.36 | 54.29 | 54.48 | 52.15 | 49.78 |
| $Al_2O_3$ | 15.41 | 14.13 | 13.39 | 14.59 | 14.21 | 13.94 | 13.43 | 13.86 | 14.38 | 14.66 | 15.41 | 16.78 |
| FeO | 10.23 | 13.89 | 14.73 | 12.93 | 13.45 | 11.16 | 14.30 | 13.42 | 13.46 | 13.28 | 10.73 | 10.13 |
| MgO | 3.75 | 5.15 | 4.48 | 3.23 | 4.55 | 4.29 | 4.42 | 2.89 | 2.97 | 2.91 | 5.89 | 8.19 |
| CaO | 10.42 | 8.80 | 8.64 | 7.00 | 8.53 | 8.68 | 8.05 | 6.39 | 6.55 | 6.54 | 9.86 | 10.80 |
| $Na_2O$ | 3.13 | 2.58 | 2.79 | 3.03 | 2.84 | 2.86 | 2.73 | 3.23 | 3.41 | 3.05 | 2.90 | 2.42 |
| $K_2O$ | 1.18 | 1.05 | 1.21 | 1.93 | 1.25 | 1.38 | 1.35 | 1.87 | 1.81 | 1.96 | 0.68 | 0.37 |
| $TiO_2$ | 3.50 | 3.22 | 3.59 | 2.67 | 3.11 | 3.52 | 3.01 | 2.45 | 2.47 | 2.71 | 1.45 | 0.97 |
| $P_2O_5$ | 0.79 | 0.73 | 0.84 | 1.15 | 0.68 | 0.71 | 0.61 | 0.90 | 0.89 | 0.75 | 0.36 | 0.17 |
| MnO | 0.15 | 0.19 | 0.20 | 0.24 | 0.25 | 0.23 | 0.22 | 0.30 | 0.26 | 0.22 | 0.15 | 0.14 |
| Total | 99.83 | 99.72 | 99.65 | 100.59 | 99.61 | 99.45 | 99.63 | 99.67 | 100.49 | 100.56 | 99.58 | 99.75 |
| | | | | | Trace elements (parts per million) | | | | | | | |
| Ba | 677 | 539 | 600 | 1043 | 556 | 812 | 549 | 991 | 1024 | 762 | 348 | 175 |
| BaX | 650 | 481 | 524 | 955 | 572 | 807 | 457 | 1001 | 972 | 761 | 327 | 135 |
| Co | 28.8 | 40.2 | 37.7 | n.a. | 38.5 | 52.9 | 38.8 | 23.9 | n.a. | n.a. | 36.9 | 46.6 |
| Cr | 102.9 | 82 | 13.6 | n.a. | 44.3 | 24.4 | 39.5 | 4.4 | 4.9 | 6.8 | 159.7 | 151.4 |
| Cs | 0.62 | 0.70 | 0.89 | 1.15 | 0.78 | 0.95 | 0.93 | 1.02 | 0.86 | 1.21 | 0.50 | n.a. |
| Hf | 5.02 | 4.66 | 5.43 | 6.40 | 4.64 | 5.08 | 4.42 | 6.16 | 6.33 | 5.63 | 2.86 | 1.48 |
| NbX | 19.0 | 15.8 | 17.0 | 20.0 | 17.0 | 17.5 | 13.0 | 19.3 | 24.0 | 18.5 | 8.7 | 6.0 |
| Rb | 28.2 | 26.6 | 34.6 | 38.9 | 31.4 | 37.5 | 35.4 | 35.5 | 36.0 | 36.7 | 15.8 | n.a. |
| RbX | 31.5 | 27.3 | 31.7 | 42.0 | 37.8 | 45.0 | 32.3 | 42.7 | 44.0 | 49.0 | 13.6 | n.a. |
| SrX | 330 | 302 | 286 | 354 | 313 | 353 | 317 | 335 | 308 | 331 | 397 | 353 |
| Ta | 1.18 | 1.09 | 1.22 | 1.26 | 1.05 | 1.22 | 0.98 | 1.33 | 1.29 | 1.29 | 0.51 | 0.31 |
| Th | 3.89 | 3.56 | 4.04 | 5.44 | 3.98 | 4.91 | 3.88 | 5.27 | 5.52 | 5.47 | 1.16 | 0.37 |
| U | 1.11 | 0.88 | 0.93 | 1.64 | 1.22 | 1.56 | 0.85 | 1.66 | 1.45 | 1.56 | 0.52 | n.a. |
| YX | 50.5 | 41.8 | 43.7 | 56.0 | 44.3 | 58.0 | 41.3 | 55.0 | 52.0 | 48.5 | 31 | 20.3 |
| Zn | 208 | 170 | 173 | 152 | 163 | 216 | 172 | 165 | 153 | 141 | 123 | 112 |
| Zr | 133 | 223 | 238 | 270 | 223 | 202 | 196 | 307 | 255 | 239 | 136 | 96 |
| ZrX | 207 | 198 | 224 | 260 | 200 | 219 | 185 | 256 | 260 | 235 | 124 | 68 |
| Sc | 39.9 | 36.0 | 37.3 | 31.5 | 36.1 | 38.6 | 35.8 | 33.4 | 33.6 | 30.6 | 40.1 | 36.7 |
| La | 30.0 | 28.0 | 31.1 | 37.1 | 27.0 | 31.1 | 25.4 | 36.1 | 35.7 | 30.0 | 15.2 | 7.6 |
| Ce | 58.9 | 57.4 | 62.7 | 82.0 | 54.2 | 57.7 | 51.0 | 75.2 | 77.7 | 64.4 | 32.3 | 16.3 |
| Nd | 37.5 | 34.4 | 35.8 | 49.9 | 34.8 | 35.9 | 30.9 | 44.7 | 47.0 | 38.4 | 20.8 | 12.8 |
| Sm | 9.4 | 7.9 | 7.6 | 11.7 | 6.9 | 9.0 | 6.1 | 11.1 | 11.2 | 9.0 | 4.2 | 2.7 |
| Eu | 2.69 | 2.56 | 2.66 | 3.35 | 2.25 | 2.34 | 2.16 | 3.24 | 3.28 | 2.48 | 1.41 | 1.00 |
| Gd | 9.2 | 8.6 | 9.4 | 11.5 | 7.9 | 8.9 | 7.9 | 10.1 | 10.5 | 8.7 | 5.0 | 3.6 |
| Tb | 1.47 | 1.37 | 1.44 | 1.87 | 1.19 | 1.39 | 1.21 | 1.60 | 1.67 | 1.36 | 0.81 | 0.63 |
| Yb | 4.62 | 3.92 | 4.62 | 5.69 | 3.89 | 4.63 | 3.52 | 5.55 | 5.62 | 4.65 | 3.08 | 2.10 |
| Lu | 0.73 | 0.62 | 0.69 | 0.92 | 0.64 | 0.78 | 0.59 | 0.86 | 0.91 | 0.78 | 0.47 | 0.35 |
| Cu | 45.0 | 37.3 | 27.7 | n.a. | 39.6 | 29.5 | 35.3 | 29.5 | n.a. | 15.0 | 105.7 | 78.7 |
| Ni | 31.5 | 35.0 | 27.0 | n.a. | 33.6 | 46.5 | 39.3 | 2.5 | n.a. | 1 | 42.7 | 117 |
| | | | | | Normalized major-oxide contents (weight percent) | | | | | | | |
| $SiO_2$ | 51.36 | 50.12 | 49.95 | 53.50 | 50.94 | 52.97 | 51.70 | 54.54 | 54.03 | 54.18 | 52.37 | 49.90 |
| $Al_2O_3$ | 15.44 | 14.17 | 13.44 | 14.50 | 14.27 | 14.02 | 13.48 | 13.91 | 14.31 | 14.58 | 15.47 | 16.82 |
| FeO | 10.25 | 13.93 | 14.78 | 12.85 | 13.50 | 11.22 | 14.35 | 13.46 | 13.39 | 13.21 | 10.78 | 10.16 |
| MgO | 3.76 | 5.16 | 4.50 | 3.21 | 4.57 | 4.31 | 4.44 | 2.90 | 2.96 | 2.89 | 5.91 | 8.21 |
| CaO | 10.44 | 8.82 | 8.67 | 6.96 | 8.56 | 8.73 | 8.08 | 6.41 | 6.52 | 6.50 | 9.90 | 10.83 |
| $Na_2O$ | 3.14 | 2.59 | 2.80 | 3.01 | 2.85 | 2.88 | 2.74 | 3.24 | 3.39 | 3.03 | 2.91 | 2.43 |
| $K_2O$ | 1.18 | 1.05 | 1.21 | 1.92 | 1.25 | 1.39 | 1.36 | 1.88 | 1.80 | 1.95 | 0.68 | 0.37 |
| $TiO_2$ | 3.51 | 3.23 | 3.60 | 2.65 | 3.12 | 3.54 | 3.02 | 2.46 | 2.46 | 2.69 | 1.46 | 0.97 |
| $P_2O_5$ | 0.79 | 0.73 | 0.84 | 1.14 | 0.68 | 0.71 | 0.61 | 0.90 | 0.89 | 0.75 | 0.36 | 0.17 |
| MnO | 0.15 | 0.19 | 0.20 | 0.24 | 0.25 | 0.23 | 0.22 | 0.30 | 0.26 | 0.22 | 0.15 | 0.14 |
| Total | 100.00 | 100.00 | 100.00 | 100.00 | 100.00 | 100.00 | 100.00 | 100.00 | 100.00 | 100.00 | 100.00 | 100.00 |

**Table 5.** Average chemical composition of geochemical units in the Saddle Mountains Basalt

[Chemical types listed in approximate stratigraphic order, see table 1. Trace elements followed by X analyzed by X-ray fluorescence; all others analyzed by instrumental neutron activation. n.a., not analyzed. Data from which these average compositions are calculated are given in Wright (1988)]

| Geochemical unit-------- | LM | GOOSE | INDIAN | MARTIN | BASIN | BUFORD | ELEPHANT | POMONA | VC WEIPE | ESQUAT | RBESQUAT | FS IC | SLIP |
|---|---|---|---|---|---|---|---|---|---|---|---|---|---|
| Chemical type- | A | B | C | D | E | F | G | H | I | J | J | K | L |
| Major oxides (weight percent) | | | | | | | | | | | | | |
| $SiO_2$ | 50.01 | 47.54 | 49.17 | 48.58 | 47.35 | 53.82 | 51.19 | 51.94 | 51.72 | 54.14 | 53.51 | 52.47 | 52.00 |
| $Al_2O_3$ | 14.12 | 12.34 | 13.76 | 13.69 | 13.74 | 14.17 | 13.26 | 15.02 | 15.30 | 13.82 | 14.35 | 13.48 | 14.29 |
| FeO | 14.16 | 17.36 | 14.36 | 14.40 | 14.98 | 11.34 | 14.77 | 10.44 | 11.26 | 12.62 | 13.33 | 13.90 | 11.69 |
| MgO | 4.87 | 4.50 | 5.40 | 5.87 | 6.03 | 4.98 | 4.17 | 7.18 | 6.49 | 3.97 | 3.70 | 4.20 | 5.47 |
| CaO | 8.60 | 8.76 | 9.13 | 9.88 | 9.72 | 8.47 | 8.34 | 10.38 | 10.39 | 7.38 | 7.53 | 7.60 | 9.60 |
| $Na_2O$ | 2.68 | 2.42 | 2.41 | 2.36 | 2.27 | 2.77 | 2.44 | 2.23 | 2.53 | 2.57 | 2.54 | 2.66 | 2.64 |
| $K_2O$ | 1.43 | 1.21 | 1.00 | 0.74 | 0.78 | 1.41 | 1.25 | 0.65 | 0.49 | 1.71 | 1.65 | 1.61 | 0.91 |
| $TiO_2$ | 2.92 | 3.80 | 3.40 | 3.31 | 3.69 | 2.21 | 3.60 | 1.62 | 1.83 | 2.91 | 3.15 | 3.16 | 2.43 |
| $P_2O_5$ | 0.64 | 1.56 | 0.84 | 0.74 | 0.87 | 0.38 | 0.60 | 0.24 | 0.29 | 0.44 | 0.42 | 0.52 | 0.53 |
| MnO | 0.20 | 0.27 | 0.23 | 0.21 | 0.24 | 0.15 | 0.23 | 0.18 | 0.19 | 0.22 | 0.19 | 0.21 | 0.15 |
| Total | 99.63 | 99.76 | 99.70 | 99.78 | 99.67 | 99.70 | 99.85 | 99.88 | 100.49 | 99.78 | 100.37 | 99.81 | 99.71 |
| Trace elements (parts per million) | | | | | | | | | | | | | |
| Ba | 541 | 852 | 701 | 638 | 611 | 425 | 485 | 243 | 292 | 592 | 611 | 592 | 423 |
| BaX | 523 | 830 | 687 | 612 | 603 | 444 | 320 | 173 | 265 | 577 | 658 | 481 | 308 |
| Co | 41.6 | 38.1 | 41.6 | 43.1 | 46.5 | 39.2 | 45.0 | 43.5 | n.a. | 40.7 | n.a. | 46.1 | 43.8 |
| Cr | 24.0 | 41.3 | 117.5 | 194.9 | 148.8 | 44.5 | 18.5 | 109.0 | 51.8 | 18.9 | 7.1 | 21.4 | 38.3 |
| Cs | 1.23 | 0.45 | 0.50 | n.a. | n.a. | 0.85 | 0.70 | 0.90 | n.a. | 0.98 | 0.89 | 0.78 | n.a. |
| Hf | 4.63 | 10.74 | 6.74 | 5.90 | 6.59 | 5.30 | 6.41 | 3.23 | 3.28 | 5.57 | 5.81 | 5.38 | 4.40 |
| NbX | 25.7 | 48.5 | 29.0 | 21.3 | 23.7 | 21.3 | 24.5 | 13.0 | 12.5 | 21.80 | 23.0 | 24.0 | 18.0 |
| Rb | 18.0 | 30.1 | 28.3 | 20.6 | 19.8 | 35.5 | 27.6 | 10.0 | 9.0 | 47.3 | 32.0 | 35.30 | 19.0 |
| RbX | 35.3 | 22.5 | 16.0 | 10.0 | 10.0 | 43.3 | 24.0 | 18.0 | 26.5 | 51.5 | 50.0 | 46.5 | 25.0 |
| SrX | 350 | 220 | 233 | 235 | 227 | 230 | 213 | 227 | 235 | 257 | 269 | 245 | 244 |
| Ta | 1.68 | 3.07 | 1.92 | 1.66 | 1.91 | 1.53 | 1.74 | 0.82 | 0.81 | 1.63 | 1.67 | 1.79 | 1.24 |
| Th | 4.98 | 4.34 | 3.53 | 2.10 | 2.19 | 7.10 | 5.91 | 2.55 | 2.47 | 8.67 | 8.93 | 7.23 | 4.70 |
| U | 1.38 | 1.12 | 0.90 | 0.65 | 0.75 | 1.70 | 1.42 | 0.77 | 0.47 | 2.08 | 1.61 | 1.80 | 1.10 |
| YX | 35.3 | 89.5 | 52.0 | 45.0 | 52.3 | 44.0 | 42.0 | 26.5 | 27.5 | 41.3 | 38.0 | 35.5 | 28.0 |
| Zn | 147 | 226 | 173 | 161 | 177 | 129 | 179 | 118 | 102 | 134 | 127 | 164 | 135 |
| Zr | 350 | 502 | 297 | 304 | 293 | n.a. | 316 | n.a. | 170 | 240 | 250 | 250 | n.a. |
| ZrX | 189 | 436 | 273 | 238 | 273 | 216 | 229 | 137 | 140 | 226 | 223 | 219 | 180 |
| Sc | 22.6 | 37.5 | 38.5 | 39.3 | 39.0 | 31.2 | 31.7 | 34.4 | 35.8 | 27.7 | 28.4 | 29.3 | 33.4 |
| La | 35.3 | 74.1 | 46.0 | 36.8 | 42.9 | 33.0 | 33.7 | 17.0 | 17.1 | 38.2 | 38.6 | 35.8 | 28.0 |
| Ce | 67.8 | 149 | 90.9 | 73.6 | 85.6 | 63.0 | 68.7 | 35.3 | 35.4 | 73.8 | 74.6 | 69.3 | 57.5 |
| Nd | 34.0 | 86.9 | 53.3 | 47.3 | 53.7 | 33.5 | 35.3 | 20.5 | 21.1 | 36.7 | 38.5 | 34.3 | 31.0 |
| Sm | 7.1 | 18.7 | 11.0 | 9.1 | 10.7 | 7.3 | 9.4 | 4.7 | 5.0 | 8.4 | 8.3 | 8.3 | 7.0 |
| Eu | 2.10 | 5.41 | 3.22 | 2.82 | 3.31 | 1.83 | 2.44 | 1.41 | 1.47 | 2.18 | 2.24 | 2.15 | 1.94 |
| Gd | 8.2 | 18.4 | 10.1 | 9.0 | 9.7 | 6.9 | 8.7 | 5.0 | 5.1 | 8.0 | 8.2 | 8.2 | 7.5 |
| Tb | 1.34 | 2.66 | 1.21 | 1.11 | 1.24 | 1.41 | 1.39 | 0.68 | 0.82 | 1.49 | 0.98 | 1.42 | 1.12 |
| Yb | 3.13 | 9.08 | 5.55 | 5.01 | 5.64 | 3.90 | 4.58 | 2.73 | 2.66 | 3.65 | 3.58 | 3.75 | 3.40 |
| Lu | 0.46 | 1.35 | 0.82 | 0.74 | 0.82 | 0.57 | 0.66 | 0.39 | 0.44 | 0.51 | 0.53 | 0.53 | 0.48 |
| Cu | 17.5 | 27.0 | 39.0 | 33.0 | 46.0 | 32.5 | 39.7 | 63.0 | n.a. | 34.5 | n.a. | 28.0 | n.a. |
| Ni | 28.5 | 9.8 | 13.0 | 34.0 | 42.0 | 40.5 | 30.7 | 51.3 | n.a. | 16.0 | n.a. | 16.0 | n.a. |
| Normalized major-oxide contents (weight percent) | | | | | | | | | | | | | |
| $SiO_2$ | 50.20 | 47.65 | 49.32 | 48.69 | 47.51 | 53.98 | 51.27 | 52.00 | 51.47 | 54.26 | 53.31 | 52.57 | 52.15 |
| $Al_2O_3$ | 14.17 | 12.37 | 13.80 | 13.72 | 13.79 | 14.21 | 13.28 | 15.04 | 15.23 | 13.85 | 14.30 | 13.51 | 14.33 |
| FeO | 14.21 | 17.40 | 14.40 | 14.43 | 15.03 | 11.37 | 14.79 | 10.45 | 11.21 | 12.65 | 13.28 | 13.93 | 11.72 |
| MgO | 4.89 | 4.51 | 5.42 | 5.88 | 6.05 | 4.99 | 4.18 | 7.19 | 6.46 | 3.98 | 3.69 | 4.21 | 5.49 |
| CaO | 8.63 | 8.78 | 9.16 | 9.90 | 9.75 | 8.50 | 8.35 | 10.39 | 10.34 | 7.40 | 7.50 | 7.61 | 9.63 |
| $Na_2O$ | 2.69 | 2.43 | 2.42 | 2.37 | 2.28 | 2.78 | 2.44 | 2.23 | 2.52 | 2.58 | 2.53 | 2.67 | 2.65 |
| $K_2O$ | 1.44 | 1.21 | 1.00 | 0.74 | 0.78 | 1.41 | 1.25 | 0.65 | 0.49 | 1.71 | 1.64 | 1.61 | 0.91 |
| $TiO_2$ | 2.93 | 3.81 | 3.41 | 3.32 | 3.70 | 2.22 | 3.61 | 1.62 | 1.82 | 2.92 | 3.14 | 3.17 | 2.44 |
| $P_2O_5$ | 0.64 | 1.56 | 0.84 | 0.74 | 0.87 | 0.38 | 0.60 | 0.24 | 0.29 | 0.44 | 0.42 | 0.52 | 0.53 |
| MnO | 0.20 | 0.27 | 0.23 | 0.21 | 0.24 | 0.15 | 0.23 | 0.18 | 0.19 | 0.22 | 0.19 | 0.21 | 0.15 |
| Total | 100.00 | 100.00 | 100.00 | 100.00 | 100.00 | 100.00 | 100.00 | 100.00 | 100.00 | 100.00 | 100.00 | 100.00 | 100.00 |

Table 5. Average chemical composition of geochemical units in the Saddle Mountains Basalt—*Continued*

| Geochemical unit-------- | LEW ORCH | SPRAGUE | SW SPRAG | NEW | SW NEW | ASOTIN | VC ASOT | SW HUNTZ | HUNTZ | VC LAP | EAGLE | WILBUR | UMATILLA |
|---|---|---|---|---|---|---|---|---|---|---|---|---|---|
| Chemical type- | M | N | N | O | O | P | P | Q | Q | R | R | S | T |
| Major oxides (weight percent) | | | | | | | | | | | | | |
| SiO2 | 49.63 | 50.76 | 49.65 | 49.22 | 50.11 | 50.76 | 51.11 | 52.37 | 52.50 | 53.08 | 52.86 | 54.23 | 54.51 |
| Al2O3 | 15.22 | 13.72 | 14.54 | 15.64 | 15.95 | 16.02 | 16.54 | 16.05 | 15.39 | 15.85 | 15.35 | 14.46 | 14.18 |
| FeO | 11.80 | 12.60 | 13.41 | 10.85 | 10.42 | 9.52 | 9.83 | 9.56 | 10.37 | 10.47 | 10.52 | 11.16 | 12.23 |
| MgO | 7.09 | 5.07 | 6.39 | 7.97 | 7.41 | 8.23 | 7.88 | 7.56 | 6.52 | 5.84 | 5.99 | 4.50 | 2.74 |
| CaO | 10.08 | 9.83 | 9.92 | 11.00 | 11.50 | 10.77 | 10.78 | 10.18 | 9.38 | 9.26 | 9.16 | 8.40 | 6.18 |
| Na2O | 2.32 | 2.64 | 2.63 | 2.19 | 2.51 | 2.29 | 1.99 | 2.43 | 2.34 | 2.33 | 2.45 | 2.64 | 3.37 |
| K2O | 0.46 | 0.87 | 0.61 | 0.40 | 0.29 | 0.39 | 0.46 | 0.65 | 1.22 | 1.32 | 1.15 | 1.76 | 2.55 |
| TiO2 | 2.42 | 3.17 | 2.73 | 1.89 | 1.93 | 1.48 | 1.48 | 1.47 | 1.63 | 1.71 | 1.70 | 1.90 | 2.78 |
| P2O5 | 0.55 | 0.79 | 0.64 | 0.47 | 0.47 | 0.19 | 0.24 | 0.28 | 0.34 | 0.41 | 0.41 | 0.51 | 0.82 |
| MnO | 0.21 | 0.18 | 0.22 | 0.15 | 0.18 | 0.14 | 0.20 | 0.20 | 0.20 | 0.17 | 0.13 | 0.23 | 0.19 |
| Total | 99.78 | 99.63 | 100.74 | 99.78 | 100.77 | 99.79 | 100.51 | 100.75 | 99.89 | 100.44 | 99.72 | 99.79 | 99.55 |
| Trace elements (parts per million) | | | | | | | | | | | | | |
| Ba | 410 | 767 | 506 | 320 | 342 | 303 | 277 | 352 | 410 | 665 | 570 | 876 | 3313 |
| BaX | 351 | 598 | 486 | 329 | 336 | 249 | 278 | 262 | n.a. | 598 | 593 | 757 | 3184 |
| Co | 43.8 | 46.2 | n.a. | 45.0 | n.a. | 46.9 | n.a. | n.a. | 42.7 | n.a. | 41.2 | 42.5 | 28.1 |
| Cr | 267.0 | 48.6 | 150.5 | 300.5 | 307.5 | 283.7 | 272.5 | 222.0 | 172.0 | 115.4 | 98.1 | 36.6 | 3.6 |
| Cs | n.a. | n.a. | n.a. | n.a. | n.a. | n.a. | n.a. | 0.34 | 0.50 | 0.63 | 0.70 | 0.80 | 0.73 |
| Hf | 3.90 | 6.35 | 5.23 | 3.05 | 3.05 | 2.78 | 2.90 | 3.23 | 4.20 | 4.89 | 5.13 | 5.90 | 10.22 |
| NbX | 18.0 | 28.0 | 23.0 | 18.0 | 16.5 | 13.0 | 12.0 | 13.0 | n.a. | 18.30 | 16 | 16.70 | 21.30 |
| Rb | n.a. | n.a. | 17.5 | n.a. | 13.4 | 10.0 | 17.5 | 22.0 | 26.5 | 31.5 | 38.8 | 38.2 | 47.0 |
| RbX | n.a. | 6.0 | n.a. | 13.0 | 9.0 | 14.5 | 10.0 | 17.0 | n.a. | 34.30 | 24.0 | 43.3 | 43.0 |
| SrX | 242 | 253 | 229 | 252 | 259 | 252 | 249 | 240 | n.a. | 274 | 296 | 277 | 276 |
| Ta | 1.23 | 1.64 | 1.49 | 0.96 | 0.88 | 0.65 | 0.62 | 0.80 | 0.72 | 0.91 | 1.18 | 1.06 | 1.49 |
| Th | 1.53 | 3.00 | 2.34 | 1.40 | 1.35 | 2.05 | 2.15 | 2.63 | 3.90 | 5.13 | 5.04 | 6.65 | 7.25 |
| U | 0.95 | 1.45 | 0.61 | n.a. | 1 | n.a. | 0.70 | 0.61 | 0.50 | 1.08 | 1.17 | 1.10 | 1.43 |
| YX | 34.5 | 47.0 | 46.5 | 35.0 | 33.0 | 26.7 | 25.0 | 24.0 | n.a. | 43.0 | 37.0 | 41.7 | 49.7 |
| Zn | 131 | 162 | 128 | 116 | 111 | 107 | 103 | 87 | 103 | 117 | 126 | 131 | 135 |
| Zr | 203 | 360 | 255 | n.a. | 160 | n.a. | 126 | 140 | 195 | 230 | 234 | 282 | 520 |
| ZrX | 172 | 274 | 228 | 141 | 134 | 121 | 120 | 141 | n.a. | 216 | 164 | 249 | 482 |
| Sc | 37.3 | 37.4 | 38.5 | 34.6 | 35.7 | 30.8 | 30.9 | 29.2 | 28.7 | 27.8 | 29.0 | 26.6 | 26.2 |
| La | 27.8 | 42.5 | 34.7 | 20.0 | 20.5 | 15.7 | 15.0 | 17.7 | 27.0 | 33.3 | 31.6 | 43.7 | 46.7 |
| Ce | 56.0 | 87.0 | 73.9 | 41.0 | 41.5 | 31.5 | 30.5 | 36.2 | 52.0 | 62.1 | 61.2 | 80.5 | 88.2 |
| Nd | 29.3 | 48.0 | 42.4 | 24.0 | 27.0 | 18.0 | 19.0 | 19.5 | 27.5 | 33.8 | 32.3 | 39.5 | 49.2 |
| Sm | 6.8 | 10.3 | 9.2 | 5.3 | 5.1 | 4.3 | 4.0 | 4.5 | 5.9 | 6.6 | 6.5 | 7.8 | 9.8 |
| Eu | 2.03 | 2.69 | 2.44 | 1.61 | 1.71 | 1.28 | 1.29 | 1.30 | 1.56 | 1.71 | 1.92 | 1.93 | 3.95 |
| Gd | 6.9 | 9.5 | 8.2 | 4.2 | 6.4 | 4.7 | 4.5 | 4.4 | 5.6 | 6.8 | 7.2 | 7.6 | 10.2 |
| Tb | 1.11 | 1.63 | 1.32 | 0.86 | 0.93 | 0.74 | 0.80 | 0.73 | 0.82 | 0.99 | 1.04 | 1.32 | 1.69 |
| Yb | 3.53 | 4.80 | 4.17 | 2.50 | 2.85 | 2.37 | 2.45 | 2.30 | 2.85 | 3.59 | 3.85 | 4.23 | 4.52 |
| Lu | 0.53 | 0.69 | 0.75 | 0.40 | 0.42 | 0.35 | 0.35 | 0.49 | 0.55 | 0.56 | 0.56 | 0.63 | 0.66 |
| Cu | 59.5 | 46.0 | 57.0 | 67.0 | 89.0 | 111.7 | 100.0 | 96.0 | n.a. | 49.0 | 52.5 | 25.0 | 19.0 |
| Ni | 84.5 | 70.0 | 85.0 | 140.0 | 140.0 | 203.3 | 140.0 | 170.0 | n.a. | 54.0 | 93.0 | 47.0 | 2.7 |
| Normalized major-oxide contents (weight percent) | | | | | | | | | | | | | |
| SiO2 | 49.74 | 50.95 | 49.29 | 49.33 | 49.73 | 50.87 | 50.85 | 51.98 | 52.56 | 52.85 | 53.01 | 54.34 | 54.76 |
| Al2O3 | 15.25 | 13.77 | 14.43 | 15.67 | 15.83 | 16.05 | 16.46 | 15.93 | 15.41 | 15.78 | 15.39 | 14.49 | 14.24 |
| FeO | 11.83 | 12.65 | 13.31 | 10.87 | 10.34 | 9.54 | 9.78 | 9.49 | 10.38 | 10.42 | 10.55 | 11.18 | 12.29 |
| MgO | 7.11 | 5.09 | 6.34 | 7.99 | 7.35 | 8.25 | 7.84 | 7.50 | 6.53 | 5.81 | 6.01 | 4.51 | 2.75 |
| CaO | 10.10 | 9.87 | 9.85 | 11.02 | 11.41 | 10.79 | 10.73 | 10.10 | 9.39 | 9.22 | 9.19 | 8.42 | 6.21 |
| Na2O | 2.33 | 2.65 | 2.61 | 2.19 | 2.49 | 2.29 | 1.98 | 2.41 | 2.34 | 2.32 | 2.46 | 2.65 | 3.39 |
| K2O | 0.46 | 0.87 | 0.61 | 0.40 | 0.29 | 0.39 | 0.46 | 0.65 | 1.22 | 1.31 | 1.15 | 1.76 | 2.56 |
| TiO2 | 2.43 | 3.18 | 2.71 | 1.89 | 1.92 | 1.48 | 1.47 | 1.46 | 1.63 | 1.70 | 1.70 | 1.90 | 2.79 |
| P2O5 | 0.55 | 0.79 | 0.64 | 0.47 | 0.47 | 0.19 | 0.24 | 0.28 | 0.34 | 0.41 | 0.41 | 0.51 | 0.82 |
| MnO | 0.21 | 0.18 | 0.22 | 0.15 | 0.18 | 0.14 | 0.20 | 0.20 | 0.20 | 0.17 | 0.13 | 0.23 | 0.19 |
| Total | 100.00 | 100.00 | 100.00 | 100.00 | 100.00 | 100.00 | 100.00 | 100.00 | 100.00 | 100.00 | 100.00 | 100.00 | 100.00 |

**Table 5.** Average chemical composition of geochemical units in the Saddle Mountains Basalt—*Continued*

| Geochemical unit------- <br> Chemical type- | UM FRAC <br> T | PH UMTIL <br> T | PH SOPHER <br> U |
|---|---|---|---|
| **Major oxides (weight percent)** | | | |
| SiO2 | 59.09 | 55.56 | 54.49 |
| Al2O3 | 16.62 | 15.04 | 15.08 |
| FeO | 5.79 | 11.77 | 11.76 |
| MgO | 0.60 | 2.49 | 2.89 |
| CaO | 5.32 | 6.01 | 6.63 |
| Na2O | 4.10 | 3.16 | 3.06 |
| K2O | 3.51 | 2.60 | 2.41 |
| TiO2 | 3.27 | 2.71 | 3.06 |
| P2O5 | 1.20 | 0.97 | 0.86 |
| MnO | 0.06 | 0.19 | 0.23 |
| Total | 99.56 | 100.50 | 100.47 |
| **Trace elements (parts per million)** | | | |
| Ba | 4410 | 3585 | 3153 |
| BaX | 4161 | 3478 | 3281 |
| Co | 12.7 | n.a. | n.a. |
| Cr | 3.2 | 1.7 | 1.4 |
| Cs | 0.69 | 0.63 | 0.65 |
| Hf | 12.48 | 10.55 | 9.83 |
| NbX | 25.0 | 20.0 | 17.5 |
| Rb | 59.8 | 56.3 | 42.3 |
| RbX | 56.0 | 44.0 | 35.0 |
| SrX | 346 | 285 | 338 |
| Ta | 1.58 | 1.62 | 1.44 |
| Th | 8.89 | 7.45 | 7.00 |
| U | 1.74 | 1.42 | 1.02 |
| YX | 54.0 | 49.0 | 43.0 |
| Zn | 199 | 135 | 139 |
| Zr | 631 | 543 | 494 |
| ZrX | 546 | 517 | 462 |
| Sc | 29.9 | 25.8 | 27.4 |
| La | 57.0 | 48.8 | 45.0 |
| Ce | 114.4 | 89.3 | 85.5 |
| Nd | 57.3 | 50.5 | 43.3 |
| Sm | 12.6 | 9.5 | 8.5 |
| Eu | 5.15 | 4.12 | 3.68 |
| Gd | 12.0 | 10.70 | 9.2 |
| Tb | 1.74 | 1.49 | 1.29 |
| Yb | 4.39 | 4.55 | 4.28 |
| Lu | 0.66 | 0.66 | 0.65 |
| Cu | 5.0 | 26.0 | 15.0 |
| Ni | n.a. | 75.0 | 5.0 |
| **Normalized major-oxide contents (weight percent)** | | | |
| SiO2 | 59.35 | 55.28 | 54.24 |
| Al2O3 | 16.69 | 14.97 | 15.01 |
| FeO | 5.82 | 11.71 | 11.70 |
| MgO | 0.60 | 2.48 | 2.88 |
| CaO | 5.34 | 5.98 | 6.60 |
| Na2O | 4.12 | 3.14 | 3.05 |
| K2O | 3.53 | 2.59 | 2.40 |
| TiO2 | 3.28 | 2.70 | 3.05 |
| P2O5 | 1.21 | 0.97 | 0.86 |
| MnO | 0.06 | 0.19 | 0.23 |
| Total | 100.00 | 100.00 | 100.00 |

## Table 6. Average chemical composition of feeder dikes in the Yakima Basalt Subgroup

[Chemical types listed in approximate stratigraphic order, see table 1. Trace elements followed by X analyzed by X-ray fluorescence; all others analyzed by instrumental neutron activation. n.a., not analyzed. Data from which these average compositions are calculated are given in Wright (1988). GRB CT1 and GRB CT3 refer to geochemical units 1 and 3 in table 3]

| Geochemical unit-------- | ELEPHANT | UMATILLA | LOLOINC | ROSALIA | ROZA | FSINC | SHUMAKER | DODGE | ROBIN | GRB CT1 | GRB CT3 | GRB CT3 | GRB LH2 | GRB MG6 |
|---|---|---|---|---|---|---|---|---|---|---|---|---|---|---|
| Chemical type- | G | T | B | C | E | F | G | I | J | A | C | C | 1 | 2 |
| Major oxides (weight percent) | | | | | | | | | | | | | | |
| $SiO_2$ | 51.25 | 54.68 | 50.75 | 50.23 | 51.07 | 51.43 | 54.43 | 51.94 | 49.43 | 54.29 | 53.22 | 54.54 | 54.48 | 52.56 |
| $Al_2O_3$ | 13.22 | 13.07 | 13.57 | 12.76 | 13.46 | 13.49 | 13.06 | 14.56 | 16.58 | 14.49 | 14.44 | 14.21 | 14.83 | 14.38 |
| FeO | 14.75 | 13.34 | 13.77 | 15.35 | 14.05 | 14.19 | 13.42 | 10.70 | 10.39 | 11.15 | 11.47 | 11.39 | 9.48 | 11.63 |
| MgO | 4.07 | 3.03 | 5.26 | 4.53 | 4.59 | 4.54 | 2.91 | 6.42 | 8.59 | 4.90 | 5.49 | 4.57 | 6.15 | 5.82 |
| CaO | 8.10 | 5.66 | 8.47 | 8.19 | 8.33 | 8.12 | 6.65 | 10.16 | 11.03 | 8.53 | 9.11 | 8.09 | 9.39 | 9.29 |
| $Na_2O$ | 2.64 | 3.24 | 2.73 | 2.47 | 2.75 | 2.73 | 3.51 | 3.16 | 2.35 | 2.86 | 2.75 | 3.15 | 2.80 | 2.72 |
| $K_2O$ | 1.22 | 2.51 | 0.84 | 1.13 | 1.43 | 1.34 | 2.01 | 0.61 | 0.23 | 1.22 | 1.11 | 1.22 | 0.96 | 1.03 |
| $TiO_2$ | 3.76 | 2.72 | 3.25 | 3.71 | 3.26 | 2.94 | 2.47 | 1.53 | 0.92 | 1.73 | 1.73 | 1.93 | 1.27 | 1.78 |
| $P_2O_5$ | 0.49 | 1.02 | 0.83 | 0.84 | 0.60 | 0.62 | 0.83 | 0.36 | 0.18 | 0.35 | 0.32 | 0.33 | 0.29 | 0.36 |
| MnO | 0.20 | 0.17 | 0.18 | 0.19 | 0.23 | 0.25 | 0.28 | 0.16 | 0.19 | 0.19 | 0.17 | 0.17 | 0.16 | 0.17 |
| Total | 99.70 | 99.44 | 99.65 | 99.40 | 99.77 | 99.65 | 99.57 | 99.60 | 99.89 | 99.71 | 99.81 | 99.60 | 99.81 | 99.74 |
| Trace elements (parts per million) | | | | | | | | | | | | | | |
| Ba | 447 | 3510 | 460 | 531 | 560 | 537 | 1070 | 357 | 145 | 487 | 401 | 524 | 390 | 419 |
| BaX | 480 | 3460 | 490 | 544 | 559 | 524 | 1050 | 345 | 151 | 498 | 427 | 525 | 433 | 434 |
| Co | 41.3 | 25.3 | 36.1 | 36.5 | 39.1 | 38.7 | 23.9 | 36.1 | 45.9 | 38.1 | 38.7 | 35.3 | 32.1 | 38.7 |
| Cr | 18.3 | 4.1 | 91.5 | 18.5 | 33.6 | 46.6 | 4.4 | 161.0 | 152.5 | 44.1 | 83.6 | 26.6 | 86.3 | 112.1 |
| Cs | 0.50 | n.a. | 1.20 | n.a. | 0.80 | 0.95 | 0.60 | n.a. | n.a. | 0.90 | 0.65 | 0.90 | 0.40 | 0.68 |
| Hf | 6.10 | 9.80 | 3.90 | 5.00 | 4.90 | 4.50 | 6.50 | 3.00 | 1.55 | 3.50 | 3.20 | 4.30 | 2.70 | 3.18 |
| NbX | 10.0 | 5.0 | 17.5 | 19.0 | 19.0 | 15.0 | 20.0 | 10.0 | 9.0 | 12.0 | 12.5 | 12.5 | 11.0 | 12.0 |
| Rb | 35.0 | 42.0 | 28.5 | 19.0 | 38.0 | 41.3 | 51.0 | 13.0 | 4.0 | 32.0 | 27.5 | 41.0 | 20.5 | 31.8 |
| RbX | 15.0 | 44.0 | 31.0 | 20.0 | 39.0 | 39.5 | 53.0 | 14.0 | 6.0 | 32.0 | 27.5 | 40.5 | 23.5 | 31.0 |
| SrX | 382 | 291 | 330 | 345 | 322 | 318 | 342 | 377 | 332 | 346 | 343 | 329 | 392 | 386 |
| Ta | 1.71 | 1.40 | 3.00 | 3.60 | 4.20 | 4.10 | 5.70 | 1.10 | 0.50 | 3.20 | 2.55 | 4.20 | 1.75 | 2.25 |
| U | 1.20 | 1.20 | 0.75 | 0.80 | 1.10 | 0.93 | 1.50 | n.a. | n.a. | 0.80 | 0.80 | 1.20 | 0.45 | 0.65 |
| YX | 29.0 | 48.0 | 40.5 | 45.0 | 40.0 | 36.5 | 59.0 | 28.0 | 21.5 | 31.0 | 29.5 | 32.0 | 25.5 | 29.3 |
| Zn | 137 | 134 | 131 | 154 | 140 | 146 | 165 | 110 | 89 | 120 | 105 | 118 | 90 | 114 |
| Zr | 190 | 519 | 150 | 210 | 200 | 145 | 270 | 90 | n.a. | 120 | 170 | 230 | 125 | 160 |
| ZrX | 125 | 484 | 180 | 216 | 200 | 185 | 263 | 124 | 74 | 151 | 143 | 172 | 126 | 140 |
| Sc | 28.9 | 25.0 | 32.7 | 36.7 | 37.4 | 35.4 | 36.0 | 46.0 | 36.5 | 33.6 | 36.3 | 33.0 | 36.4 | 38.8 |
| La | 31.0 | 45.0 | 24.0 | 28.0 | 27.0 | 24.3 | 38.0 | 14.0 | 7.0 | 18.0 | 16.0 | 20.5 | 14.5 | 16.5 |
| Ce | 60.0 | 86.0 | 49.0 | 55.0 | 56.0 | 49.3 | 79.0 | 30.0 | 15.0 | 36.0 | 33.0 | 39.5 | 30.0 | 32.8 |
| Nd | 34.0 | 47.0 | 30.5 | 33.0 | 33,0 | 27.8 | 47.0 | 21.0 | 10.5 | 21.0 | 22.0 | 22.5 | 17.5 | 19.5 |
| Sm | 8.3 | 10.2 | 7.6 | 7.5 | 8.4 | 5.6 | 10.8 | 4.9 | 2.9 | 49.0 | 4.6 | 5.7 | 4.1 | 13.4 |
| Eu | 2.41 | 4.24 | 2.34 | 2.45 | 2.42 | 2.02 | 3.58 | 1.40 | 0.94 | 1.48 | 1.50 | 1.68 | 1.22 | 1.52 |
| Gd | 8.8 | 10.5 | 6.5 | 7.8 | 8.2 | 7.9 | 12.7 | 6.4 | 2.3 | 55.0 | 4.8 | 7.0 | 4.0 | 4.4 |
| Tb | 1.22 | 1.39 | 1.09 | 1.17 | 1.21 | 1.10 | 1.72 | 0.73 | 0.55 | 0.81 | 0.71 | 0.95 | 0.60 | 0.70 |
| Yb | 4.30 | 4.20 | 3.65 | 4.40 | 4.10 | 3.73 | 5.80 | 3.10 | 2.35 | 3.00 | 2.85 | 3.25 | 2.40 | 3.00 |
| Lu | 0.63 | 0.63 | 0.54 | 0.63 | 0.60 | 0.54 | 0.86 | 0.48 | 0.35 | 0.44 | 0.45 | 0.47 | 0.37 | 0.44 |
| Cu | 25.0 | 2.0 | 43.5 | 30.0 | 32.0 | 29.5 | 17.0 | 110.0 | 92.0 | 50.0 | 55.0 | 35.5 | 67.0 | 54.7 |
| Ni | 14.0 | 1.0 | 44.0 | 14.0 | 19.0 | 10.0 | 1.0 | 41.0 | 93.0 | 21.0 | 23.5 | 12.0 | 23.5 | 20.3 |
| Normalized major-oxide contents (weight percent) | | | | | | | | | | | | | | |
| $SiO_2$ | 51.40 | 54.99 | 50.93 | 50.53 | 51.19 | 51.61 | 54.67 | 52.15 | 49.48 | 54.45 | 53.32 | 54.76 | 54.58 | 52.70 |
| $Al_2O_3$ | 13.26 | 13.14 | 13.62 | 12.84 | 13.49 | 13.54 | 13.12 | 14.62 | 16.60 | 14.53 | 14.47 | 14.27 | $14.86_3$ | 14.42 |
| FeO | 14.79 | 13.42 | 13.82 | 15.44 | 14.08 | 14.24 | 13.48 | 10.74 | 10.40 | 11.18 | 11.49 | 11.44 | 9.50 | 11.66 |
| MgO | 4.08 | 3.05 | 5.28 | 4.56 | 4.60 | 4.56 | 2.92 | 6.45 | 8.60 | 4.91 | 5.50 | 4.59 | 6.16 | 5.84 |
| CaO | 8.12 | 5.69 | 8.50 | 8.24 | 8.35 | 8.15 | 6.68 | 10.20 | 11.04 | 8.55 | 9.13 | 8.12 | 9.41 | 9.31 |
| $Na_2O$ | 2.65 | 3.26 | 2.74 | 2.48 | 2.76 | 2.74 | 3.53 | 3.17 | 2.35 | 2.87 | 2.76 | 3.16 | 2.81 | 2.73 |
| $K_2O$ | 1.22 | 2.52 | 0.84 | 1.14 | 1.43 | 1.34 | 2.02 | 0.61 | 0.23 | 1.22 | 1.11 | 1.22 | 0.96 | 1.03 |
| $TiO_2$ | 3.77 | 2.74 | 3.26 | 3.73 | 3.27 | 2.95 | 2.48 | 1.54 | 0.92 | 1.74 | 1.73 | 1.94 | 1.27 | 1.78 |
| $P_2O_5$ | 0.49 | 1.03 | 0.83 | 0.85 | 0.60 | 0.62 | 0.83 | 0.36 | 0.18 | 0.35 | 0.32 | 0.33 | 0.29 | 0.36 |
| MnO | 0.20 | 0.17 | 0.18 | 0.19 | 0.23 | 0.25 | 0.28 | 0.16 | 0.19 | 0.19 | 0.17 | 0.17 | 0.16 | 0.17 |
| Total | 100.00 | 100.00 | 100.00 | 100.00 | 100.00 | 100.00 | 100.00 | 100.00 | 100.00 | 100.00 | 100.00 | 100.00 | 100.00 | 100.00 |

## **Table 7.** Ratios of incompatible trace elements in samples of the Grande Ronde Basalt

[Geochemical units listed in approximate stratigraphic order, see table 1. n.a., not analyzed]

| Geochemical unit------- | 1A N2 | 1A* N2 | 2A N2 | UNC N2 | 3A N2 | 3A* N2 | UNC N2 | 4A N2 | 4A* N2 | Unc N2 | 3B N2 | UNC N2 | 4B N2 |
|---|---|---|---|---|---|---|---|---|---|---|---|---|---|
| Chemical type- | A | A | B | X | C | C | X | D | D | X | C | X | D |
| K/Rb | 3.48 | 3.18 | n.a. | n.a. | 3.28 | 3.10 | 3.19 | 3.20 | 3.58 | n.a. | 3.16 | n.a. | n.a. |
| K/Th | 27.14 | 30.44 | n.a. | n.a. | 24.53 | 26.86 | 28.93 | 25.07 | 28.82 | n.a. | 26.99 | n.a. | n.a. |
| K/P | 7.04 | 8.96 | 5.58 | 4.99 | 6.82 | 9.09 | 7.09 | 5.93 | 7.92 | 13.03 | 8.01 | 6.45 | 5.33 |
| K/Ba | 19.71 | 20.41 | n.a. | n.a. | 18.25 | 20.11 | 20.97 | 18.60 | 23.64 | n.a. | 19.59 | n.a. | n.a. |
| K/Sr | 34.05 | 33.72 | n.a. | n.a. | 25.70 | 27.26 | 31.71 | 26.75 | 30.70 | n.a. | 29.87 | n.a. | n.a. |
| Rb/Sr | 9.79 | 10.62 | n.a. | n.a. | 7.83 | 8.81 | 9.94 | 8.36 | 8.58 | n.a. | 9.45 | n.a. | n.a. |
| Hf/Th | 0.99 | 1.03 | n.a. | n.a. | 1.11 | 1.13 | 1.14 | 1.13 | 1.08 | n.a. | 1.05 | n.a. | n.a. |
| Hf/Ba | 7.20 | 6.90 | n.a. | n.a. | 8.20 | 8.50 | 8.30 | 8.40 | 8.90 | n.a. | 7.60 | n.a. | n.a. |
| Hf/Zr | 24.40 | 22.20 | n.a. | n.a. | 24.10 | 24.40 | 24.60 | 24.00 | 23.80 | n.a. | 23.60 | n.a. | n.a. |
| Hf/Ta | 5.52 | 5.14 | n.a. | n.a. | 5.42 | 5.27 | 5.45 | 5.28 | 5.42 | n.a. | 5.51 | n.a. | n.a. |
| Hf/La | 18.73 | 20.00 | n.a. | n.a. | 19.70 | 19.74 | 20.25 | 20.52 | 20.53 | n.a. | 18.91 | n.a. | n.a. |
| Th/Ba | 7.30 | 6.70 | n.a. | n.a. | 7.40 | 7.50 | 7.20 | 7.40 | 8.20 | n.a. | 7.30 | n.a. | n.a. |
| La/Sm | 2.25 | 2.13 | n.a. | n.a. | 2.16 | 2.12 | 2.17 | 2.03 | 2.23 | n.a. | 2.19 | n.a. | n.a. |
| La/Yb | 4.66 | 4.21 | n.a. | n.a. | 4.15 | 3.96 | 4.15 | 4.08 | 4.05 | n.a. | 4.25 | n.a. | n.a. |

| Geochemical unit------- | LH2 N2 | MG6 N2 | 2B N2 | 5A N2 | 5A* N2 | UNC N2 | 2C N2 | 4C N2 | 5B N2 | 3C N2 | 3C* N2 | UNC N2 | 5C N2R2 |
|---|---|---|---|---|---|---|---|---|---|---|---|---|---|
| Chemical type- | 1 | 2 | B | E | E | X | B | D | E | C | C | X | E |
| K/Rb | 2.49 | 2.14 | n.a. | 2.99 | 2.69 | n.a. | 2.95 | n.a. | 2.99 | 3.46 | 3.13 | n.a. | n.a. |
| K/Th | 32.31 | 23.97 | 27.67 | 24.89 | 23.04 | n.a. | 26.55 | n.a. | 25.99 | 29.29 | 29.69 | n.a. | n.a. |
| K/P | 4.72 | 4.25 | 9.14 | 11.00 | 11.41 | 5.81 | 8.65 | 5.50 | 11.35 | 8.22 | 7.96 | 5.95 | 9.45 |
| K/Ba | 16.11 | 14.15 | n.a. | 22.02 | 20.52 | n.a. | 21.52 | n.a. | 22.18 | 24.38 | 19.79 | n.a. | n.a. |
| K/Sr | 13.80 | 14.60 | n.a. | 47.05 | 43.38 | n.a. | 44.97 | n.a. | 49.70 | 30.81 | 26.50 | n.a. | n.a. |
| Rb/Sr | 5.54 | 6.82 | n.a. | 15.73 | 16.13 | n.a. | 15.27 | n.a. | 16.61 | 8.90 | 8.47 | n.a. | n.a. |
| Hf/Th | 1.50 | 1.36 | 0.83 | 0.77 | 0.76 | n.a. | 0.86 | n.a. | 0.76 | 1.06 | 1.13 | n.a. | n.a. |
| Hf/Ba | 7.50 | 8.00 | n.a. | 6.80 | 6.70 | n.a. | 7.00 | n.a. | 6.40 | 8.90 | 7.60 | n.a. | n.a. |
| Hf/Zr | 22.20 | 24.10 | n.a. | 25.10 | 25.10 | n.a. | 25.10 | n.a. | 25.10 | 25.20 | 24.20 | n.a. | n.a. |
| Hf/Ta | 6.44 | 5.10 | 7.66 | 5.23 | 5.28 | n.a. | 5.41 | n.a. | 5.30 | 5.00 | 4.97 | n.a. | n.a. |
| Hf/La | 17.76 | 19.04 | 16.33 | 18.02 | 17.21 | n.a. | 17.63 | n.a. | 17.87 | 19.62 | 19.14 | n.a. | n.a. |
| Th/Ba | 5.00 | 5.90 | n.a. | 8.80 | 8.90 | n.a. | 8.10 | n.a. | 8.50 | 8.30 | 6.70 | n.a. | n.a. |
| La/Sm | 2.21 | 2.30 | 2.44 | 2.48 | 2.59 | n.a. | 2.40 | n.a. | 2.50 | 2.10 | 2.11 | n.a. | n.a. |
| La/Yb | 5.34 | 3.91 | 5.24 | 5.46 | 5.34 | n.a. | 5.13 | n.a. | 5.15 | 4.53 | 3.98 | n.a. | n.a. |

| Geochemical unit-------- | 5C* N2R2 | 3D R2 | 5D R2 | 5D* R2 | 5D* R2 | UNC R2 | 2D R2 | 2D* R2 | UNC R2 | AS16 R2 | 2E R2N1 | UNC* N1 | KB5 N1 |
|---|---|---|---|---|---|---|---|---|---|---|---|---|---|
| Chemical type- | E | C | E | E | E | X | B | B | X | 3 | B | X | 4 |
| K/Rb | n.a. | 2.52 | n.a. | n.a. | n.a. | n.a. | 3.28 | 2.89 | 2.81 | n.a. | n.a. | n.a. | 3.10 |
| K/Th | n.a. | 26.39 | 26.71 | n.a. | n.a. | 27.57 | 27.72 | 24.63 | 24.65 | 28.76 | n.a. | n.a. | 31.18 |
| K/P | 12.83 | 8.04 | 10.36 | 10.53 | 11.06 | 7.32 | 8.40 | 9.30 | 7.64 | 7.84 | 10.46 | 6.95 | 6.84 |
| K/Ba | n.a. | 18.83 | n.a. | n.a. | n.a. | n.a. | 23.13 | 21.04 | 18.35 | n.a. | n.a. | n.a. | 21.00 |
| K/Sr | n.a. | 29.65 | n.a. | n.a. | n.a. | n.a. | 47.51 | 45.39 | 48.55 | n.a. | n.a. | n.a. | 36.65 |
| Rb/Sr | n.a. | 11.79 | n.a. | n.a. | n.a. | n.a. | 14.49 | 15.71 | 17.27 | n.a. | n.a. | n.a. | 11.84 |
| Hf/Th | n.a. | 1.08 | 0.86 | n.a. | n.a. | 0.90 | 0.87 | 0.80 | 0.75 | 1.06 | n.a. | n.a. | 1.06 |
| Hf/Ba | n.a. | 7.70 | n.a. | n.a. | n.a. | n.a. | 7.20 | 6.80 | 5.60 | n.a. | n.a. | n.a. | 7.10 |
| Hf/Zr | n.a. | 22.70 | n.a. | n.a. | n.a. | n.a. | 25.30 | 25.10 | 25.40 | n.a. | n.a. | n.a. | 24.00 |
| Hf/Ta | n.a. | 5.03 | 4.55 | n.a. | n.a. | 4.84 | 5.42 | 5.47 | 5.52 | 5.66 | n.a. | n.a. | 5.12 |
| Hf/La | n.a. | 20.33 | 19.05 | n.a. | n.a. | 18.28 | 18.33 | 17.97 | 17.61 | 21.38 | n.a. | n.a. | 20.05 |
| Th/Ba | n.a. | 7.10 | n.a. | n.a. | n.a. | n.a. | 8.30 | 8.50 | 7.40 | n.a. | n.a. | n.a. | 6.70 |
| La/Sm | n.a. | 2.10 | 2.29 | n.a. | n.a. | 2.19 | 2.22 | 2.36 | 2.40 | 1.88 | n.a. | n.a. | 1.96 |
| La/Yb | n.a. | 4.44 | 5.11 | n.a. | n.a. | 5.13 | 5.12 | 5.04 | 5.25 | 4.07 | n.a. | n.a. | 4.14 |

| Geochemical unit-------- | 3E N1 | UNC N1 | 3F N1 | 5E N1 | AS16 N1 | 3G N1 | 5F N1 | UNC N1 | AS16 N1 | 5G N1 | AS16 N1 | 5H N1 | AS16 N1 |
|---|---|---|---|---|---|---|---|---|---|---|---|---|---|
| Chemical type- | C | X | C | E | 3 | C | E | X | 3 | E | 3 | E | 3 |
| K/Rb | 3.18 | n.a. | 3.21 | n.a. | 2.96 | n.a. | 3.43 | n.a. | 2.89 | n.a. | n.a. | n.a. | n.a. |
| K/Th | 26.52 | 33.47 | 25.97 | 32.36 | 27.61 | 28.59 | 29.69 | n.a. | 29.56 | n.a. | 25.60 | 29.43 | 28.74 |
| K/P | 9.11 | 7.14 | 8.52 | 9.19 | 7.71 | 8.73 | 9.63 | 5.50 | 8.62 | 9.87 | 8.10 | 10.95 | 9.97 |
| K/Ba | 27.59 | n.a. | 17.61 | n.a. | 19.74 | n.a. | 20.14 | n.a. | 20.02 | n.a. | n.a. | n.a. | n.a. |
| K/Sr | 32.04 | n.a. | 26.87 | n.a. | 36.40 | n.a. | 40.23 | n.a. | 36.90 | n.a. | n.a. | n.a. | n.a. |
| Rb/Sr | 10.07 | n.a. | 8.38 | n.a. | 12.31 | n.a. | 11.73 | n.a. | 12.75 | n.a. | n.a. | n.a. | n.a. |
| Hf/Th | 1.00 | 1.10 | 1.01 | 1.10 | 0.97 | 1.05 | 1.09 | n.a. | 1.11 | n.a. | 1.08 | 0.98 | 1.01 |
| Hf/Ba | 10.40 | n.a. | 6.80 | n.a. | 6.90 | n.a. | 7.40 | n.a. | 7.50 | n.a. | n.a. | n.a. | n.a. |
| Hf/Zr | 24.90 | n.a. | 23.40 | n.a. | 23.80 | n.a. | 24.40 | n.a. | 23.80 | n.a. | n.a. | n.a. | n.a. |
| Hf/Ta | 5.23 | 5.70 | 5.31 | 5.94 | 5.46 | 5.74 | 5.71 | n.a. | 5.96 | n.a. | 5.69 | 5.13 | 5.34 |
| Hf/La | 21.75 | 20.00 | 20.75 | 21.03 | 20.19 | 20.71 | 22.22 | n.a. | 21.58 | n.a. | 21.85 | 21.29 | 21.82 |
| Th/Ba | 10.40 | n.a. | 6.80 | n.a. | 7.10 | n.a. | 6.80 | n.a. | 6.80 | n.a. | n.a. | n.a. | n.a. |
| La/Sm | 1.91 | 1.95 | 1.96 | 1.95 | 2.04 | 2.07 | 1.97 | n.a. | 2.02 | n.a. | 1.98 | 2.00 | 1.93 |
| La/Yb | 4.44 | 4.27 | 4.58 | 4.09 | 4.51 | 4.51 | 4.43 | n.a. | 4.36 | n.a. | 4.57 | 4.64 | 4.20 |

**Table 7.** Ratios of incompatible trace elements in samples of the Grande Ronde Basalt—*Continued*

| Geochemical unit--------<br>Chemical type- | UNC N1<br>X | AS16 N1<br>3 | 2F R1<br>B | 5I R1<br>E | AS16 R1<br>3 |
|---|---|---|---|---|---|
| K/Rb | 2.58 | 2.60 | 3.08 | n.a. | n.a. |
| K/Th | 28.43 | 26.98 | 29.50 | 25.41 | 31.54 |
| K/P | 11.82 | 10.37 | 7.42 | 9.87 | 8.05 |
| K/Ba | 26.06 | 20.60 | 22.21 | n.a. | n.a. |
| K/Sr | 49.02 | 42.90 | 42.46 | n.a. | n.a. |
| Rb/Sr | 18.99 | 16.51 | 13.77 | n.a. | n.a. |
| Hf/Th | 0.90 | 0.95 | 1.17 | 0.92 | 1.22 |
| Hf/Ba | 8.20 | 7.20 | 8.80 | n.a. | n.a. |
| Hf/Zr | 24.10 | 23.90 | 25.70 | n.a. | n.a. |
| Hf/Ta | 5.49 | 5.93 | 6.18 | 5.54 | 5.27 |
| Hf/La | 21.05 | 21.21 | 22.40 | 21.71 | 21.89 |
| Th/Ba | 9.20 | 7.60 | 7.50 | n.a. | n.a. |
| La/Sm | 2.10 | 2.05 | 1.94 | 2.11 | 1.93 |
| La/Yb | 4.83 | 4.89 | 4.14 | 5.11 | 4.12 |

**Table 8.** Ratios of incompatible trace elements in samples of the Wanapum Basalt

[Geochemical units listed in approximate stratigraphic order, see table 1. n.a., not analyzed]

| Geochemical unit--------<br>Chemical type- | PV<br>A | LOLO INC<br>B | ROSALIA<br>C | PH POWAT<br>D | ROZA<br>E | FS ANOM<br>F | FS INC<br>F | SHUMAKER<br>G | PH SHUM<br>G | SW LOOK<br>H | DODGE<br>I | ROBIN<br>J |
|---|---|---|---|---|---|---|---|---|---|---|---|---|
| K/Rb | 3.11 | 3.19 | 3.17 | 3.81 | 2.75 | 2.55 | 3.47 | 3.64 | 3.41 | 3.32 | 4.15 | n.a. |
| K/Th | 25.18 | 24.48 | 24.86 | 29.45 | 26.07 | 23.33 | 28.88 | 29.46 | 27.22 | 29.75 | 48.66 | 48.23 |
| K/P | 2.84 | 2.73 | 2.74 | 3.19 | 3.50 | 3.70 | 4.21 | 3.95 | 3.87 | 4.97 | 3.59 | 2.40 |
| K/Ba | 15.07 | 18.12 | 19.17 | 16.78 | 18.14 | 14.20 | 24.52 | 15.51 | 15.46 | 21.38 | 17.26 | 11.86 |
| K/Sr | 29.68 | 28.86 | 35.12 | 45.26 | 33.15 | 32.45 | 35.35 | 46.34 | 48.78 | 49.16 | 14.22 | 5.03 |
| Rb/Sr | 9.55 | 9.04 | 11.08 | 11.86 | 12.08 | 12.75 | 10.19 | 12.75 | 14.29 | 14.80 | 3.43 | n.a. |
| Hf/Th | 1.29 | 1.31 | 1.34 | 1.18 | 1.17 | 1.03 | 1.14 | 1.17 | 1.15 | 1.03 | 2.47 | 4.00 |
| Hf/Ba | 7.70 | 9.70 | 10.40 | 6.70 | 8.10 | 6.30 | 9.70 | 6.20 | 6.50 | 7.40 | 8.70 | 11.00 |
| Hf/Zr | 24.30 | 23.50 | 24.20 | 24.60 | 23.20 | 23.20 | 23.90 | 24.10 | 24.30 | 24.00 | 23.10 | 21.80 |
| Hf/Ta | 4.25 | 4.28 | 4.45 | 5.08 | 4.42 | 4.16 | 4.51 | 4.63 | 4.91 | 4.36 | 5.61 | 4.77 |
| Hf/La | 16.73 | 16.64 | 17.46 | 17.25 | 17.19 | 16.33 | 17.40 | 17.06 | 17.73 | 18.77 | 18.82 | 19.47 |
| Th/Ba | 6.00 | 7.40 | 7.70 | 5.70 | 7.00 | 6.10 | 8.50 | 5.30 | 5.70 | 7.20 | 3.50 | 2.70 |
| La/Sm | 1.95 | 2.16 | 2.49 | 1.93 | 2.39 | 2.11 | 2.54 | 1.98 | 1.94 | 2.03 | 2.21 | 1.72 |
| La/Yb | 4.29 | 4.72 | 4.44 | 4.31 | 4.58 | 4.44 | 4.76 | 4.30 | 4.19 | 4.26 | 3.26 | 2.39 |

**Table 9.** Ratios of incompatible trace elements in samples of the Saddle Mountain Basalt

[Geochemical units listed in approximate stratigraphic order, see table 1. n.a., not analyzed]

| Geochemical unit | LM | GOOSE | INDIAN | MARTIN | BASIN | BUFORD | ELEPHANT | POMONA | VC WEIPE | ESQUAT | RBESQUAT | FS IC | SLIP |
|---|---|---|---|---|---|---|---|---|---|---|---|---|---|
| Chemical type | A | B | C | D | E | F | G | H | I | J | J | K | L |
| K/Rb | 3.36 | 4.46 | 5.19 | 6.14 | 6.48 | 2.70 | 4.32 | 3.00 | 1.53 | 2.76 | 2.74 | 2.87 | 3.02 |
| K/Th | 23.84 | 23.14 | 23.52 | 29.25 | 29.57 | 16.49 | 17.56 | 21.16 | 16.47 | 16.37 | 15.34 | 18.49 | 16.07 |
| K/P | 4.25 | 1.47 | 2.26 | 1.90 | 1.70 | 7.05 | 3.96 | 5.15 | 3.21 | 7.39 | 7.47 | 5.89 | 3.26 |
| K/Ba | 22.70 | 12.10 | 12.08 | 10.04 | 10.74 | 26.36 | 32.43 | 31.19 | 15.35 | 24.60 | 20.82 | 27.79 | 24.53 |
| K/Sr | 33.92 | 45.66 | 35.63 | 26.14 | 28.52 | 50.89 | 48.72 | 23.77 | 17.31 | 55.24 | 50.92 | 54.55 | 30.96 |
| Rb/Sr | 10.09 | 10.23 | 6.87 | 4.26 | 4.41 | 18.83 | 11.27 | 7.93 | 11.28 | 20.04 | 18.59 | 18.98 | 10.25 |
| Hf/Th | 0.93 | 2.47 | 1.91 | 2.81 | 3.01 | 0.75 | 1.08 | 1.27 | 1.33 | 0.64 | 0.65 | 0.74 | 0.94 |
| Hf/Ba | 8.90 | 12.90 | 9.80 | 9.60 | 10.90 | 11.90 | 20.00 | 18.70 | 12.40 | 9.70 | 8.80 | 11.20 | 14.30 |
| Hf/Zr | 24.50 | 24.60 | 24.70 | 24.80 | 24.10 | 24.50 | 28.00 | 23.60 | 23.40 | 24.60 | 26.10 | 24.60 | 24.40 |
| Hf/Ta | 2.76 | 3.50 | 3.51 | 3.55 | 3.45 | 3.46 | 3.68 | 3.94 | 4.05 | 3.42 | 3.48 | 3.01 | 3.55 |
| Hf/La | 13.12 | 14.49 | 14.65 | 16.03 | 15.36 | 16.06 | 19.02 | 19.00 | 19.18 | 14.58 | 15.05 | 15.03 | 15.71 |
| Th/Ba | 9.50 | 5.20 | 5.10 | 3.40 | 3.60 | 16.00 | 18.50 | 14.70 | 9.30 | 15.00 | 13.60 | 15.00 | 15.30 |
| La/Sm | 3.03 | 2.42 | 2.55 | 2.46 | 2.44 | 2.76 | 2.19 | 2.20 | 2.08 | 2.77 | 2.83 | 2.63 | 2.44 |
| La/Yb | 7.45 | 5.39 | 5.47 | 4.85 | 5.02 | 5.59 | 4.86 | 4.11 | 4.24 | 6.91 | 7.12 | 6.30 | 5.44 |

| Geochemical unit | LEW ORCH | SPRAGUE | SW SPRAG | NEW | SW NEW | ASOTIN | VC ASOT | SW HUNTZ | HUNTZ | VC LAP | EAGLE | WILBUR | UMATILLA |
|---|---|---|---|---|---|---|---|---|---|---|---|---|---|
| Chemical type | M | N | N | O | O | P | P | Q | Q | R | R | S | T |
| K/Rb | n.a. | 12.04 | 0.00 | 2.55 | 2.67 | 2.23 | 3.82 | 3.17 | 0.00 | 3.19 | 3.98 | 3.37 | 4.92 |
| K/Th | 4.96 | 24.07 | 21.64 | 23.72 | 17.83 | 15.79 | 17.76 | 20.52 | 25.97 | 21.36 | 18.94 | 21.97 | 29.20 |
| K/P | .59 | 2.09 | 1.81 | 1.62 | 1.17 | 3.90 | 3.64 | 4.41 | 6.82 | 6.12 | 5.33 | 6.56 | 5.91 |
| K/Ba | 0.88 | 12.08 | 10.42 | 10.09 | 7.16 | 13.00 | 13.74 | 20.60 | 0.00 | 18.32 | 16.10 | 19.30 | 6.65 |
| K/Sr | 5.78 | 28.55 | 22.11 | 13.18 | 9.30 | 12.85 | 15.34 | 22.48 | 0.00 | 39.99 | 32.25 | 52.75 | 76.70 |
| Rb/Sr | .00 | 2.37 | 0.00 | 5.16 | 3.47 | 5.75 | 4.02 | 7.08 | 0.00 | 12.52 | 8.11 | 15.63 | 15.58 |
| Hf/Th | .55 | 2.12 | 2.24 | 2.18 | 2.26 | 1.36 | 1.35 | 1.23 | 1.08 | 0.95 | 1.02 | 0.89 | 1.41 |
| Hf/Ba | 1.10 | 10.60 | 10.80 | 9.30 | 9.10 | 11.20 | 10.40 | 12.30 | 0.00 | 8.20 | 8.70 | 7.80 | 3.20 |
| Hf/Zr | 2.70 | 23.20 | 22.90 | 21.60 | 22.80 | 23.00 | 24.20 | 22.90 | 0.00 | 22.60 | 31.30 | 23.70 | 21.20 |
| Hf/Ta | .17 | 3.87 | 3.51 | 3.18 | 3.47 | 4.28 | 4.68 | 4.04 | 5.83 | 5.37 | 4.35 | 5.57 | 6.86 |
| Hf/La | 4.03 | 14.94 | 15.07 | 15.25 | 14.88 | 17.71 | 19.33 | 18.25 | 15.56 | 14.68 | 16.23 | 13.50 | 21.88 |
| Th/Ba | .40 | 5.00 | 4.80 | 4.30 | 4.00 | 8.20 | 7.70 | 10.00 | 0.00 | 8.60 | 8.50 | 8.80 | 2.30 |
| La/Sm | .49 | 2.52 | 2.30 | 2.30 | 2.45 | 2.23 | 2.29 | 2.40 | 2.79 | 3.08 | 2.96 | 3.41 | 2.90 |
| La/Yb | .20 | 5.85 | 5.49 | 5.28 | 4.75 | 4.37 | 4.04 | 5.08 | 6.26 | 6.12 | 5.42 | 6.82 | 6.82 |

| Geochemical unit | UM FRAC | PH UMTIL | PHSOPHER |
|---|---|---|---|
| Chemical type | T | T | U |
| K/Rb | 5.20 | 4.91 | 5.72 |
| K/Th | 32.78 | 28.97 | 28.58 |
| K/P | 5.56 | 5.10 | 5.33 |
| K/Ba | 7.00 | 6.21 | 6.10 |
| K/Sr | 84.21 | 75.73 | 59.19 |
| Rb/Sr | 16.18 | 15.44 | 10.36 |
| Hf/Th | 1.40 | 1.42 | 1.40 |
| Hf/Ba | 3.00 | 3.00 | 3.00 |
| Hf/Zr | 22.90 | 20.40 | 21.30 |
| Hf/Ta | 7.90 | 6.51 | 6.83 |
| Hf/La | 21.89 | 21.62 | 21.84 |
| Th/Ba | 2.10 | 2.10 | 2.10 |
| La/Sm | 2.76 | 3.13 | 3.23 |
| La/Yb | 8.57 | 7.08 | 6.94 |

## Table 10. Corrected and normalized major-oxide chemistry of naturally quenched glass from the Grande Ronde Basalt

[Geochemical units listed in approximate stratigraphic order, see table 1. Chemical type names for glasses correspond to the chemical types for whole rocks. Data are averages computed from original data given in Wright (1988)]

| Geochemical unit------- | 1A* GL | 3A* GL | 4A* GL | LH2N2 GL | MG6N2 GL | 5A* GL | 3C* GL | 5C* GL | 5D* GL | 2D* GL |
|---|---|---|---|---|---|---|---|---|---|---|
| Chemical type- | A | C | D | 1 | 2 | E | C | E | E | B |
| $SiO_2$ | 54.82 | 54.36 | 54.30 | 55.41 | 52.47 | 56.26 | 54.51 | 57.37 | 55.98 | 55.74 |
| $Al_2O_3$ | 13.89 | 13.59 | 13.43 | 14.38 | 14.08 | 13.24 | 13.45 | 13.10 | 12.92 | 12.96 |
| FeO | 11.90 | 12.27 | 12.77 | 10.42 | 12.57 | 12.51 | 12.79 | 12.24 | 12.98 | 12.98 |
| MgO | 4.08 | 4.39 | 4.08 | 5.00 | 5.25 | 3.18 | 3.96 | 2.83 | 3.03 | 2.80 |
| CaO | 8.18 | 8.71 | 8.21 | 9.21 | 9.67 | 7.04 | 7.93 | 6.69 | 6.89 | 6.75 |
| $Na_2O$ | 3.15 | 3.04 | 3.10 | 3.01 | 2.97 | 3.39 | 3.30 | 3.21 | 3.41 | 3.44 |
| $K_2O$ | 1.60 | 1.35 | 1.50 | 0.88 | 0.81 | 1.90 | 1.45 | 2.01 | 2.05 | 2.13 |
| $TiO_2$ | 2.04 | 2.03 | 2.26 | 1.41 | 1.87 | 2.16 | 2.26 | 2.22 | 2.38 | 2.77 |
| $P_2O_5$ | 0.34 | 0.27 | 0.36 | 0.28 | 0.31 | 0.32 | 0.35 | 0.33 | 0.35 | 0.44 |
| Total | 100.00 | 100.01 | 100.01 | 100.00 | 100.00 | 100.00 | 100.00 | 100.00 | 99.99 | 100.01 |

## Table 11. Corrected and normalized major-oxide chemistry of naturally quenched glaass from the Wanapum Basalt

[Geochemical units listed in approximate stratigraphic order, see table 1. Chemical type names for glasses correspond to the chemical types for whole rocks. Data are averages computed from original data given in Wright (1988)]

| Geochemical unit-------- | LOLO GL | ROSAL GL | ROZA GL | FRSP GL | DODGE GL | ROBIN GL |
|---|---|---|---|---|---|---|
| Chemical type- | 2 | 3 | 4 | 5 | 6 | 7 |
| $SiO_2$ | 50.31 | 50.42 | 51.32 | 52.36 | 52.54 | 49.72 |
| $Al_2O_3$ | 12.24 | 12.08 | 12.77 | 12.44 | 14.07 | 16.06 |
| FeO | 15.37 | 15.91 | 14.95 | 15.08 | 12.39 | 10.83 |
| MgO | 4.31 | 3.85 | 3.90 | 3.51 | 5.31 | 7.71 |
| CaO | 9.13 | 8.56 | 8.39 | 8.05 | 9.74 | 11.39 |
| $Na_2O$ | 2.73 | 2.88 | 2.95 | 2.89 | 3.04 | 2.51 |
| $K_2O$ | 1.19 | 1.35 | 1.44 | 1.56 | 0.76 | 0.44 |
| $TiO_2$ | 3.92 | 4.18 | 3.58 | 3.51 | 1.76 | 1.12 |
| $P_2O_5$ | 0.80 | 0.78 | 0.69 | 0.60 | 0.39 | 0.20 |
| Total | 100.00 | 100.01 | 99.99 | 100.00 | 100.00 | 99.98 |

## Table 12. Corrected and normalized major-oxide chemistry of naturally quenched glass from the Saddle Mountains

[Geochemical units listed in approximate stratigraphic order, see table 1. Chemical type names for glasses correspond to the chemical types for whole rocks. Data are averages computed from original data given in Wright (1988)]

| Geochemical unit------- | LM GL | GOOSE GL | INDIAN GL | MARTIN GL | BASIN GL | BUFORD GL | EM GL | POMONA GL | WEIPE GL | ESQUAT GL | SPRAGE GL | NEW GL | ASOTIN GL |
|---|---|---|---|---|---|---|---|---|---|---|---|---|---|
| Chemical type- | A | B | C | D | E | F | G | H | I | K | N | O | P |
| $SiO_2$ | 51.68 | 48.17 | 49.55 | 48.25 | 47.47 | 55.15 | 51.71 | 52.98 | 52.17 | 54.88 | 49.63 | 49.76 | 53.60 |
| $Al_2O_3$ | 11.61 | 10.96 | 11.54 | 12.62 | 11.55 | 12.47 | 11.81 | 13.74 | 13.52 | 12.72 | 11.99 | 14.96 | 14.09 |
| FeO | 15.96 | 18.33 | 16.59 | 15.88 | 17.36 | 13.71 | 16.12 | 11.90 | 12.66 | 14.02 | 15.99 | 11.38 | 11.66 |
| MgO | 3.35 | 3.77 | 3.84 | 5.29 | 4.61 | 3.11 | 3.56 | 5.46 | 5.71 | 3.07 | 4.46 | 7.04 | 5.00 |
| CaO | 8.16 | 9.02 | 8.95 | 10.13 | 9.90 | 7.57 | 8.29 | 10.26 | 10.31 | 7.07 | 9.43 | 11.58 | 9.75 |
| $Na_2O$ | 2.86 | 2.55 | 2.68 | 2.47 | 2.50 | 3.06 | 2.54 | 2.46 | 2.68 | 2.72 | 2.73 | 2.37 | 2.80 |
| $K_2O$ | 1.92 | 1.34 | 1.39 | 0.81 | 1.00 | 1.84 | 1.43 | 0.85 | 0.58 | 1.92 | 1.10 | 0.44 | 0.70 |
| $TiO_2$ | 3.88 | 4.09 | 4.56 | 3.80 | 4.62 | 2.73 | 4.01 | 2.10 | 2.13 | 3.24 | 3.91 | 2.04 | 2.04 |
| $P_2O_5$ | 0.59 | 1.77 | 0.90 | 0.76 | 0.99 | 0.37 | 0.53 | 0.25 | 0.23 | 0.37 | 0.75 | 0.44 | 0.35 |
| Total | 100.01 | 100.00 | 100.00 | 100.01 | 100.00 | 100.01 | 100.00 | 100.00 | 99.99 | 100.01 | 99.99 | 100.01 | 99.99 |

| Geochemical unit------- | LAP GL | WILBUR GL | UM GL |
|---|---|---|---|
| Chemical type- | R | S | T |
| $SiO_2$ | 54.69 | 55.41 | 56.10 |
| $Al_2O_3$ | 13.48 | 13.45 | 13.23 |
| FeO | 12.20 | 12.26 | 12.41 |
| MgO | 4.07 | 3.30 | 2.39 |
| CaO | 8.28 | 7.53 | 6.05 |
| $Na_2O$ | 2.69 | 2.83 | 3.21 |
| $K_2O$ | 1.77 | 2.26 | 3.03 |
| $TiO_2$ | 2.34 | 2.42 | 2.56 |
| $P_2O_5$ | 0.48 | 0.53 | 1.02 |
| Total | 100.00 | 99.99 | 100.00 |

**Table 13.** Summary of chemical chracteristics for geochemical units in the Yakima Basalt Subgroup

[Geochemical units listed in approximate stratigraphic order, see table 1; differences from most similar units indicated by: >, greater content in unit labeled in column 1; <, smaller content in unit labeled in column 1; differences based on MgO variation diagrams. LREE, light rare-earth elements; HREE, heavy rare-earth elements; Eu*, europium anomaly (+ or -) Diagnostic oxides and elements are those that stand out on the MgO variation diagrams. Sources of data for $^{87}Sr/^{86}Sr$ ratio: a, Carlson (1984a); b, Carlson and others (1981); c, Nelson (1980); d, J. Arth (unpublished data); e, McDougall (1976)]

| Geochemical unit | Most similar unit (differences) |  | Diagnostic oxides and elements |  | $^{87}Sr/^{86}Sr$ |
|---|---|---|---|---|---|
|  | By major oxides | By trace elements | High | Low |  |
|  |  | Saddle Mountains Basalt |  |  |  |
| LM | LOLO INC (>$K_2O$,Cs,Nb,Ta,Th,U,LREE; <Sc,HREE) | LOLO INC (<Cr) | Nb | Sc | .71087(a)<br>.71076,.71094(c) |
| GOOSE | Unique | Unique | FeO,Hf,Ta,$P_2O_5$, Nb,Y,Zn,REE | $SiO_2$,Co | .70769(d) |
| INDIAN | MARTIN (<MgO) | MARTIN |  |  | .70780(a),.70762(d) |
| MARTIN | Unique | Unique |  |  | .70764(a),.70770(b),<br>.70785,.7076(d) |
| BASIN | MARTIN (<$SiO_2$; >$TiO_2$,$P_2O_5$) |  | $SiO_2$ |  | .70782(a),.70774(d) |
| BUFORD | GR INC (>$K_2O$,$TiO_2$,$P_2O_5$) | GR INC (>Hf,Ta,Th,U, LREE,HREE; <Sc,Sr) | Th |  |  |
| ELEPHANT | ROSALIA (<$Na_2O$,$P_2O_5$) | ROSALIA (>Co,Hf,Nb,Cu,Ni; <Ba,Rb,Sr,HREE | FeO,$TiO_2$ | Ba,Rb | .70762(b)<br>.70807,.70772(c)<br>.70788-.70829(e) |
| POMONA<br>VC WEIPE | DODGE (<$Na_2O$; >$TiO_2$,LREE)<br>ROBIN (<MgO) | DODGE (<Cr,Sr,Sc; >Ta,Hf)<br>ROBIN (<Sr,Sc; >Ta,Th, Hf,LREE) |  | Ba,Cr | .70750(b),.70780(c)<br>.70761-.70784(e) |
| ESQUAT<br>RBESQUAT | FS IC | FS IC (>Th) | Th, Ta |  | .71317(a),.71448(b)<br>.71471,.71449(e) |
| FS IC | FS INC (<$P_2O_5$) | FS INC (>Co,Nb) | Ta |  | .71310(e) |
| SLIP | GR INC,(<$Na_2O$,Sc; >$TiO_2$,$P_2O_5$,LREE) | GR INC (>Co,Hf,Ta,Th; <Cr,<Sr) |  | Ba,Cr |  |
| LEW ORCH<br>SPRAGUE<br>SW SPRAG<br>NEW<br>SW NEW | LOLO INC (>MgO; <$K_2O$) | LOLO INC (<Cr,Rb,Sr; >Ba,Hf,Nb,Ta,Zr,LREE, HREE,-Eu*) | FeO, $TiO_2$,$P_2O_5$, Nb,Ta,Sc,REE |  |  |
| ASOTIN<br>VC ASOT | ROBIN (>$SiO_2$; <$TiO_2$,) | ROBIN (>Hf,Nb,Sc,LREE; <Rb,Th) |  | Sc | .70755(a) |
| SW HUNTZ<br>HUNTZ | POMONA (<CaO; >$K_2O$) | POMONA (>Ba,Cr,Th, LREE; <Cs,Sc) |  | Sc | .70884(a) |
| VC LAP<br>EAGLE | DODGE (<CaO,$Na_2O$; >$K_2O$) | DODGE (>Ba,Nb,Rb,Ta, Th,LREE,HREE,Ni; <Cr, <Hf<Sc,<Zr,<Cu) |  | Sc |  |
| WILBUR | GR INC (<$Na_2O$; >$K_2O$,$P_2O_5$) | GR INC (>Ba,Hf,Ta,Th, Zr,LREE,HREE; <Sr,Sc) |  | Sc | .71047,.71063(a) |
| UMATILLA<br>UM FRAC<br>PH UMTIL | SHUMAKER (<FeO; >$K_2O$) | SHUMAKER (>Ba,Co,Hf, Ta,Th,Zr,LREE; <Cs,Sr, Sc,HREE) | Ba,Hf,Zr,Eu | Co,Cr | .70892(b)<br>.70935(e) |
| PH SOPHER | PH UMTIL (<$TiO_2$,$P_2O_5$) | PH UMTIL (<Sc,Rb) |  |  |  |

**Table 13.** Summary of chemical chracteristics for geochemical units in the Yakima Basalt Subgroup—*Continued*

| Geochemical unit | Most similar unit (differences) | | Diagnostic oxides and elements | | $^{87}Sr/^{86}Sr$ |
|---|---|---|---|---|---|
| | By major oxides | By trace elements | High | Low | |
| | | Wanapum Basalt | | | |
| PV | Unique | | CaO,Cr,Sc | FeO,$K_2O$,Co | .70521(a) |
| LOLO INC | LM (see above) | ROZA (>Cr) | | Sc | .70506(a),.70439(c) |
| ROSALIA | LOLO INC (<MgO; >$TiO_2$) | | $TiO_2$ | Cr | .70507(a),<br>.70538,.70558(e) |
| | ELEPHANT (>$P_2O_5$) | ELEPHANT (>Ba,Rb,Sc; <Nb,Ta) | | | |
| PH POWAT | SHUMAKER (>$P_2O_5$) | SHUMAKER (<Sc; >REE) | | Cr | |
| ROZA | FS INC (>MgO) | FS INC | | | .70517(b),.70498(c)<br>.70545(e) |
| FS ANOM | FS INC (<FeO; >CaO,$TiO_2$,$P_2O_5$) | FS INC (>Ba,Ta,Hf,Th,Zn, Sc,REE) | Co | | |
| FS INC | ROZA (<MgO) | ROZA | | | .70510,.70520(b)<br>.70517(a),.70530<br>.70559(e) |
| SHUMAKER<br>PH SHUM | GR INC (<$SiO_2$,$K_2O$; >$P_2O_5$) | GR INC (>Ba,Hf,Nb,Ta,Y,Sc, HREE; <Cr,Cs,Rb,Th) | | Cr | .70481(a) |
| SW LOOK | SHUMAKER (<$P_2O_5$) | SHUMAKER (<Ba,Hf,Nb,Sc; >HREE) | | | .70546(a) |
| DODGE | GR INC | GR INC (>Cr,Sc; <Th) | | | .70435(a) |
| ROBIN | ASOTIN (see above) | | MgO | Rb,REE,Cr | .70438(a) |
| | | Grande Ronde Basalt | | | |
| GR INC | | | $SiO_2$,Cs,Rb | $TiO_2$,$P_2O_5$,<br>Ta,REE | .70489-.70504(a)<br>.70438-.70507(b)<br>.70440-.70606(e)<br>.70454-.70552(c) |

**Table 14.** Relation between stratigraphic position and chemistry, additional flows for which chemical data are available, Columbia River Plateau

[MP, magnetic polarity as determined in the field using a fluxgate magnetometer: N, normal; R, reversed, T, transitional]

| Formation<br>Member<br>Flow<br>Informal name | Age (Ma) | MP | Geochemical unit |
|---|---|---|---|
| SADDLE MOUNTAINS BASALT | | | |
| Unclassified flows in Idaho [Clearwater Embayment; Craigmont, Swamp Creek, Icicle Flat, and Grangeville Members of Camp (1981)] | | N | VC CRAIG[1] |
| | | N | VC SWAMP[1] |
| | | N | VC IFLAT[1] |
| | | R | VC GRNGE[1] |
| WANAPUM BASALT | | | |
| Basalt of Feary Creek[3] (Camp, 1981) | | N | VC FEARY[1] |
| Basalt of Potlatch[4] (Camp,1981) | | N | VC POT[2] |
| UNCLASSIFIED | | | |
| Local flows in NE Oregon (basalts of Powder River of Hooper(1984); mapping of W.T. Taubeneck, D.A. Swanson, T.L. Wright, and P.R. Hooper) | 11.6 | N | WT NEPH[2] |
| | 13.8-9.5 | N | WT ANDES[2] |
| | | N | WT JONES[2] |
| | | N | WT SUGMT[2] |
| | | N | WT SPRMT[2] |
| | | N | WT WBRMT[2] |
| | | N | PH EDEN[1] |
| | | N | WT OBHTI[1] |
| | | N | WT OBLTI[1] |

[1] Chemistry falls within the fields defined for the Yakima Basalt Subgroup

[2] Chemistry falls outside of the fields defined for the Yakima Basalt Subgroup

[3] Included in Frenchman Springs Member

[4] Included in Onaway Member of Camp (1981)

**Table 15.** Average chemical composition of additional analyzed flows of table 14

[Chemical types listed in approximate stratigraphic order, see table 14. Trace elements followed by X analyzed by X-ray fluorescence; all others analyzed by instrumental neutron activation. n.a., not analyzed Data from which these average compositions are calculated are given in Wright (1988)]

| Geochemical unit-------- | WT NEPH | WT ANDES | WT JONES | WT SUGMT | WT SPRMT | WT WBRMT | PH EDEN | WT OBHTI | WT OBLTI | VC CRAIG | VC SWAMP | VC IFLAT | VC GRNGE |
|---|---|---|---|---|---|---|---|---|---|---|---|---|---|
| Chemical type- | A | B | C | D | E | F | G | H | I | J | K | L | M |
| Major oxides (weight percent) | | | | | | | | | | | | | |
| SiO2 | 43.71 | 59.31 | 62.89 | 53.68 | 51.14 | 53.56 | 52.07 | 50.80 | 50.69 | 52.77 | 51.74 | 52.06 | 53.38 |
| Al2O3 | 15.26 | 18.01 | 19.32 | 17.09 | 16.10 | 17.45 | 14.28 | 16.76 | 17.41 | 14.73 | 14.91 | 16.01 | 16.21 |
| FeO | 15.58 | 5.97 | 3.36 | 7.99 | 9.18 | 7.63 | 13.96 | 9.87 | 9.37 | 13.82 | 12.93 | 11.54 | 8.78 |
| MgO | 7.97 | 3.12 | 2.43 | 3.78 | 4.98 | 4.43 | 3.52 | 8.86 | 8.11 | 3.83 | 4.89 | 5.36 | 6.62 |
| CaO | 9.00 | 6.31 | 6.56 | 8.39 | 9.32 | 8.69 | 7.44 | 9.34 | 10.78 | 7.12 | 8.53 | 9.56 | 10.57 |
| Na2O | 4.32 | 4.63 | 4.29 | 4.33 | 4.24 | 4.66 | 2.58 | 2.47 | 2.36 | 2.73 | 2.96 | 3.12 | 2.55 |
| K2O | 0.71 | 1.78 | 1.09 | 2.39 | 2.29 | 1.70 | 2.24 | 0.47 | 0.37 | 1.74 | 1.15 | 0.78 | 0.68 |
| TiO2 | 3.06 | 0.97 | 0.45 | 1.85 | 2.08 | 1.56 | 2.75 | 1.44 | 1.02 | 2.96 | 2.73 | 1.46 | 1.36 |
| P2O5 | 0.84 | 0.49 | 0.25 | 1.05 | 1.16 | 0.83 | 1.39 | 0.42 | 0.28 | 0.53 | 0.39 | 0.37 | 0.21 |
| MnO | 0.22 | 0.13 | 0.11 | 0.16 | 0.15 | 0.15 | 0.25 | 0.18 | 0.17 | 0.19 | 0.22 | 0.26 | 0.17 |
| Total | 100.67 | 100.72 | 100.75 | 100.71 | 100.64 | 100.66 | 100.48 | 100.61 | 100.56 | 100.42 | 100.45 | 100.52 | 100.53 |
| Trace elements (parts per million) | | | | | | | | | | | | | |
| Ba | 294 | 848 | 592 | 1234 | 1088 | 776 | 1788 | 334 | 272 | 715 | 549 | 414 | 311 |
| BaX | 198 | 821 | n.a. | n.a. | 711 | n.a. | 1774 | 428 | 245 | n.a. | n.a. | n.a. | n.a. |
| Co | n.a. | n.a. | n.a. | n.a. | n.a. | n.a. | n.a. | 46.5 | n.a. | n.a. | n.a. | n.a. | n.a. |
| Cr | 85.1 | 46.8 | 24.1 | 33.0 | 60.0 | 104.4 | 34.8 | 363.5 | 32.0 | 7.4 | 38.1 | 82.2 | 133.0 |
| Cs | n.a. | 0.42 | 0.82 | 0.60 | 0.36 | 0.58 | 0.81 | 0.20 | n.a. | 0.68 | 0.67 | n.a. | n.a. |
| Hf | 1.73 | 3.05 | 2.05 | 4.03 | 3.11 | 3.00 | 10.80 | 2.18 | 1.70 | 6.08 | 5.41 | 2.60 | 3.21 |
| NbX | 6.0 | n.a. | n.a. | n.a. | 20.0 | n.a. | 34.0 | 14.0 | n.a. | n.a. | n.a. | n.a. | n.a. |
| Rb | n.a. | 16.0 | 17.5 | 20.8 | 13.0 | 14.0 | 52.8 | 15.7 | 23.9 | 41.7 | 23.7 | n.a. | 24.0 |
| RbX | n.a. | 12.5 | n.a. | n.a. | 36.0 | n.a. | 49.0 | 10.0 | 8.0 | n.a. | n.a. | n.a. | n.a. |
| SrX | 980 | 1012 | n.a. | n.a. | 2443 | n.a. | 238 | 479 | 467 | n.a. | n.a. | n.a. | n.a. |
| Ta | 0.45 | 0.57 | 0.46 | 0.60 | 0.52 | 0.45 | 2.37 | 0.51 | 0.37 | 1.67 | 1.53 | 0.52 | 0.97 |
| Th | n.a. | 1.75 | 2.05 | 3.07 | 1.83 | 2.58 | 7.73 | 0.85 | 0.61 | 7.15 | 3.15 | 1.05 | 2.85 |
| U | n.a. | 0.75 | 0.73 | 0.83 | 0.63 | 0.65 | 1.67 | 0.37 | n.a. | 1.47 | 1.03 | 0.49 | 0.82 |
| YX | 13.5 | 20.5 | n.a. | n.a. | n.a. | n.a. | 59.0 | 27.0 | 21.0 | n.a. | n.a. | n.a. | n.a. |
| Zn | 133 | 86 | 65 | 121 | 138 | 110 | 152 | 95 | 88 | 149 | 160 | 156 | 123 |
| Zr | n.a. | 142 | 117 | 163 | 135 | 173 | 487 | 98 | 81 | 243 | 420 | 160 | 147 |
| ZrX | 67 | 125 | n.a. | n.a. | 122 | n.a. | 480 | 136 | 81 | n.a. | n.a. | n.a. | n.a. |
| Sc | 25.8 | 13.5 | 8.6 | 16.1 | 15.9 | 16.6 | 27.1 | 28.1 | 32.6 | 26.1 | 33.8 | 39.5 | 33.0 |
| La | 16.7 | 30.5 | 14.5 | 52.3 | 46.7 | 37.9 | 58.7 | 13.2 | 8.4 | 42.9 | 32.3 | 13.3 | 19.9 |
| Ce | 44.3 | 51.1 | 25.8 | 112.8 | 105.0 | 80.4 | 116.8 | 27.2 | 18.4 | 81.5 | 56.4 | 26.7 | 36.7 |
| Nd | 32.4 | 28.3 | 12.5 | 62.2 | 57.6 | 43.2 | 63.5 | 17.2 | 12.5 | 44.9 | 34.5 | 19.5 | 19.2 |
| Sm | 6.9 | 5.3 | 2.3 | 8.8 | 8.8 | 7.0 | 13.7 | 3.8 | 2.9 | 8.8 | 7.8 | 4.5 | 4.7 |
| Eu | 2.11 | 1.52 | 0.75 | 2.47 | 2.33 | 1.86 | 4.42 | 1.26 | 0.95 | 2.41 | 2.24 | 1.32 | 1.25 |
| Gd | 4.50 | 4.50 | 2.20 | 6.40 | 5.80 | 5.30 | 14.10 | 3.70 | 2.70 | 8.90 | 8.00 | 4.70 | 4.70 |
| Tb | 0.83 | 0.60 | 0.28 | 0.70 | 0.68 | 0.58 | 2.08 | 0.69 | 0.57 | 1.25 | 1.36 | 0.84 | 0.72 |
| Yb | 1.12 | 1.76 | 0.90 | 1.32 | 1.10 | 1.22 | 5.79 | 2.22 | 2.03 | 3.99 | 4.15 | 3.34 | 2.50 |
| Lu | 0.14 | 0.25 | 0.12 | 0.18 | 0.17 | 0.19 | 0.83 | 0.33 | 0.33 | 0.67 | 0.74 | 0.67 | 0.46 |
| Cu | n.a. | n.a. | n.a. | n.a. | n.a. | n.a. | n.a. | n.a. | n.a. | n.a. | n.a. | n.a. | n.a. |
| Ni | n.a. | n.a. | n.a. | n.a. | n.a. | n.a. | n.a. | n.a. | n.a. | n.a. | n.a. | n.a. | n.a. |
| Normalized major-oxide contents (weight percent) | | | | | | | | | | | | | |
| SiO2 | 43.42 | 58.89 | 62.42 | 53.30 | 50.81 | 53.21 | 51.82 | 50.49 | 50.41 | 52.55 | 51.51 | 51.79 | 53.10 |
| Al2O3 | 15.16 | 17.88 | 19.18 | 16.97 | 16.00 | 17.34 | 14.21 | 16.66 | 17.31 | 14.67 | 14.84 | 15.93 | 16.12 |
| FeO | 15.48 | 5.93 | 3.33 | 7.93 | 9.12 | 7.58 | 13.89 | 9.81 | 9.32 | 13.76 | 12.87 | 11.48 | 8.73 |
| MgO | 7.92 | 3.10 | 2.41 | 3.75 | 4.95 | 4.40 | 3.50 | 8.81 | 8.06 | 3.81 | 4.87 | 5.33 | 6.59 |
| CaO | 8.94 | 6.26 | 6.51 | 8.33 | 9.26 | 8.63 | 7.40 | 9.28 | 10.72 | 7.09 | 8.49 | 9.51 | 10.51 |
| Na2O | 4.29 | 4.60 | 4.26 | 4.30 | 4.21 | 4.63 | 2.57 | 2.46 | 2.35 | 2.72 | 2.95 | 3.10 | 2.54 |
| K2O | 0.71 | 1.77 | 1.08 | 2.37 | 2.28 | 1.69 | 2.23 | 0.47 | 0.37 | 1.73 | 1.14 | 0.78 | 0.68 |
| TiO2 | 3.04 | 0.96 | 0.45 | 1.84 | 2.07 | 1.55 | 2.74 | 1.43 | 1.01 | 2.95 | 2.72 | 1.45 | 1.35 |
| P2O5 | 0.83 | 0.49 | 0.25 | 1.04 | 1.15 | 0.82 | 1.38 | 0.42 | 0.28 | 0.53 | 0.39 | 0.37 | 0.21 |
| MnO | 0.22 | 0.13 | 0.11 | 0.16 | 0.15 | 0.15 | 0.25 | 0.18 | 0.17 | 0.19 | 0.22 | 0.26 | 0.17 |
| Total | 100.00 | 100.00 | 100.00 | 100.00 | 100.00 | 100.00 | 100.00 | 100.00 | 100.00 | 100.00 | 100.00 | 100.00 | 100.00 |

**Table 15.** Average chemical composition of additional analyzed flows of table 14—*Continued*

| Geochemical unit-------- | VC FEARY | VC POT | JOSEPH | IMNAHA |
|---|---|---|---|---|
| Chemical type- | N | O | # | * |
| **Major oxides (weight percent)** | | | | |
| SiO2 | 51.70 | 48.41 | 55.40 | 47.80 |
| Al2O3 | 14.41 | 16.82 | 15.05 | 15.32 |
| FeO | 14.12 | 12.96 | 12.43 | 10.61 |
| MgO | 4.08 | 5.04 | 3.24 | 12.02 |
| CaO | 7.66 | 7.45 | 6.73 | 10.19 |
| Na2O | 3.00 | 3.52 | 2.82 | 2.14 |
| K2O | 1.60 | 1.69 | 1.72 | 0.22 |
| TiO2 | 3.25 | 3.84 | 2.36 | 1.25 |
| P2O5 | 0.40 | 0.72 | 0.47 | 0.09 |
| MnO | 0.18 | 0.18 | 0.20 | 0.18 |
| Total | 100.40 | 100.63 | 100.42 | 99.82 |
| **Trace elements (parts per million)** | | | | |
| Ba | 550 | 367 | 857 | 140 |
| BaX | 521 | 360 | n.a. | 89 |
| Co | n.a. | 42.9 | n.a. | 49.1 |
| Cr | 20.7 | 8.9 | 6.5 | 861.5 |
| Cs | 0.83 | 0.37 | 1.27 | n.a. |
| Hf | 5.38 | 6.84 | 4.85 | 1.73 |
| NbX | 24.0 | 42.0 | n.a. | 10.0 |
| Rb | 42.0 | 29.8 | 43.5 | n.a. |
| RbX | 45.0 | 26.0 | n.a. | n.a. |
| SrX | 245 | 540 | n.a. | 384 |
| Ta | 1.70 | 3.61 | 0.90 | 0.26 |
| Th | 7.10 | 3.13 | 5.39 | 0.29 |
| U | 1.76 | 1.21 | 1.64 | n.a. |
| YX | 45.0 | 27.0 | n.a. | 17.0 |
| Zn | 152 | 129 | 134 | 89 |
| Zr | 237 | 281 | 227 | n.a. |
| ZrX | 190 | 298 | n.a. | 82 |
| Sc | 29.1 | 19.1 | 30.6 | 26.9 |
| La | 35.9 | 37.4 | 26.9 | 5.1 |
| Ce | 64.2 | 74.8 | 52.3 | 12.9 |
| Nd | 36.2 | 41.3 | 30.1 | 10.5 |
| Sm | 7.5 | 9.2 | 7.5 | 2.9 |
| Eu | 2.11 | 2.69 | 1.96 | 0.93 |
| Gd | 8.3 | 7.8 | 7.5 | 2.9 |
| Tb | 1.09 | 1.19 | 1.07 | 0.43 |
| Yb | 3.73 | 2.29 | 3.83 | 1.69 |
| Lu | 0.66 | 0.39 | 0.58 | 0.27 |
| Cu | n.a. | n.a. | n.a. | n.a. |
| Ni | n.a. | n.a. | n.a. | n.a. |
| **Normalized major-oxide contents (weight percent)** | | | | |
| SiO2 | 51.49 | 48.11 | 55.17 | 47.89 |
| Al2O3 | 14.35 | 16.71 | 14.99 | 15.35 |
| FeO | 14.06 | 12.88 | 12.38 | 10.63 |
| MgO | 4.06 | 5.01 | 3.23 | 12.04 |
| CaO | 7.63 | 7.40 | 6.70 | 10.21 |
| Na2O | 2.99 | 3.50 | 2.81 | 2.14 |
| K2O | 1.59 | 1.68 | 1.71 | 0.22 |
| TiO2 | 3.24 | 3.82 | 2.35 | 1.25 |
| P2O5 | 0.40 | 0.72 | 0.47 | 0.09 |
| MnO | 0.18 | 0.18 | 0.20 | 0.18 |
| Total | 100.00 | 100.00 | 100.00 | 100.00 |

## Table 16. Ratios of incorpatible trace elements in additional analyzed flows of table 14

[Geochemical units listed in approximate stratigraphic order, see table 14. n.a., not analyzed]

| Geochemical unit-------- | WT NEPH | WT ANDES | WT JONES | WT SUGMT | WT SPRMT | WT WBRMT | PH EDEN | WT OBHTI | WT OBLTI | VC CRAIG | VC SWAMP | VC IFLAT | VC GRNGE |
|---|---|---|---|---|---|---|---|---|---|---|---|---|---|
| Chemical type- | A | B | C | D | E | F | G | H | I | J | K | L | M |
| K/Rb | n.a. | 11.82 | n.a. | n.a. | 5.28 | n.a. | 3.79 | 3.90 | 3.84 | n.a. | n.a. | n.a. | n.a. |
| K/Th | n.a. | 84.44 | 44.14 | 64.63 | 99.99 | 54.70 | 24.06 | 45.90 | 50.35 | 20.20 | 30.31 | 61.67 | 19.81 |
| K/P | 1.61 | 6.91 | 8.29 | 4.33 | 3.75 | 3.89 | 3.06 | 2.13 | 2.51 | 6.24 | 5.61 | 4.01 | 6.16 |
| K/Ba | 29.77 | 18.00 | n.a. | n.a. | 26.74 | n.a. | 10.48 | 9.12 | 12.54 | n.a. | n.a. | n.a. | n.a. |
| K/Sr | 6.01 | 14.60 | n.a. | n.a. | 7.78 | n.a. | 78.13 | 8.15 | 6.58 | n.a. | n.a. | n.a. | n.a. |
| Rb/Sr | n.a. | 1.24 | n.a. | n.a. | 1.47 | n.a. | 20.59 | 2.09 | 1.71 | n.a. | n.a. | n.a. | n.a. |
| Hf/Th | n.a. | 1.74 | 1.00 | 1.31 | 1.70 | 1.16 | 1.40 | 2.56 | 2.79 | 0.85 | 1.72 | 2.48 | 1.13 |
| Hf/Ba | 8.70 | 3.70 | n.a. | n.a. | 4.40 | n.a. | 6.10 | 5.10 | 6.90 | n.a. | n.a. | n.a. | n.a. |
| Hf/Zr | 25.80 | 24.40 | n.a. | n.a. | 25.50 | n.a. | 22.50 | 16.00 | 21.00 | n.a. | n.a. | n.a. | n.a. |
| Hf/Ta | 3.84 | 5.35 | 4.46 | 6.72 | 5.98 | 6.67 | 4.56 | 4.27 | 4.59 | 3.64 | 3.54 | 5.00 | 3.31 |
| Hf/La | 10.36 | 10.00 | 14.14 | 7.71 | 6.66 | 7.92 | 18.40 | 16.52 | 20.24 | 14.17 | 16.75 | 19.55 | 16.13 |
| Th/Ba | n.a. | 2.10 | n.a. | n.a. | 2.60 | n.a. | 4.40 | 2.00 | 2.50 | n.a. | n.a. | n.a. | n.a. |
| La/Sm | 1.48 | 3.51 | 3.84 | 3.62 | 3.23 | 3.30 | 2.61 | 2.12 | 1.77 | 2.97 | 2.52 | 1.80 | 2.58 |
| La/Yb | 9.85 | 11.44 | 10.64 | 26.16 | 28.03 | 20.51 | 6.69 | 3.93 | 2.73 | 7.10 | 5.14 | 2.63 | 5.26 |

| Geochemical unit-------- | VC FEARY | VC POT | JOSEPH | IMNAHA |
|---|---|---|---|---|
| Chemical type- | N | O | # | * |
| K/Rb | 2.95 | 5.40 | n.a. | n.a. |
| K/Th | 18.71 | 44.82 | 26.34 | 62.98 |
| K/P | 7.61 | 4.46 | 6.92 | 4.65 |
| K/Ba | 25.49 | 38.97 | n.a. | 20.52 |
| K/Sr | 54.21 | 25.98 | n.a. | 4.76 |
| Rb/Sr | 18.37 | 4.81 | n.a. | n.a. |
| Hf/Th | 0.76 | 2.19 | 0.90 | 5.97 |
| Hf/Ba | 10.30 | 19.00 | n.a. | 19.40 |
| Hf/Zr | 28.30 | 23.00 | n.a. | 21.10 |
| Hf/Ta | 3.16 | 1.89 | 5.39 | 6.65 |
| Hf/La | 14.99 | 18.29 | 18.03 | 33.92 |
| Th/Ba | 13.60 | 8.70 | n.a. | 3.30 |
| La/Sm | 2.92 | 2.48 | 2.19 | 1.07 |
| La/Yb | 6.36 | 10.78 | 4.64 | 1.99 |

**Table 17.** Summary of chemical characteristics of additional flows for which chemical data are available, Columbia River Plateau

[Chemical analyses on which this table is based are given in table 15; geochemical units listed in approximate stratigraphic order, see table 14. The chemistries of these flows are compared with chemistries of basalts erupted in Saddle Mountains, Wanapum, or Grande Ronde time, using MgO variation diagrams (Fig. 4). Differences from most similar units indicated by: >, greater content in unit labeled in column 1; <, smaller content in unit labeled in column 1; differences based on MgO variation diagrams. LREE, light rare-earth elements; HREE, heavy rare-earth elements; Eu*, europium anomaly (+ or −). Diagnostic oxides and elements are those that stand out on the MgO variation diagrams. Sources of data for $^{87}Sr/^{86}Sr$ ratio: a, Carlson (1984a); b, Carlson and others (1981); c, Nelson (1980); d, J. Arth (unpublished data); e, McDougall (1976). The column labeled 'comment' gives a qualitative assessment of chemical classification and possible petrologic connections to units closely related in time. See text for discussion of specific examples]

| Geochemical unit | Most similar unit (differences) | | Diagnostic oxides and elements | | $^{87}Sr/^{86}Sr$ | comment |
|---|---|---|---|---|---|---|
| | By major oxides | By trace elements | High | Low | | |
| WT NEPH | unique | unique | $Na_2O$,Sr | $SiO_2$,Cr,Nb, Rb (n.d.) | 0.70343(b) | The only nepheline-normative basalt (basanite) in the Columbia Plateau. |
| WT ANDES | unique | unique | $SiO_2$,Sr<br>$Na_2O$ | Sc | 0.70354(b) | The only true andesites in the Columbia River Plateau |
| WT JONES | WT ANDES (<MgO) | WT ANDES | $SiO_2$,$Na_2O$ | Sc | | |
| WT SUGMT | unique | unique | $Na_2O$,$K_2O$ | Sc | | More evolved andesite, related to WT ANDES |
| WT SPRMT | unique | unique | $Na_2O$,$K_2O$,Sr | Hf,Sc | | Parental to WT ANDES? |
| WT WBRMT | WT SUGMT (<$K_2O$) | WT SUGMT (<Hf,REE) | $Na_2O$ | Sc | | Low silica 'andesite'-related to WT NEPH? |
| PH EDEN | UMATILLA (>MgO, $P_2O_5$,Y,REE) | UMATILLA (<Ba; >Hf, Nb,Ta,Y,REE) | 'FeO',$P_2O_5$<br>Ba,Hf,Rb,Ta<br>Th,Zr,REE | $SiO_2$,$Al_2O_3$,<br>$Na_2O$ | | |
| WT OBLTI | WT OBHTI (>$TiO_2$) | | | | | Olivine basalt |
| WT OBLTI | ROBIN (>$P_2O_5$) | ROBIN (>Ba,Cr,Rb,Th) | | | 0.70353(b) | Olivine basalt |
| VC CRAIG | ESQUAT | ESQUAT (<Th,<Sc; >LREE,HREE) | | Sc | | |
| VC SWAMP | unique | unique | | Th | | |
| VC IFLAT | GR INC (<$SiO_2$; >$Al_2O_3$,$P_2O_5$) | GR INC (<Hf,Ta,Th,U, LREE;>HREE | Sc | $TiO_2$,Hf,Ta,<br>Th,Zr,LREE | | Flatter REE pattern than other units of Saddle Mountains Basalt. |
| | DODGE (<MgO) | DODGE,(<Hf,LREE; >HREE) | | | | |
| VC GRANGE | GR INC (>MgO,$TiO_2$; <$Na_2O$) | GR INC (>Hf,Rb,Th,Ta, REE; <Sc) | $SiO_2$ | 'FeO',$P_2O_5$ | | Most like GR LH 2 N2 type |
| VC FEARY | FS IC | FS IC | | | | Magnetic polarity opposite to that of FS IC. |
| VC POT | unique | unique | $TiO_2$,Nb,Ta | $SiO_2$,CaO,<br>Ba,Cr,Sc | | Columbia River(?) Basalt Group. Resembles ROZA in field appearance. |

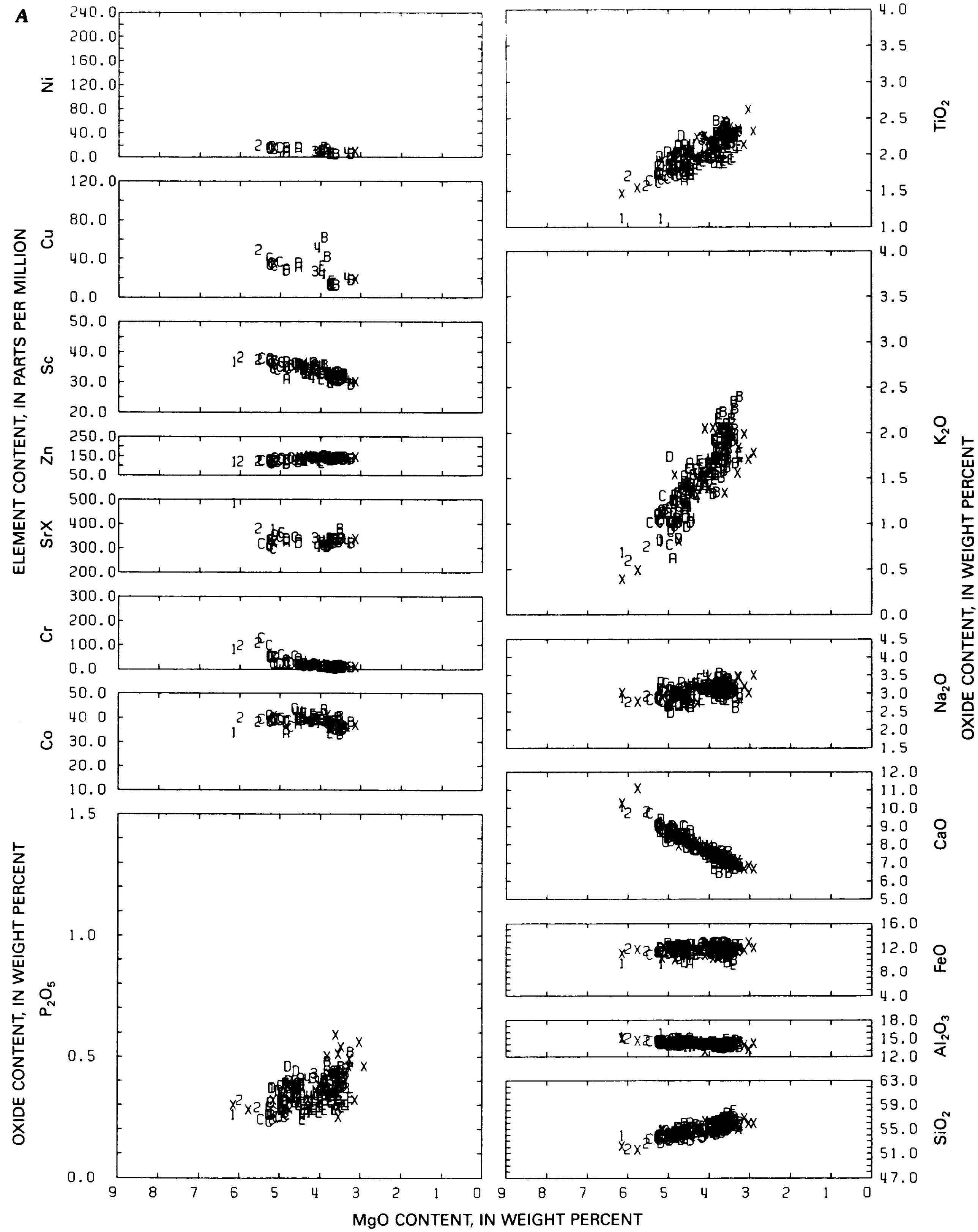

**Figure 4.** Major-oxide and trace-element chemistry of units of the Yakima Basalt Subgroup, presented as MgO variation diagrams. Diagrams scaled so that symbol size reflects approximately two standard deviations. Plotted data are averages of at least two samples from each geochemical unit; analyses recalculated to 100 percent dry weight with total iron expressed as FeO (see tables 3–5). Except where otherwise noted, symbols refer to chemical types identified in table 3 (Grande Ronde Basalt), 4 (Wanapum Basalt), and 5 (Saddle Mountains Basalt). *A*, Grande Ronde Basalt, major oxides and compatible trace elements. Symbol # is the Joseph volcanics of Kleck (1976). *B*, Grande Ronde Basalt, incompatible trace elements. *C*, Grande Ronde Basalt, selected trace-element ratios. *D*, Wanapum Basalt,

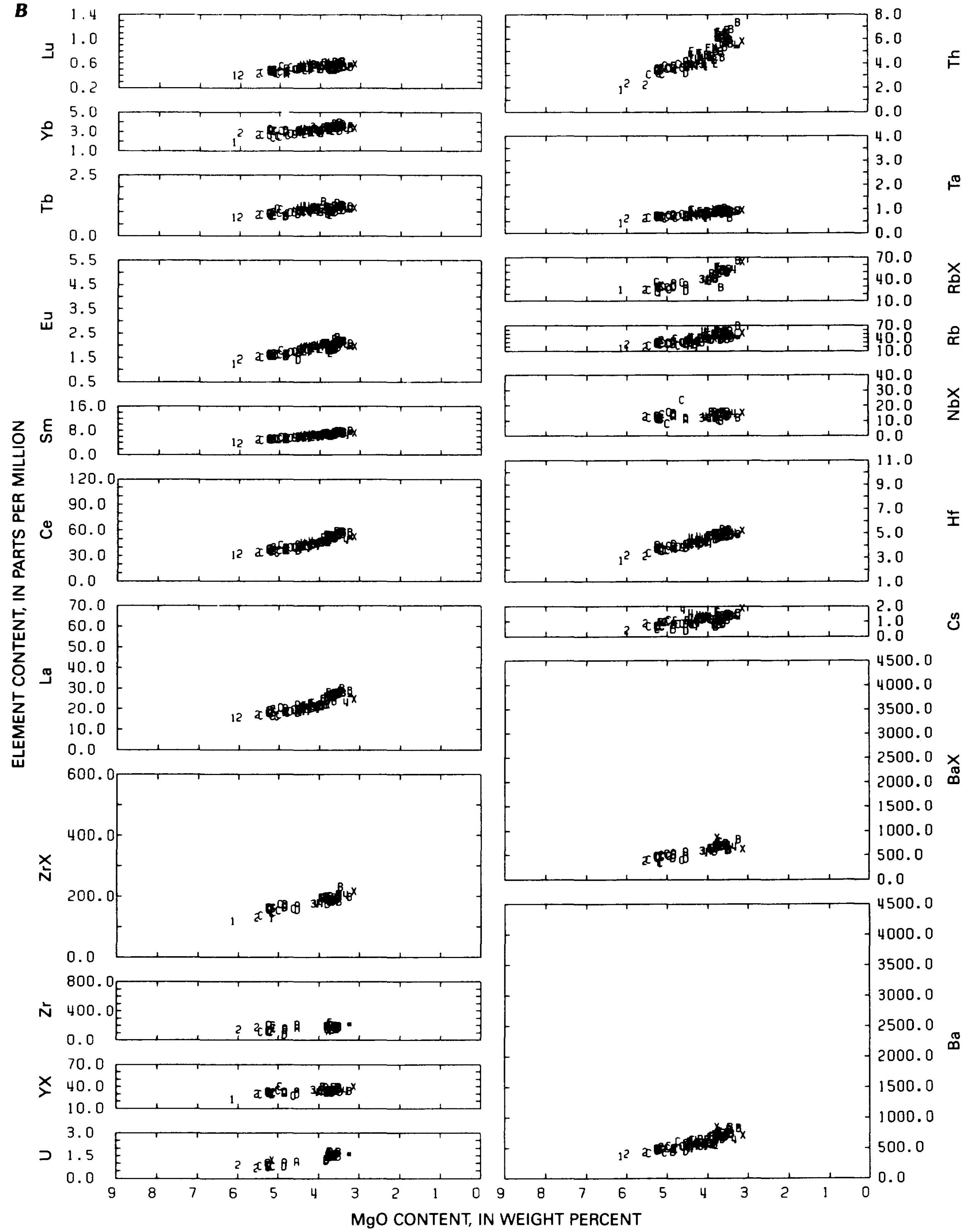

major oxides and compatible trace elements. *E*, Wanapum Basalt, incompatible trace elements. *F*, Wanapum Basalt, selected trace-element ratios. *G*, Saddle Mountains Basalt, major oxides and compatible trace elements for geochemical units with relatively high $SiO_2$ and low FeO and $TiO_2$ (that is, of Grande Ronde affinity). *H*, Saddle Mountains Basalt, incompatible trace elements for units of Grande Ronde affinity. *I*, Saddle Mountains Basalt, selected trace-element ratios for units of Grande Ronde affinity. *J*, Saddle Mountains Basalt, major oxides and compatible trace elements for geochemical units with relatively low $SiO_2$ and high FeO and $TiO_2$ (that is, of Wanapum affinity). *K*, Saddle Mountains Basalt, incompatible trace elements for units of Wanapum affinity. *L*, Saddle Mountains Basalt, selected trace-element ratios for units of Wanapum affinity.

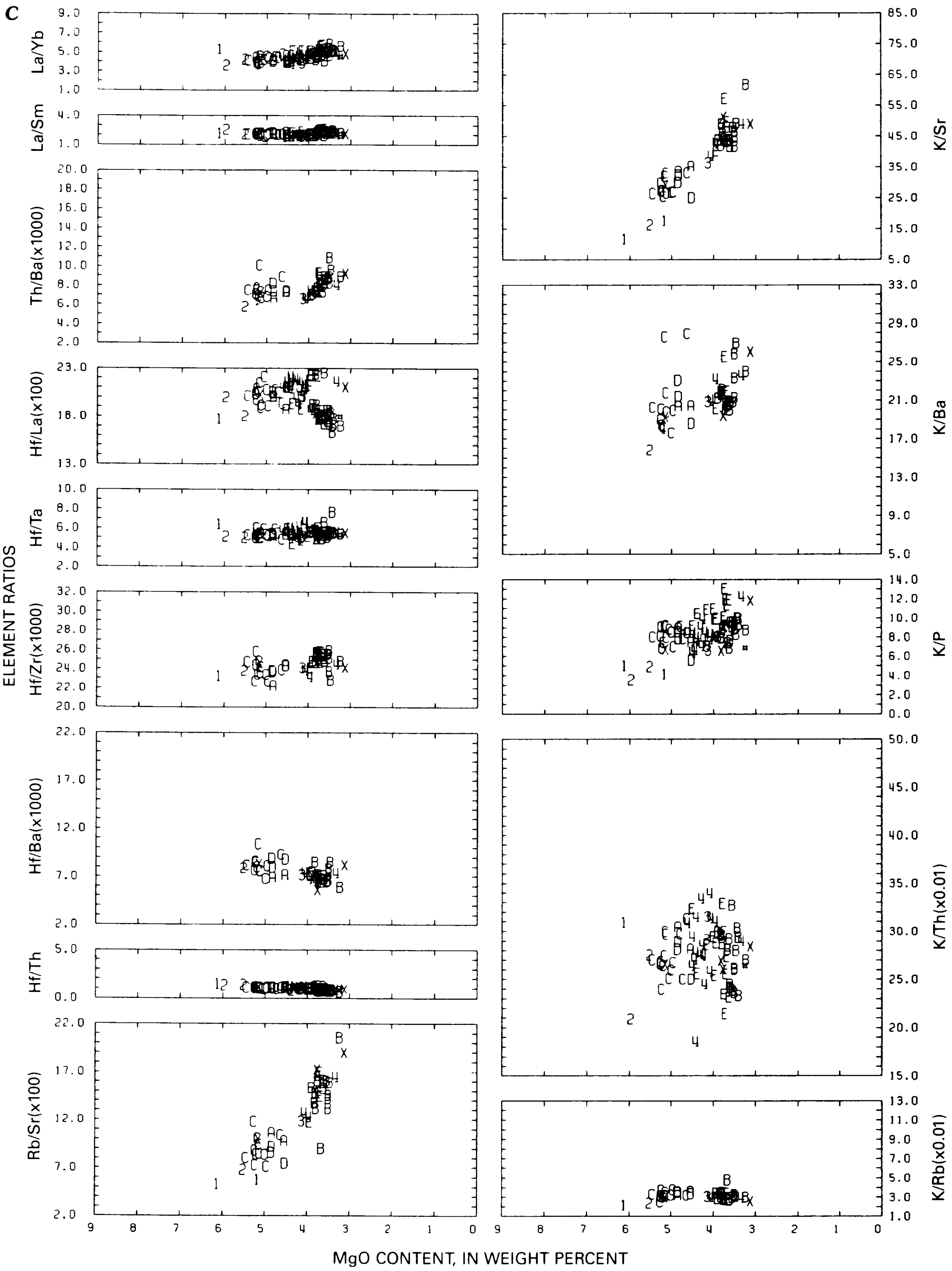

Figure 4. Continued.

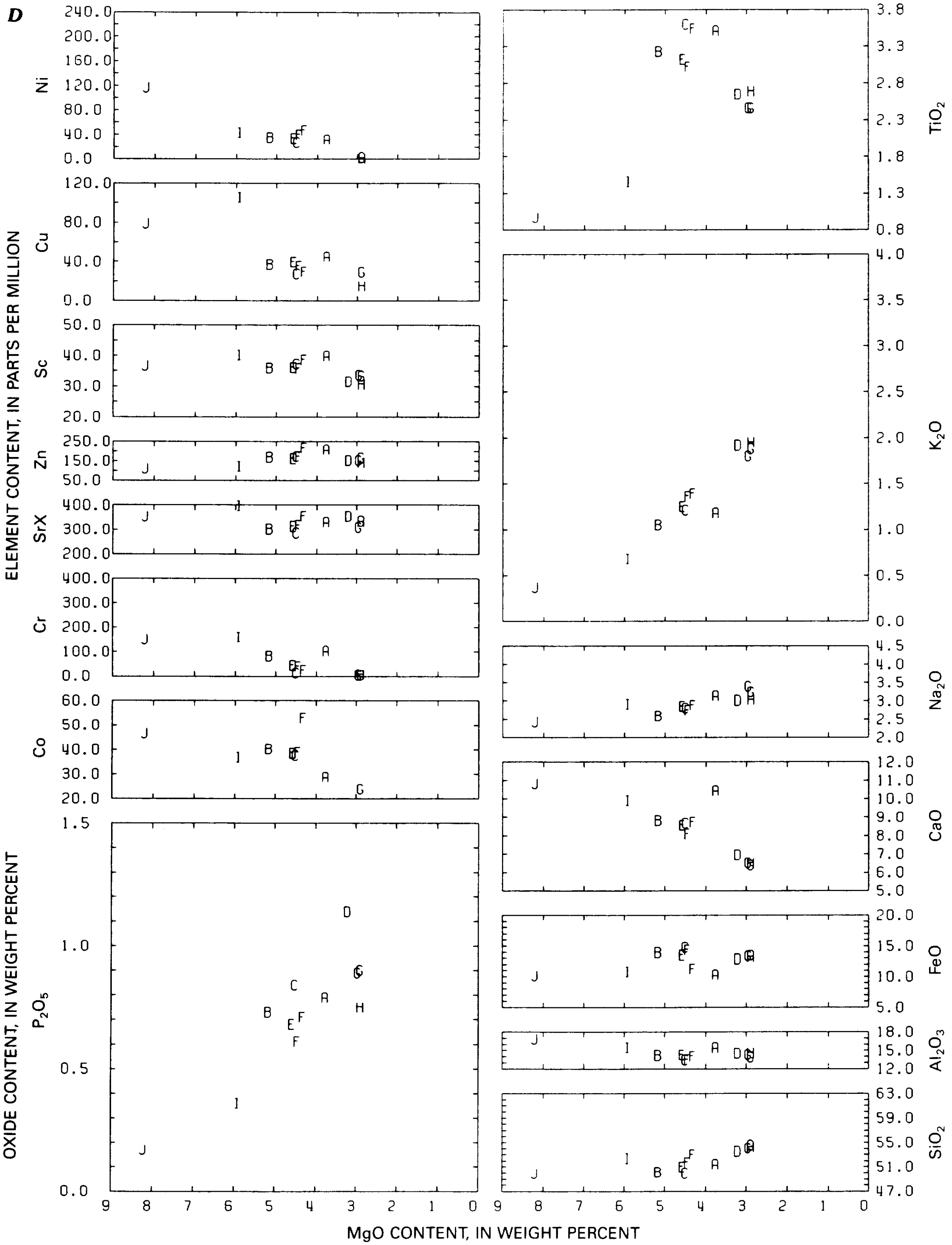

**Figure 4.** Continued.

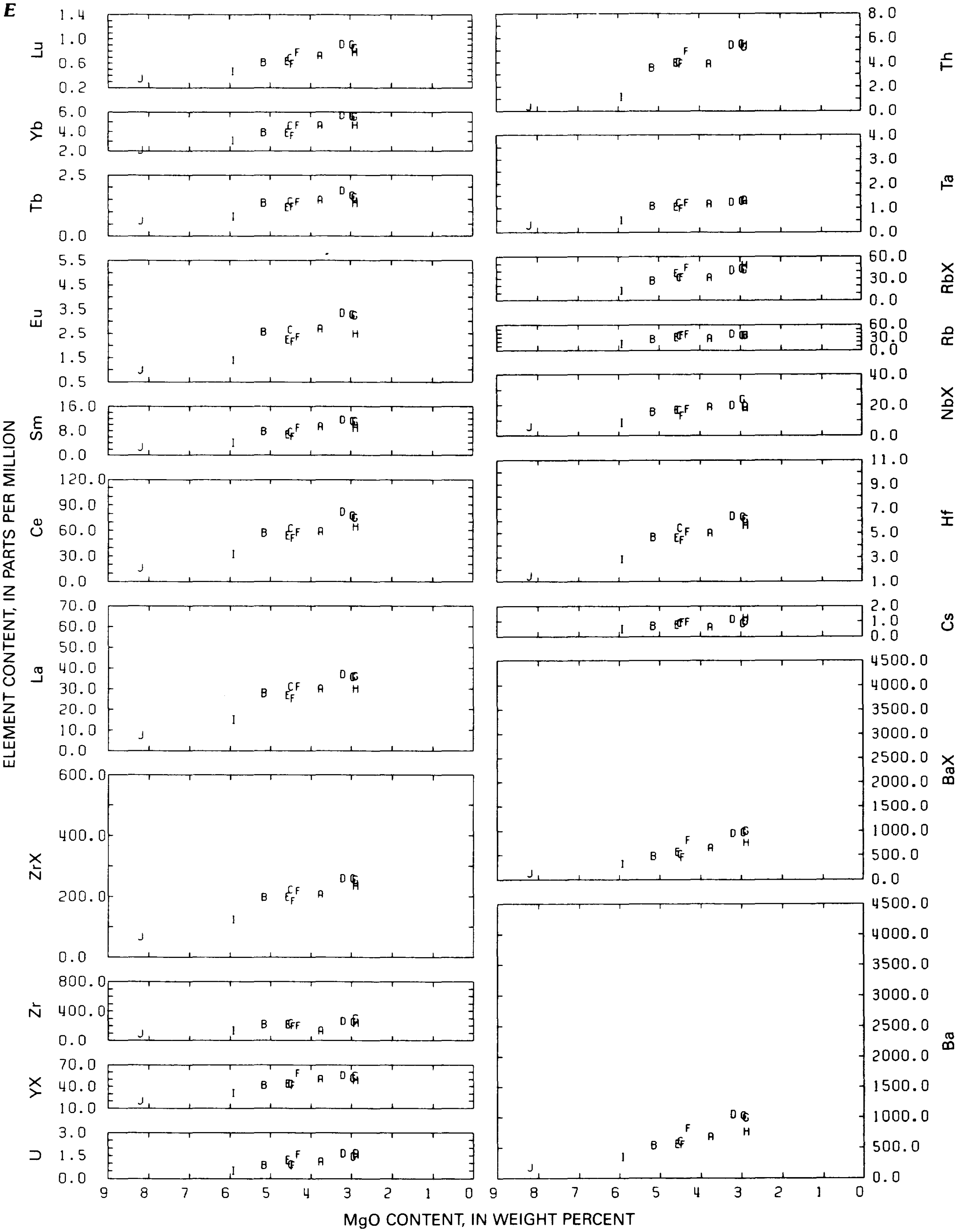

**Figure 4.** Continued.

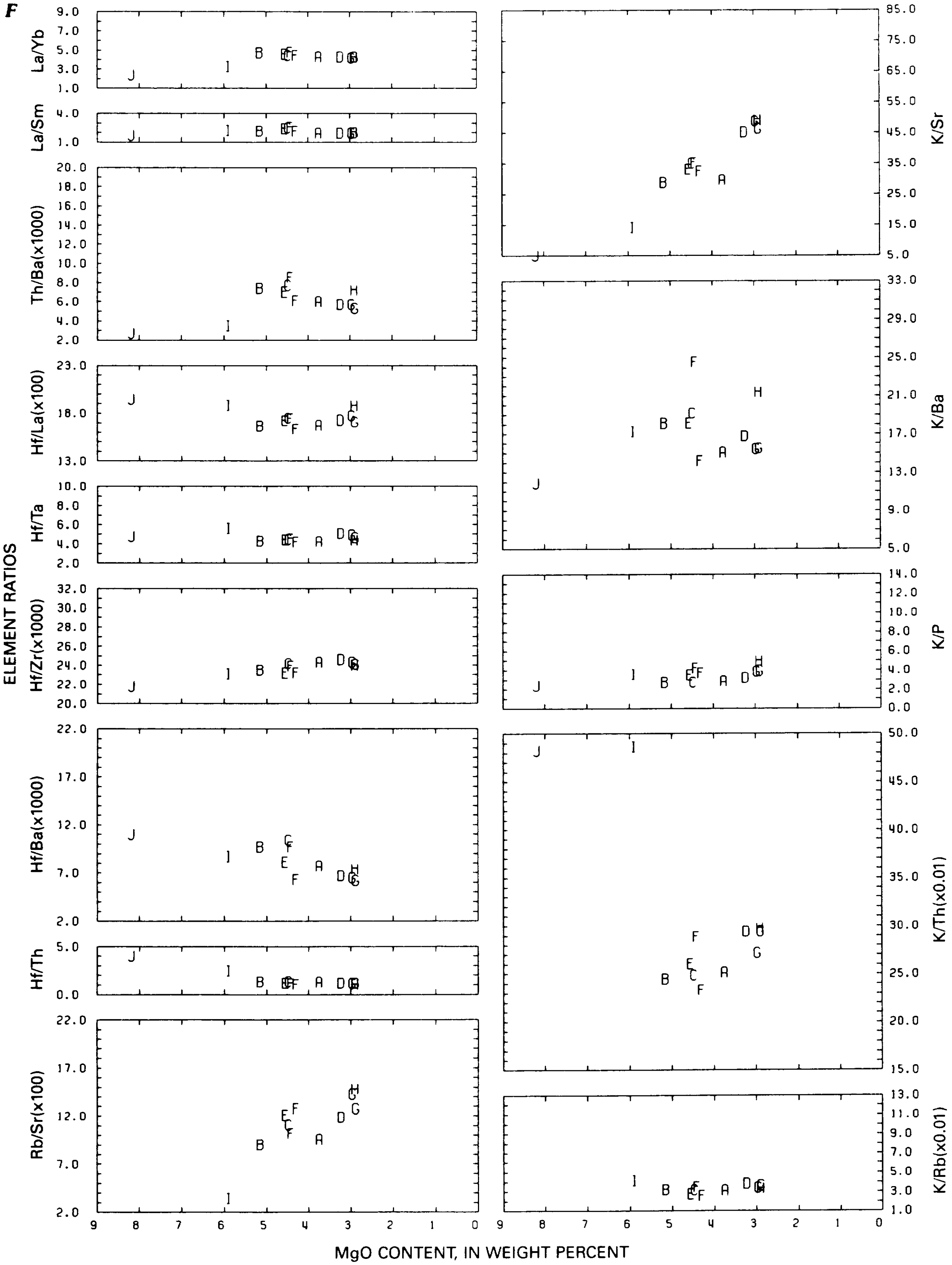

**Figure 4.** Continued.

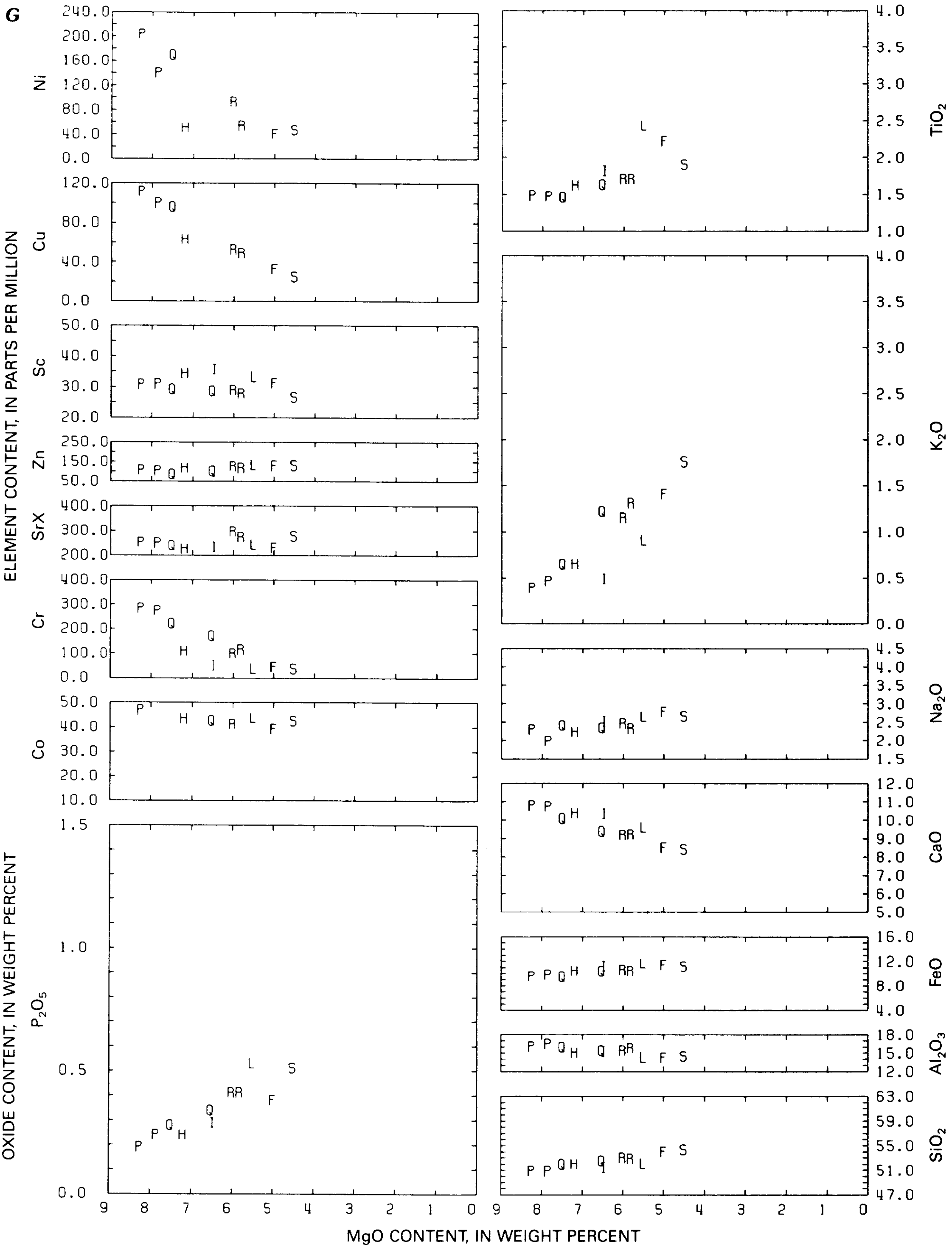

Figure 4. Continued.

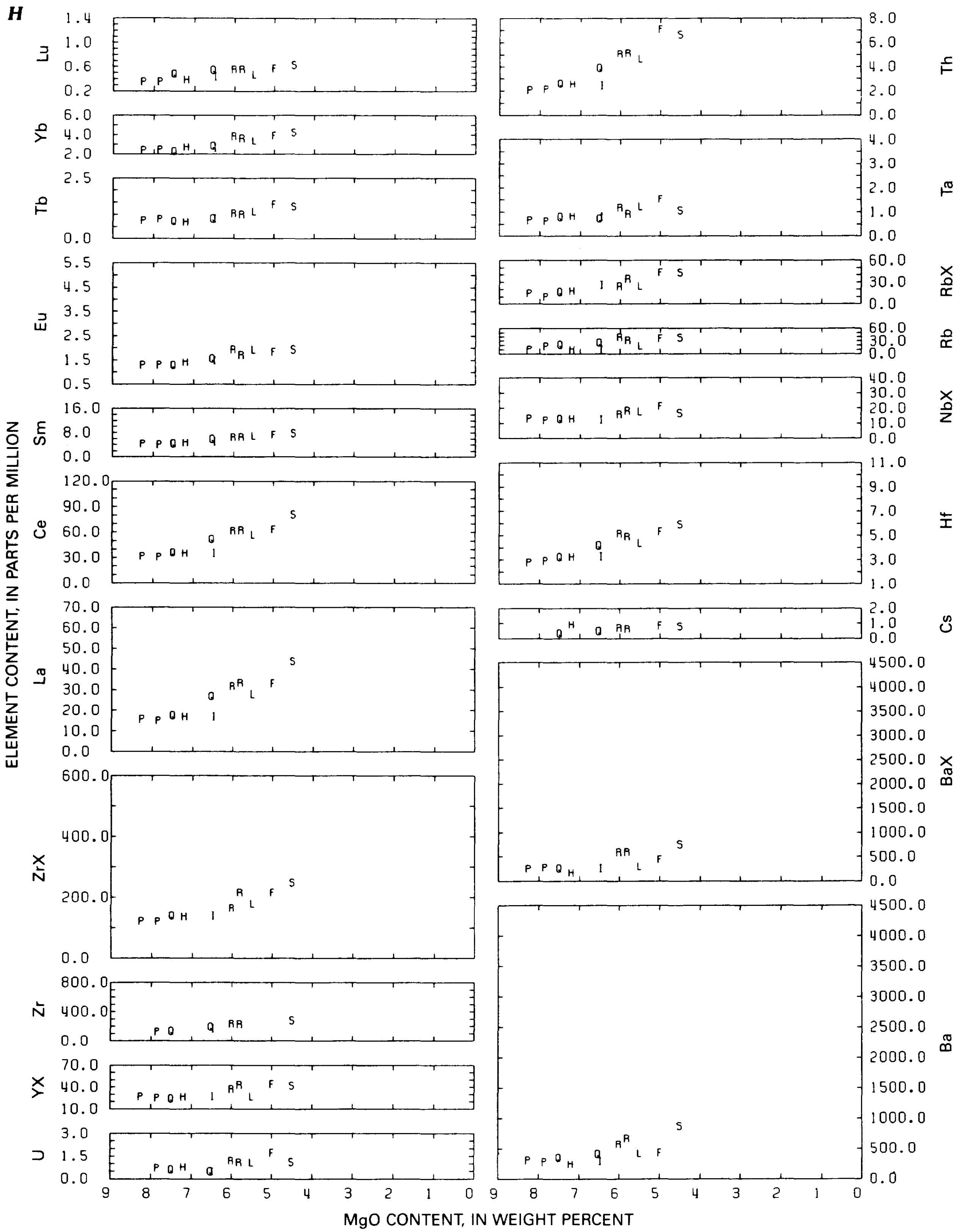

**Figure 4.** Continued.

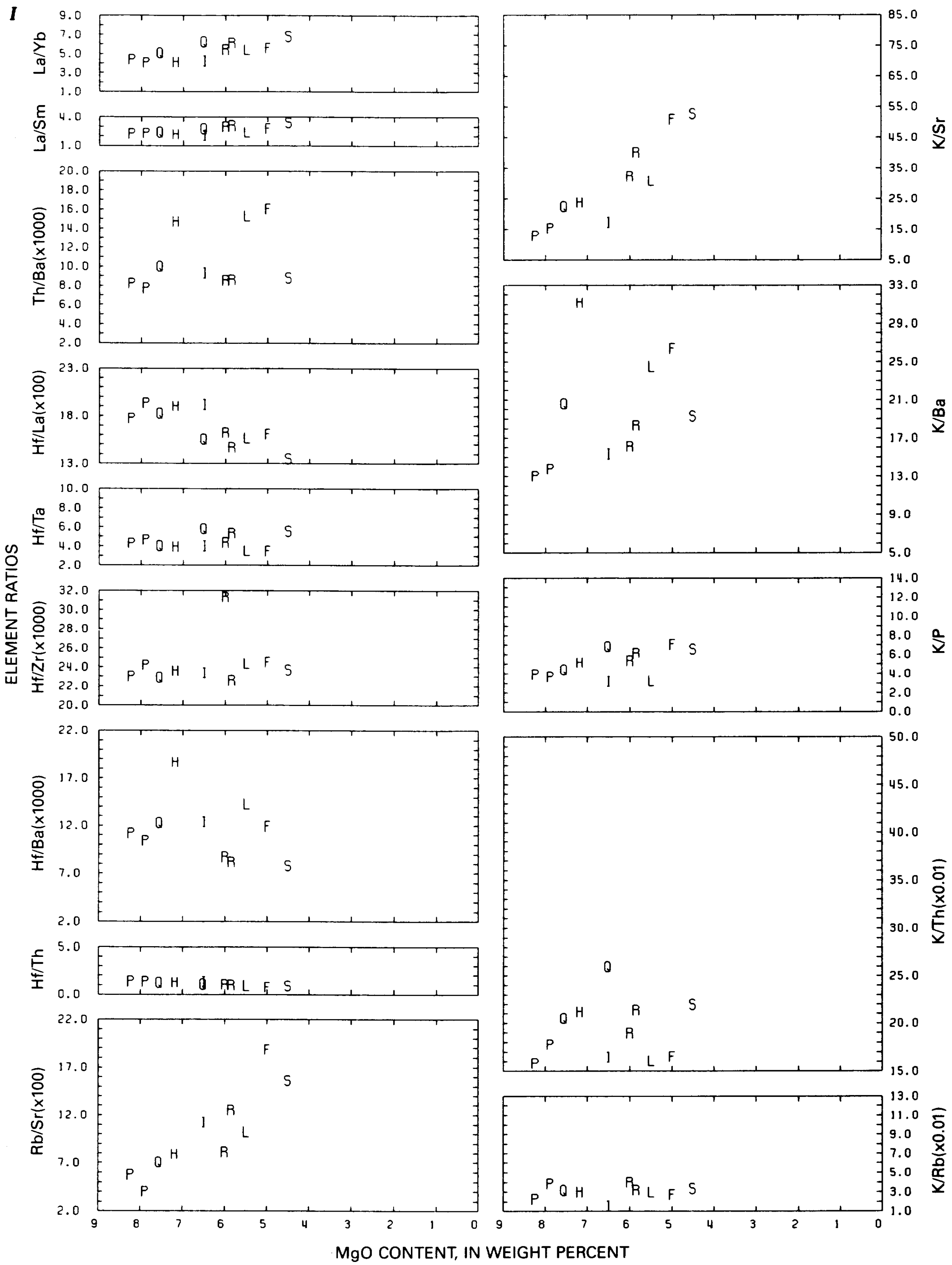

**Figure 4.** Continued.

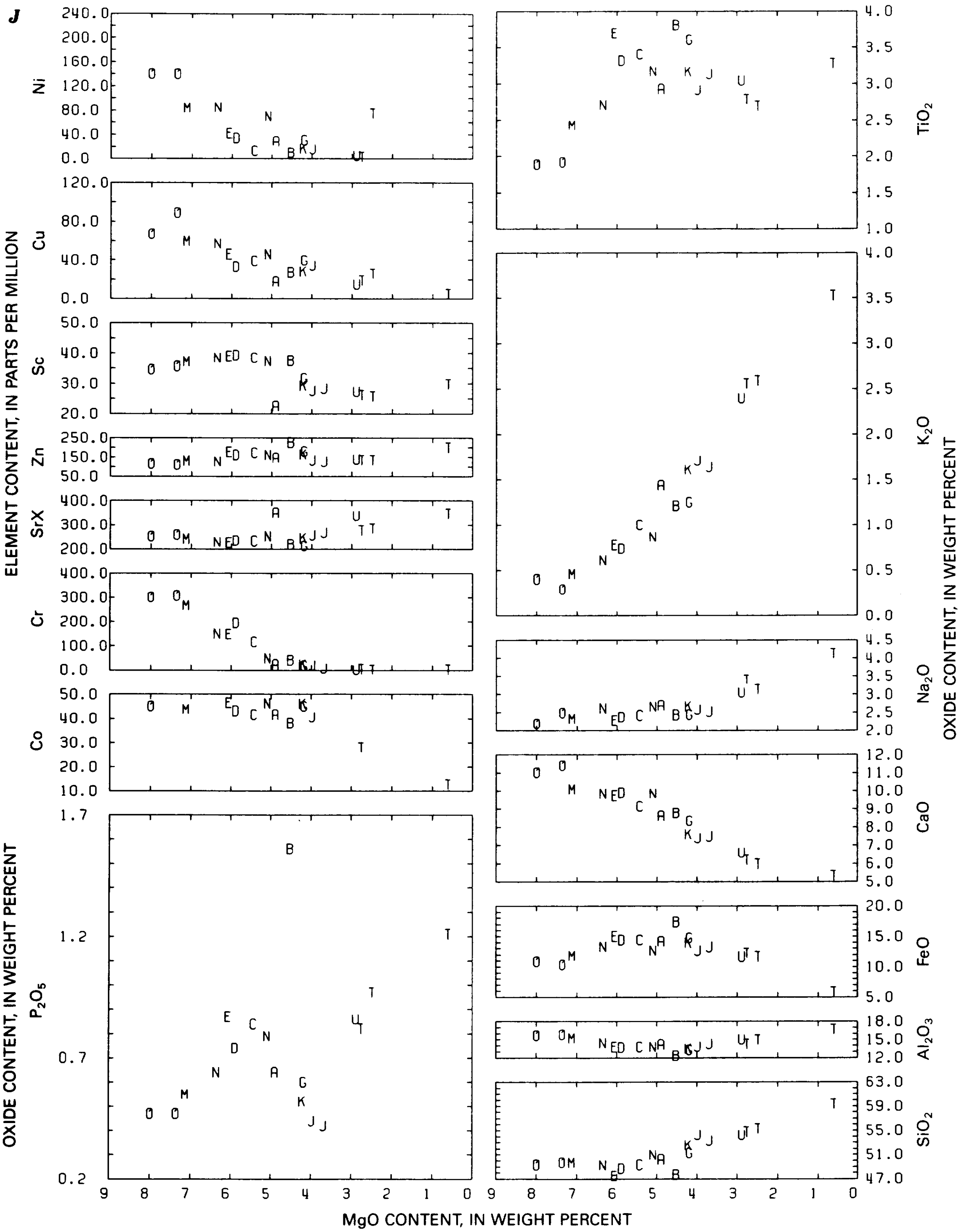

**Figure 4.** Continued.

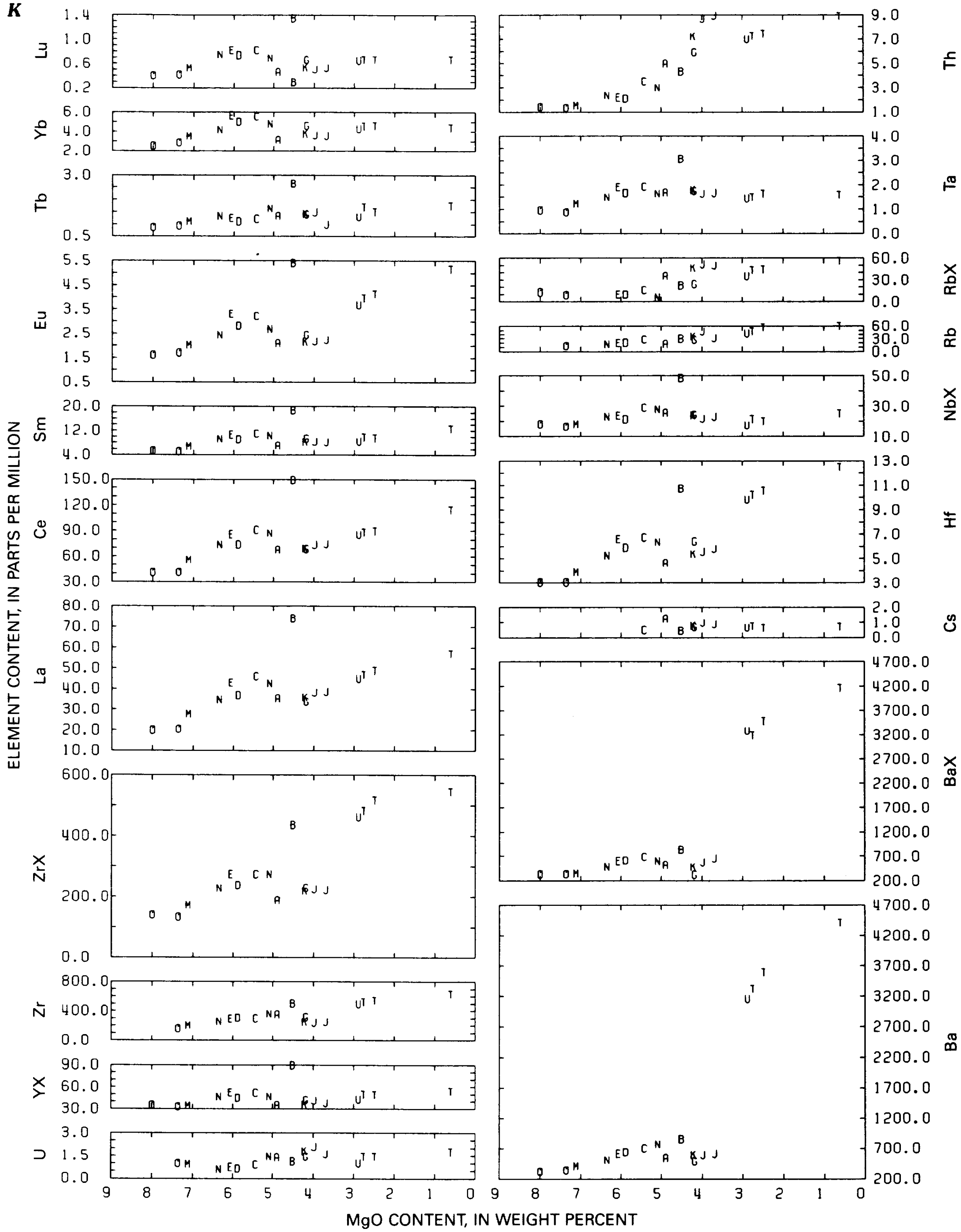

**Figure 4.** Continued.

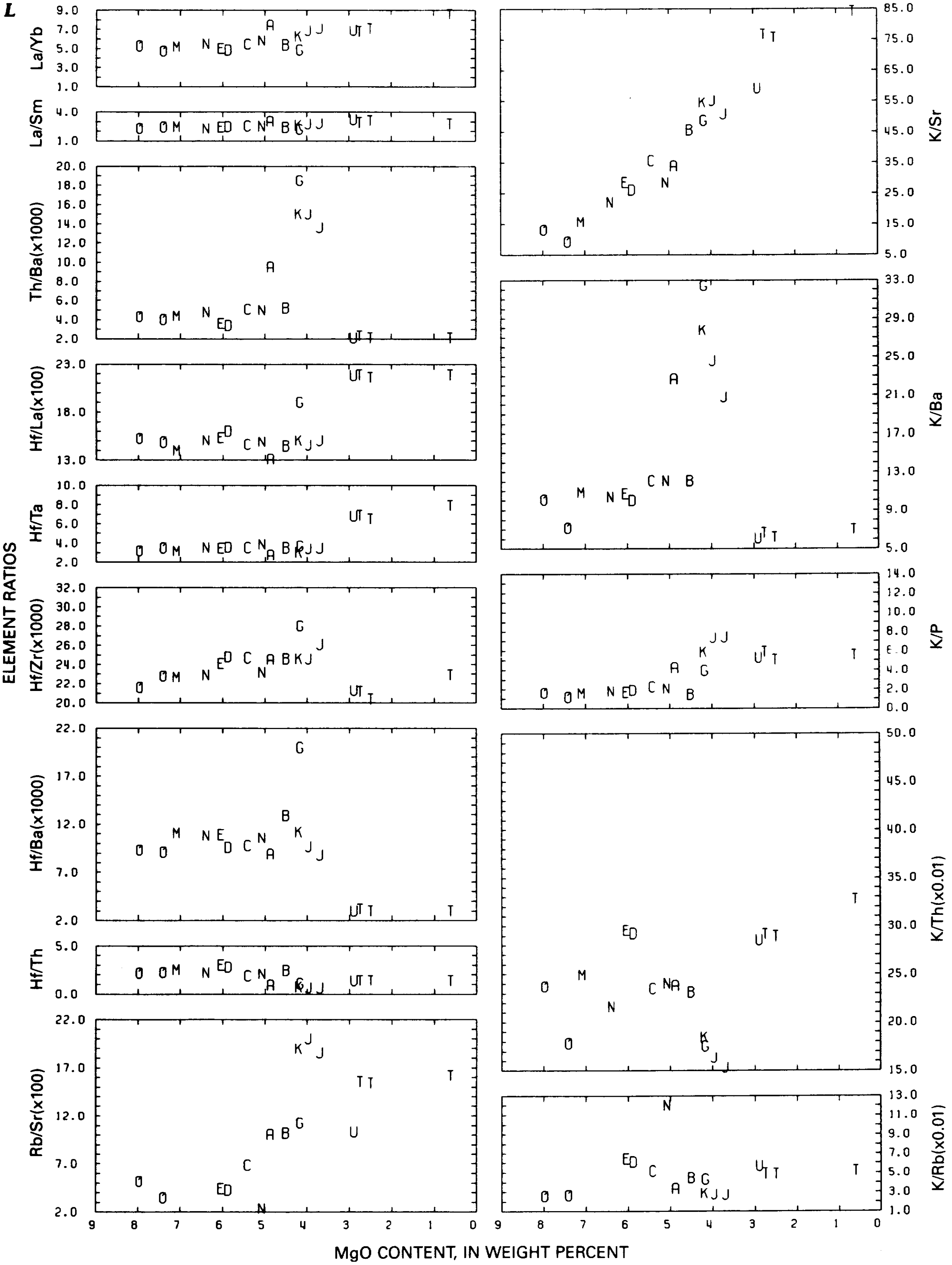

**Figure 4.** Continued.

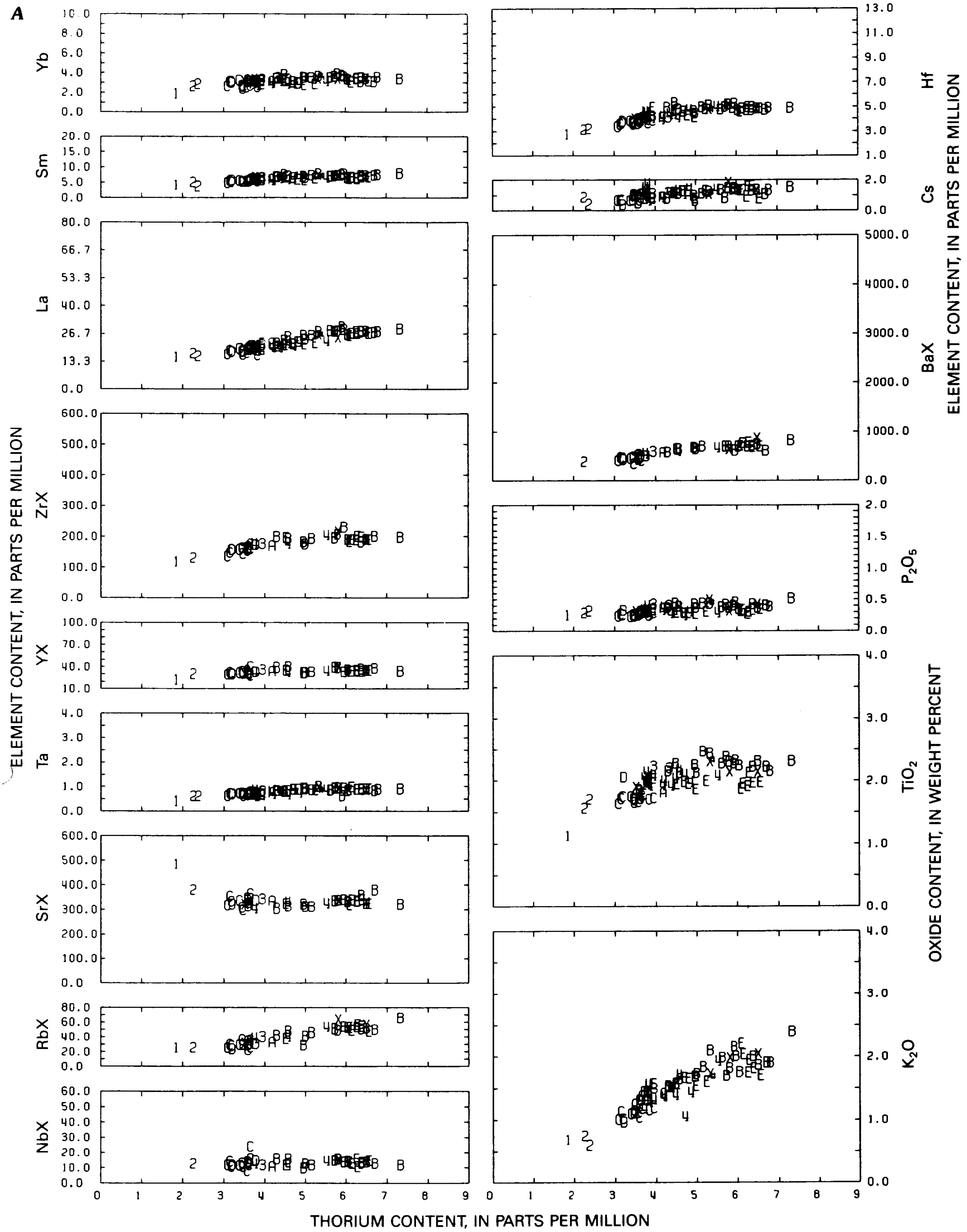

**Figure 5.** Chemistry of selected oxides and elements in units of the Yakima Basalt Subgroup, presented as thorium variation diagrams. Data from tables 3–5; symbols as in figure 4. *A*, Grande Ronde Basalt, minor and trace incompatible oxides and elements. *B*, Grande Ronde Basalt, trace-element ratios. *C*, Wanapum Basalt, minor and trace incompatible oxides and elements. *D*, Wanapum Basalt, trace-element ratios. *E*, Saddle Mountains Basalt (of Grande

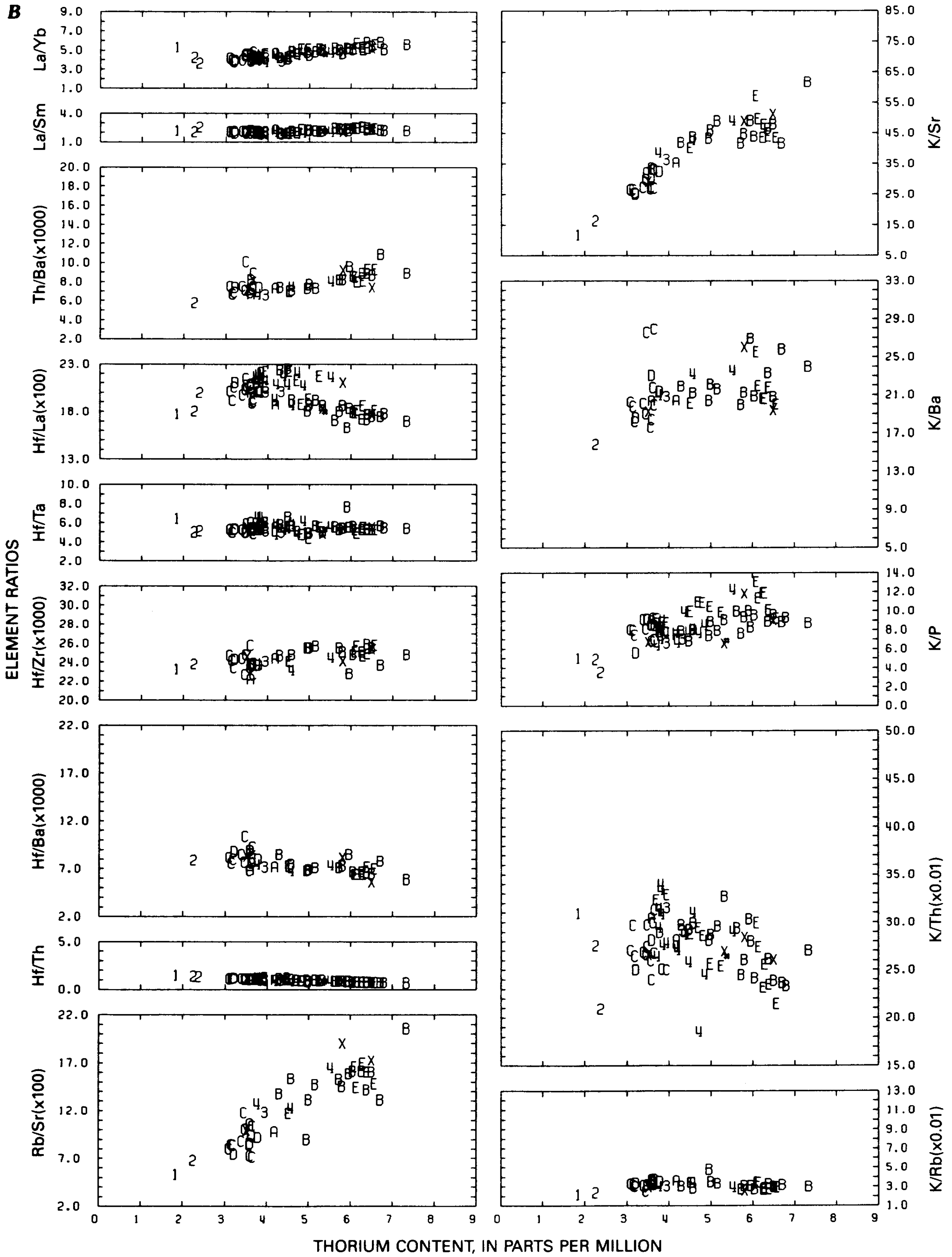

Ronde affinity), minor and trace incompatible oxides and elements. *F*, Saddle Mountains Basalt (of Grande Ronde affinity), trace-element ratios. *G*, Saddle Mountains Basalt (of Wanapum affinity), minor and trace incompatible oxides and elements. *H*, Saddle Mountains Basalt (of Wanapum affinity), trace-element ratios.

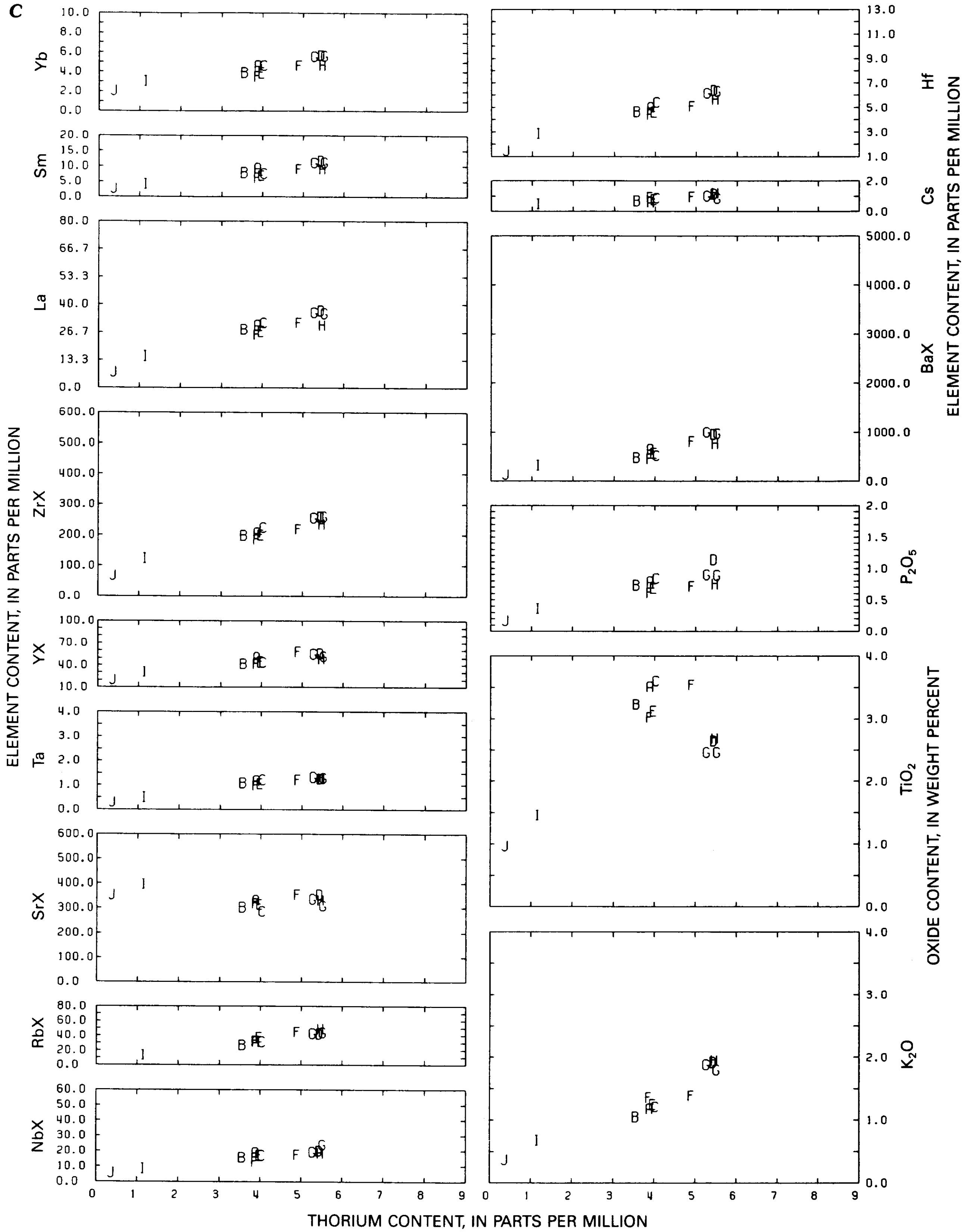

**Figure 5.** Continued.

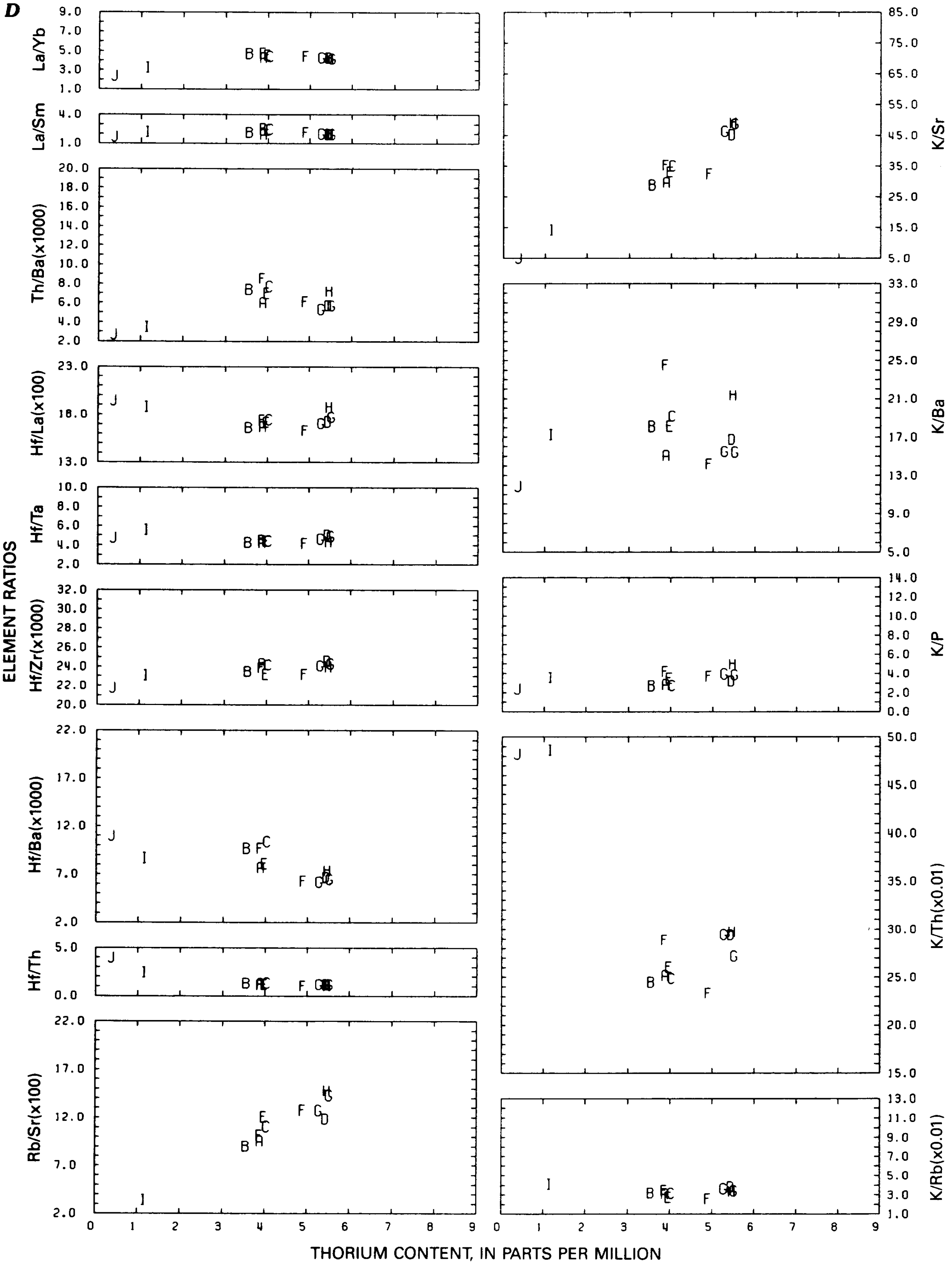

Figure 5. Continued.

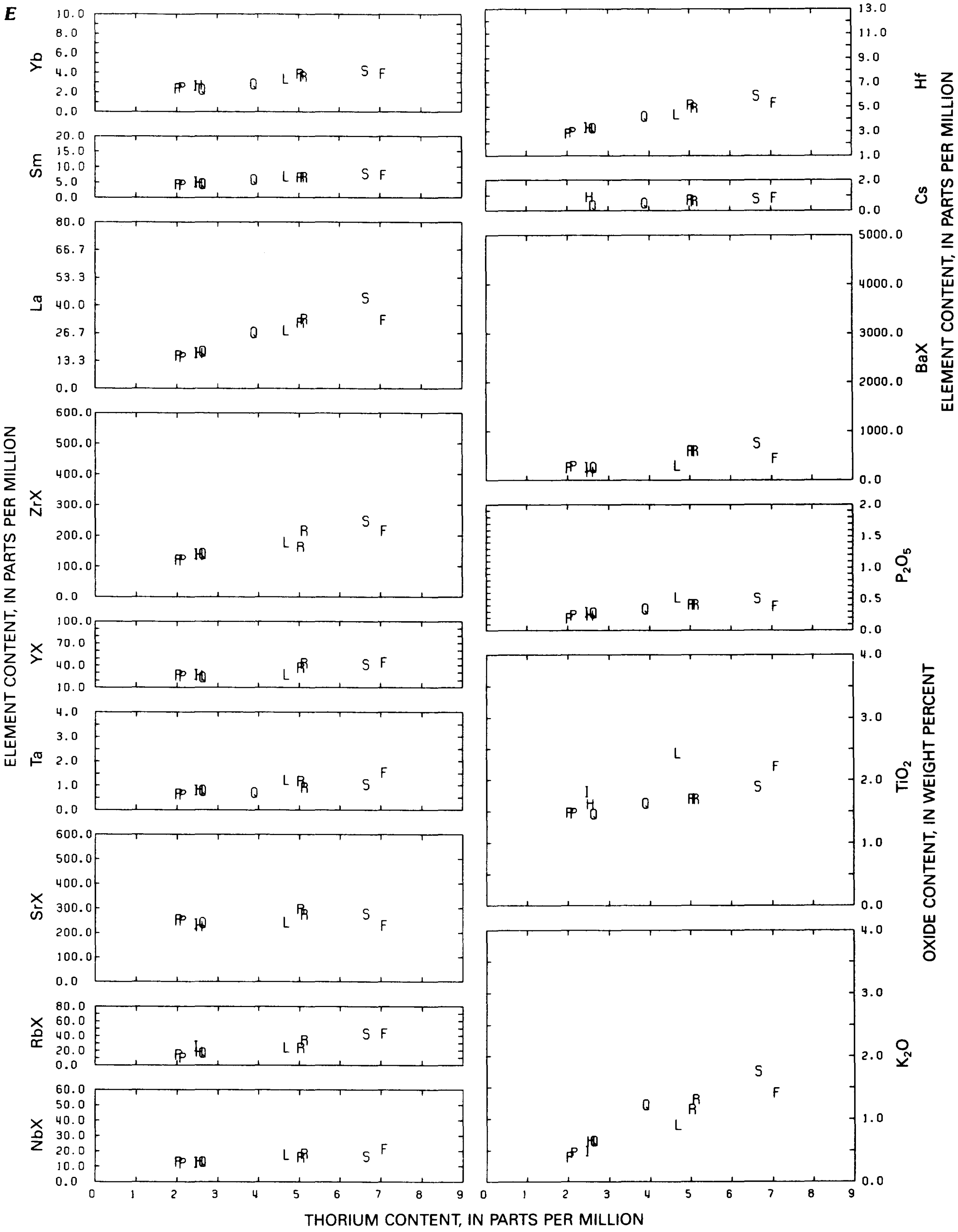

**Figure 5.** Continued.

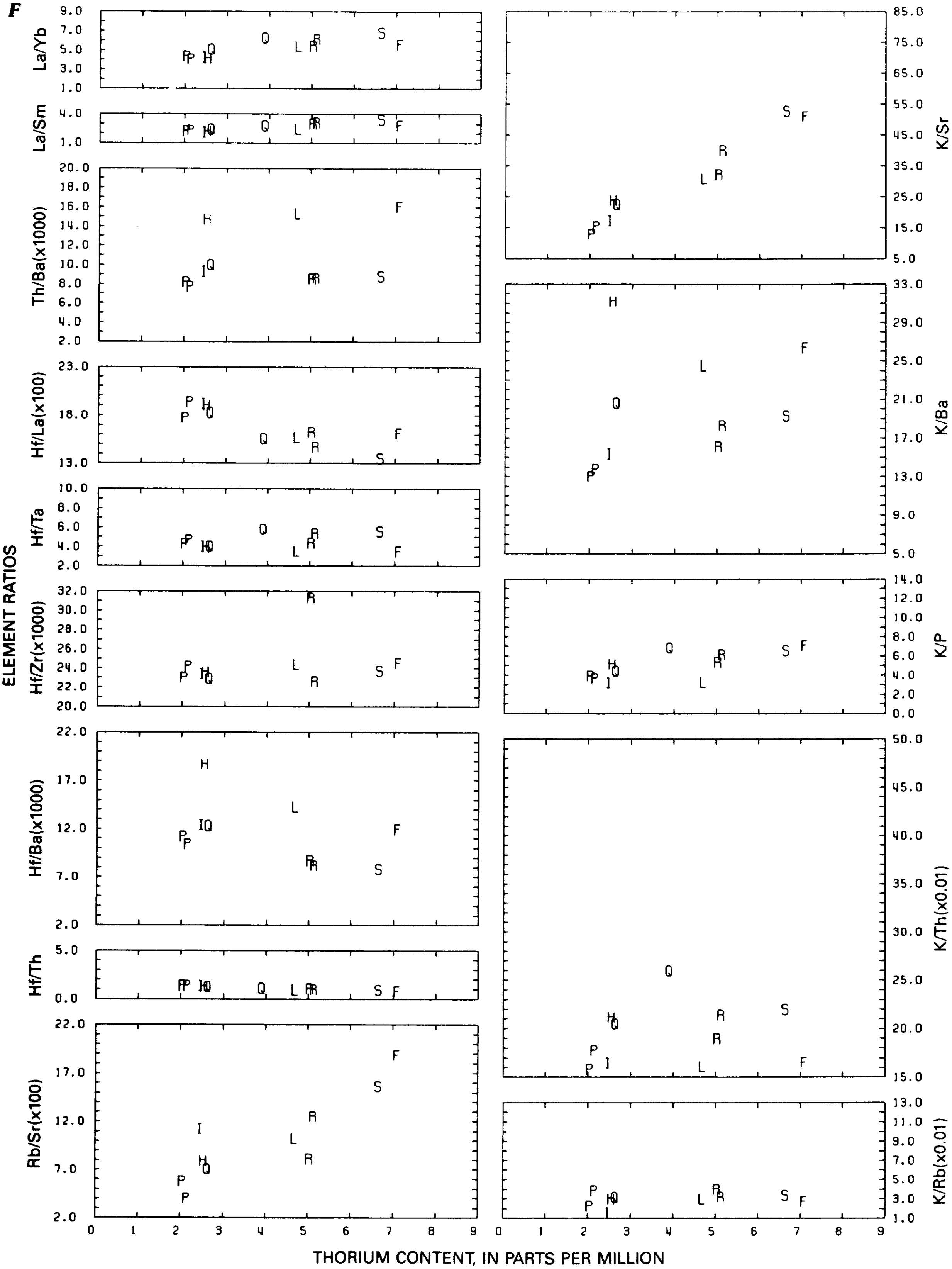

Figure 5. Continued.

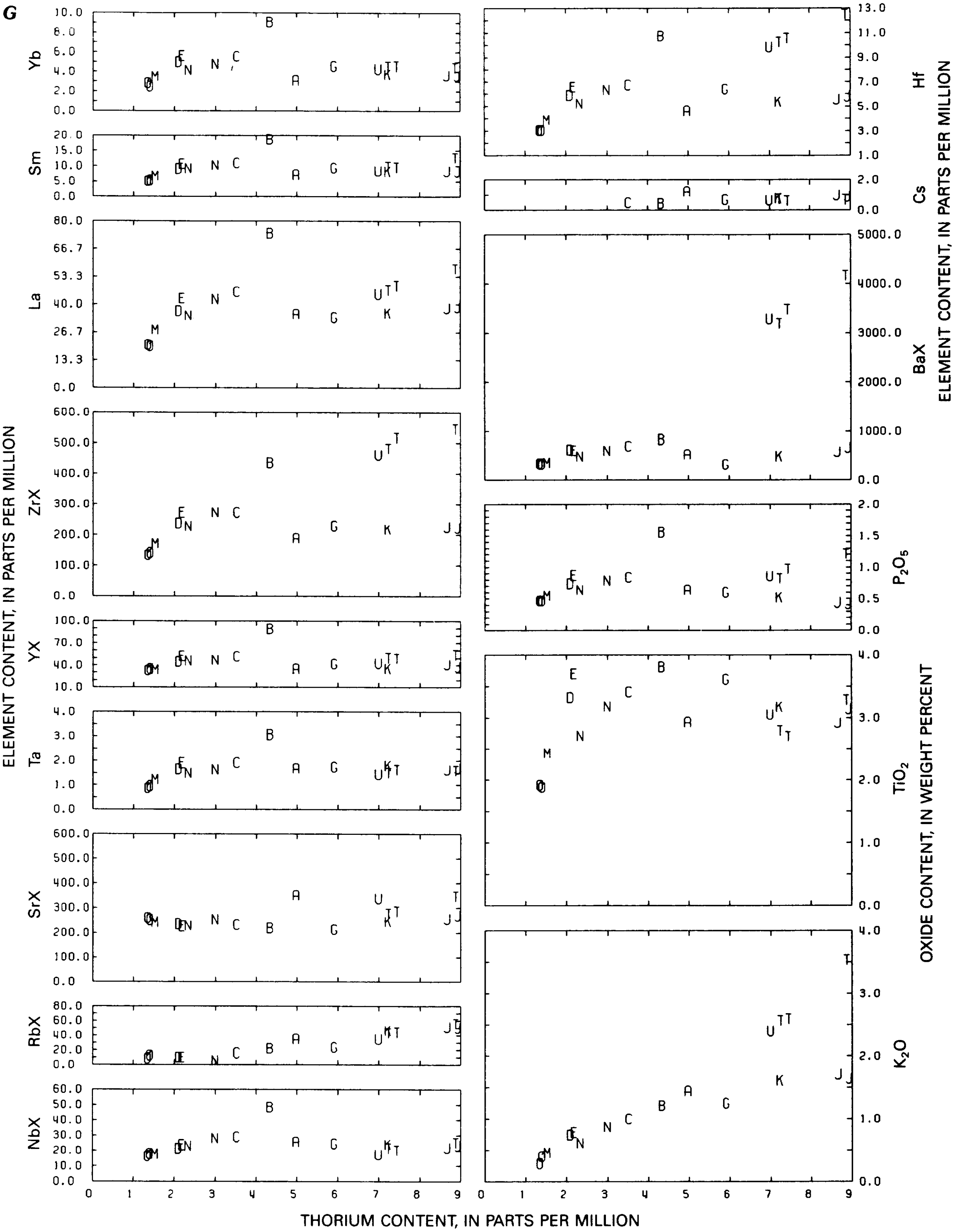

Figure 5. Continued.

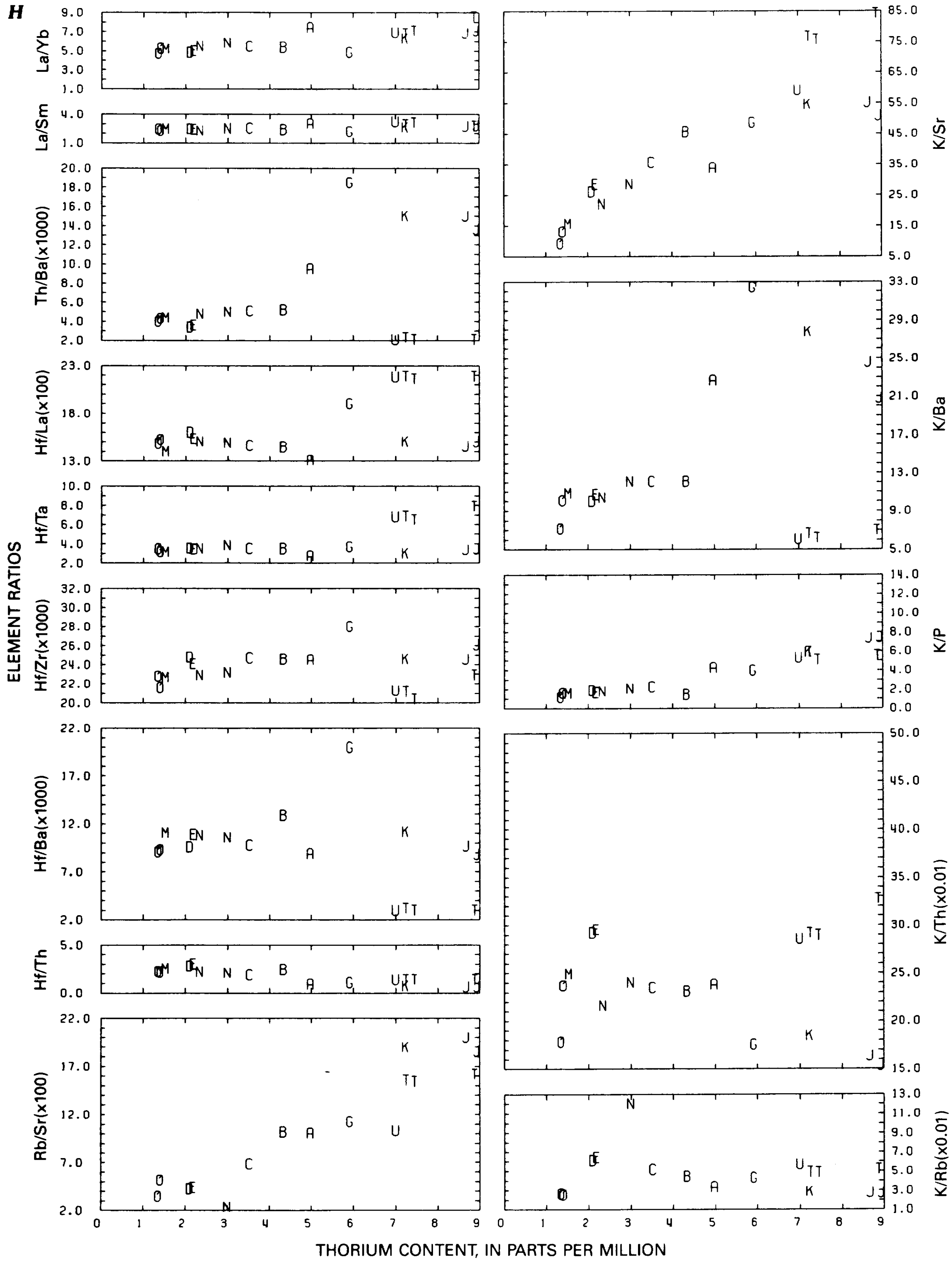

**Figure 5.** Continued.

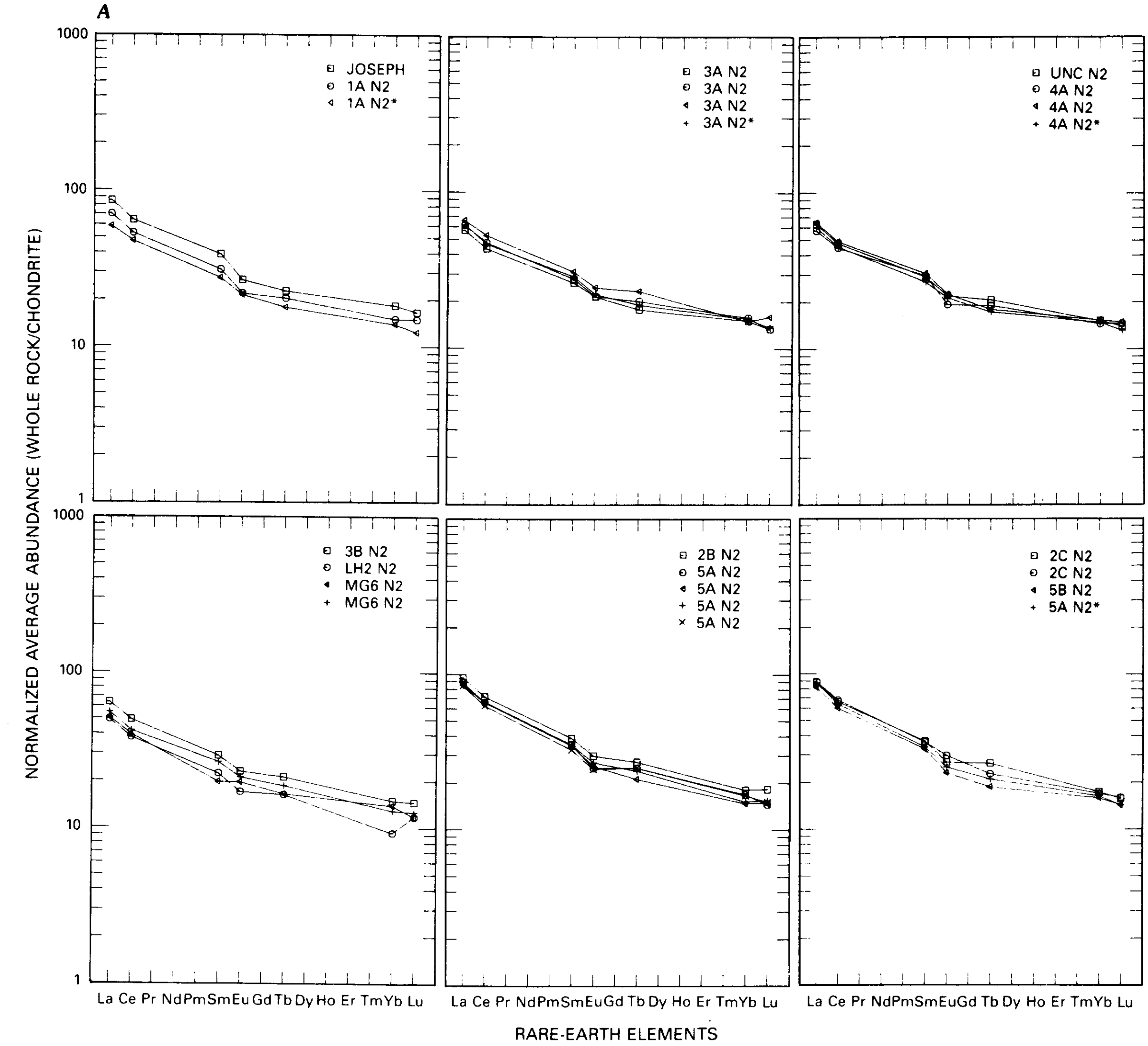

**Figure 6.** Chondrite-normalized abundances of selected rare-earth elements (La, Ce, Sm, Eu, Tb, Yb, and Lu) in flows of the Yakima Basalt Subgroup. Values used in normalizing are those of Haskin and others (1968). Names of geochemical units as in tables 3–5 and figures 4–5. See table 1 for stratigraphic association of units. *A*, Grande Ronde Basalt. Data arranged in stratigraphic order from youngest (1A N2) to oldest (AS 16 R1), using terminology of Mangan and others (1985, 1986); data for the Joseph volcanics unit of Kleck (1976) (JOSEPH in upper left box) and one sample of the Imnaha Basalt (IMNAHA in lowermost right-hand box) shown for comparison. *B*, Wanapum Basalt. Data shown in two boxes at upper left, arranged in stratigraphic order from youngest to oldest within members. Priest Rapids Member (PV, LOLO INC, ROSALIA); Powatka flow (PH POWAT); Roza Member (ROZA); Frenchman Springs Member (FS INC; FS ANOM); Eckler Mountain Member (SHUMAKER=PH SHUM; SW LOOK; DODGE; ROBIN). *C*, Saddle Mountains Basalt. Data arranged by member, from youngest to oldest, from Lower Monumental Member (LM at upper right) to Umatilla Member (UMATILLA at lower right).

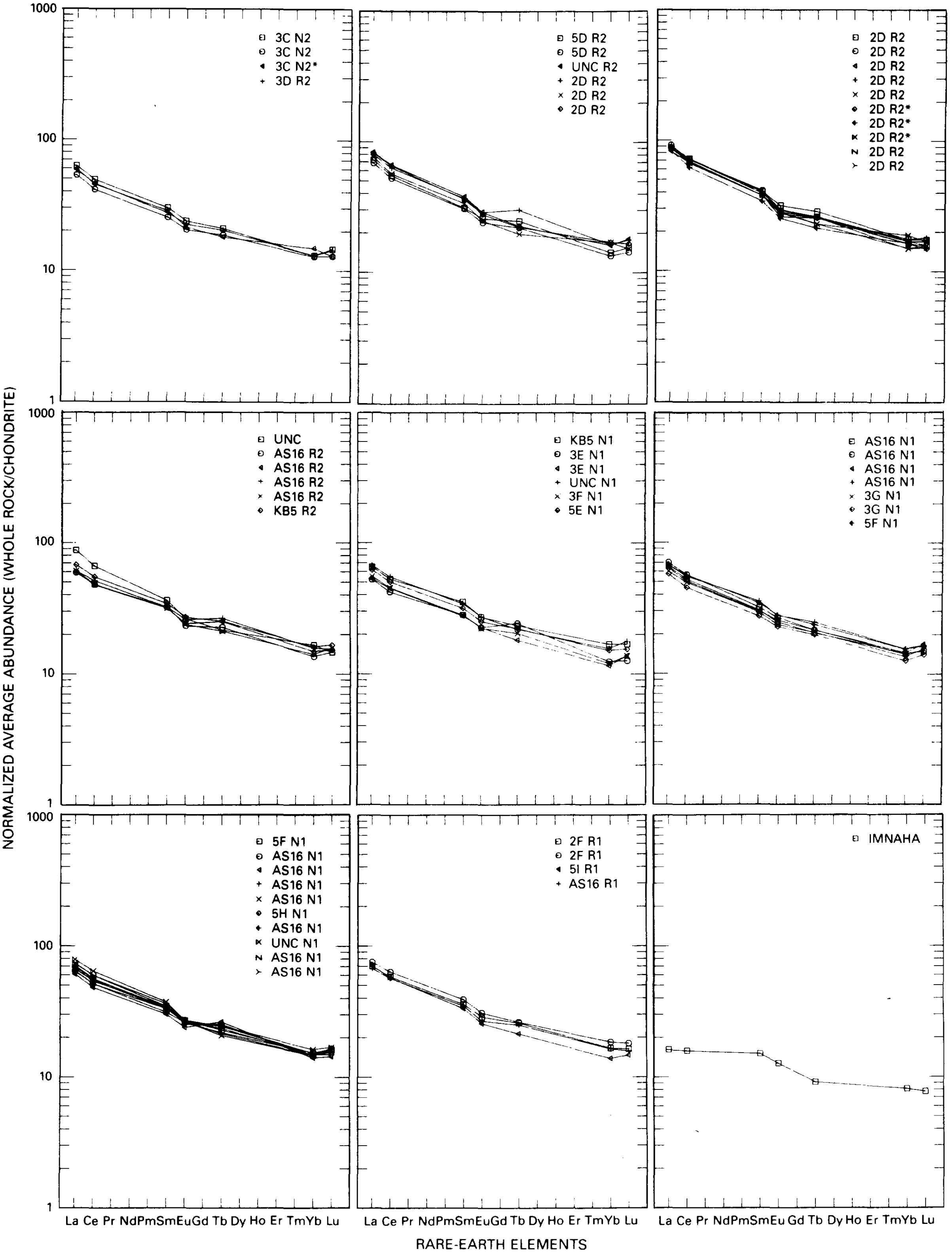

Figure 6. Continued.

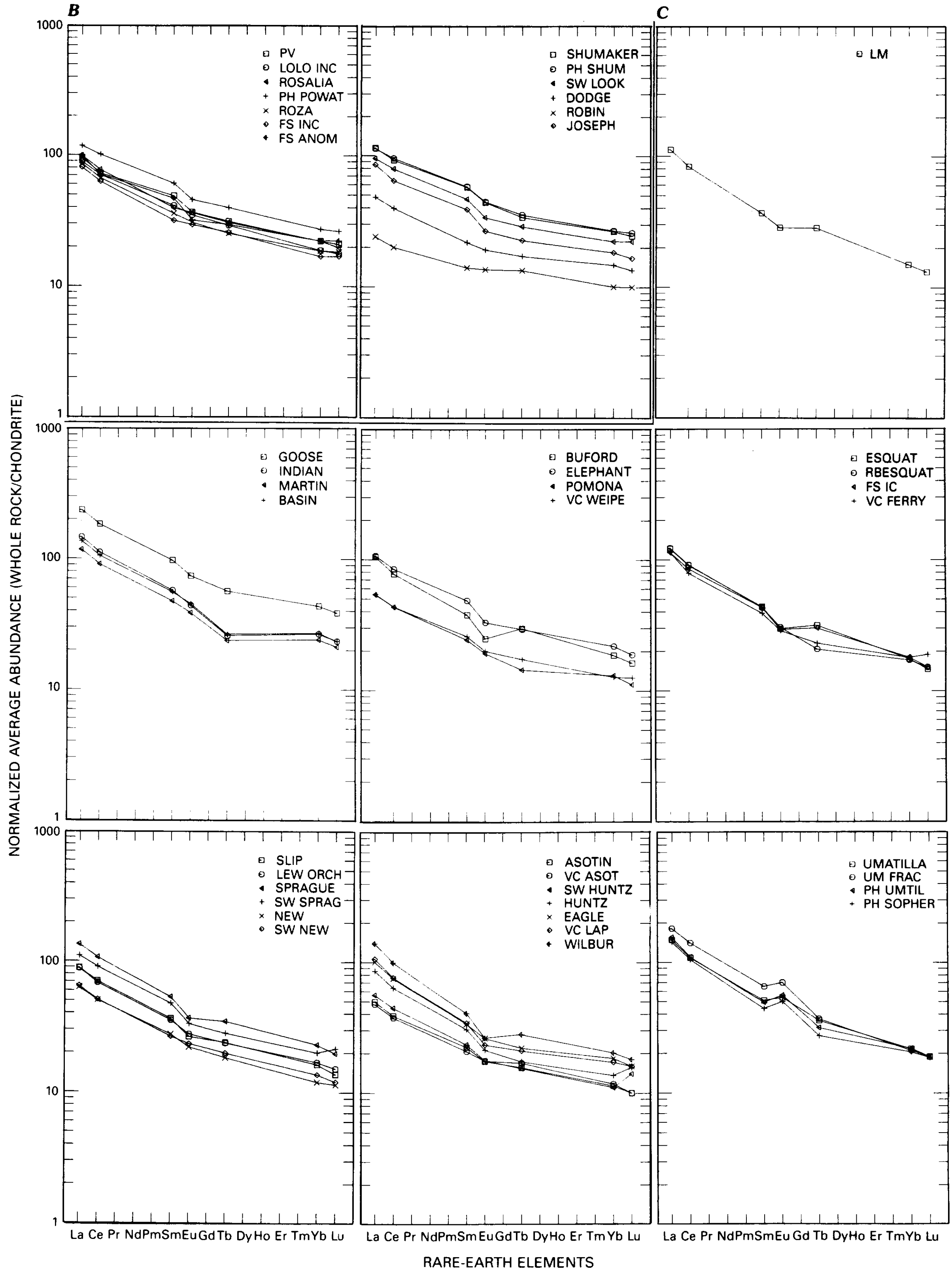

Figure 6. Continued.

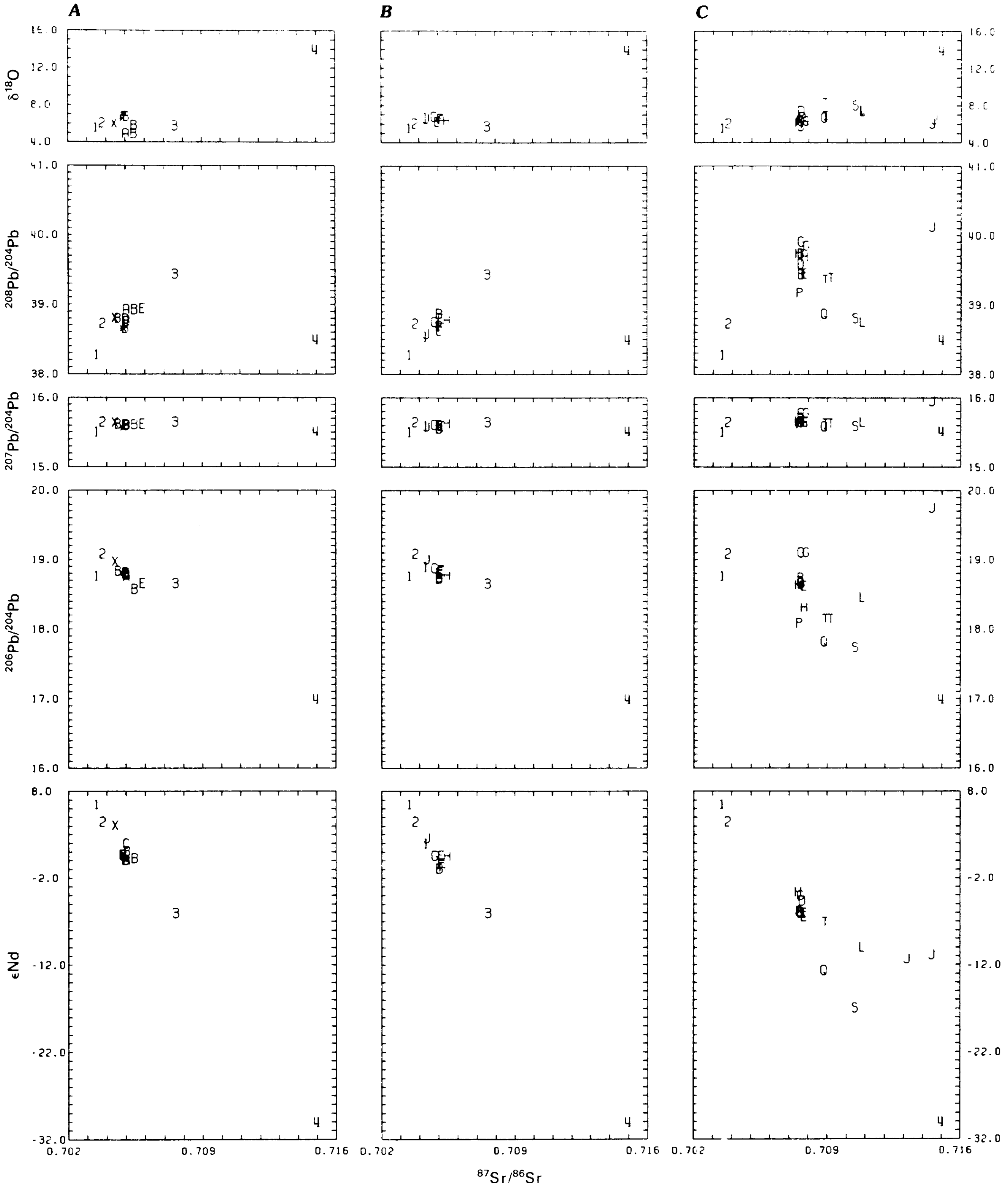

Figure 7. Isotope data for units of the Yakima Basalt Subgroup. Symbols 1, 2, 3, and 4 represent Carlson's (1984a, table 3) end-member compositions C1, C2, C3, and C4. See text for further discussion. *A*, Grande Ronde Basalt. *, LH2 N2 geochemical unit; #, MG6 N2 geochemical unit; other symbols as in table 3. *B*, Wanapum Basalt. Symbols as in table 4. *C*, Saddle Mountains Basalt. Symbols as in table 5.

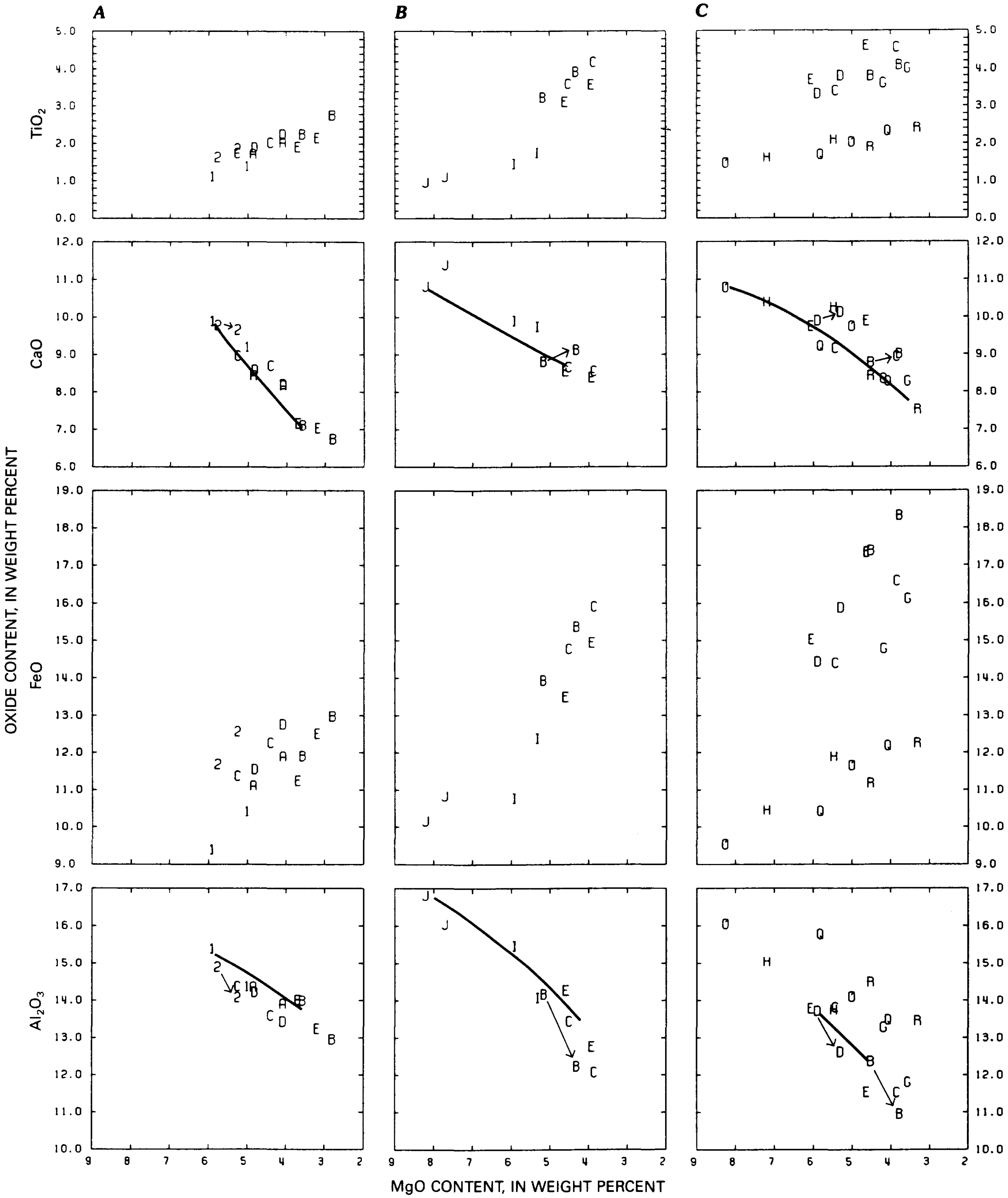

**Figure 8.** MgO variation diagrams comparing major-oxide chemistry of representative rocks and coexisting glasses in units of the Yakima Basalt Subgroup. Glass analyses adjusted before plotting (see text). Plots of CaO-MgO and $Al_2O_3$-MgO are annotated to show average trends of bulk-rock chemistry (heavy solid lines) and representative trends connecting coexisting rock and glass (short solid lines, arrows point toward glass composition). *A*, Grande Ronde Basalt. Symbols as in table 3. *B*, Wanapum Basalt. Symbols as in table 4. *C*, Saddle Mountains Basalt. Symbols as in table 5, except O, SW NEW only; Q, HUNTZ only; R, VC LAP only.

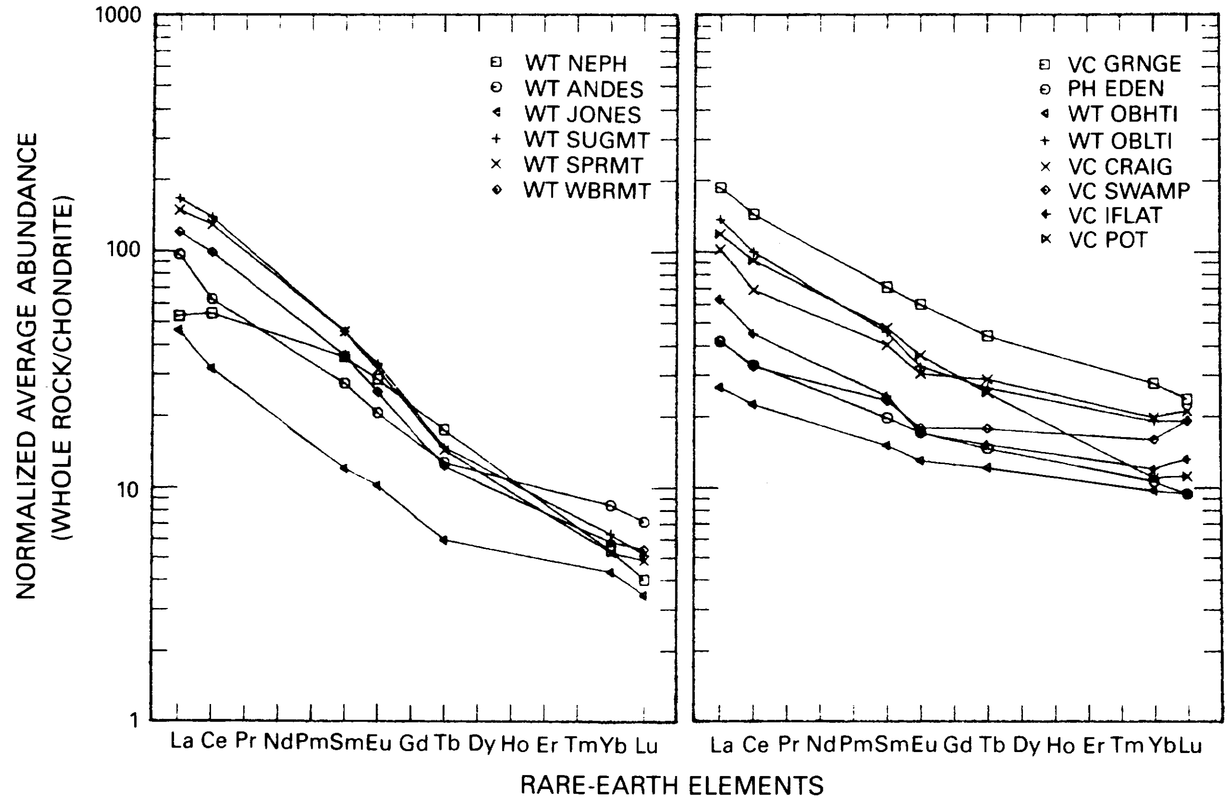

**Figure 9.** Patterns of chondrite-normalized abundances of rare-earth elements in additional analyzed flows. Symbols for flows as in tables 14 and 15.

GPO 685-041/9779

# SELECTED SERIES OF U.S. GEOLOGICAL SURVEY PUBLICATIONS

## Periodicals

**Earthquakes & Volcanoes** (issued bimonthly).
**Preliminary Determination of Epicenters** (issued monthly).

## Technical Books and Reports

**Professional Papers** are mainly comprehensive scientific reports of wide and lasting interest and importance to professional scientists and engineers. Included are reports on the results of resource studies and of topographic, hydrologic, and geologic investigations. They also include collections of related papers addressing different aspects of a single scientific topic.

**Bulletins** contain significant data and interpretations that are of lasting scientific interest but are generally more limited in scope or geographic coverage than Professional Papers. They include the results of resource studies and of geologic and topographic investigations; as well as collections of short papers related to a specific topic.

**Water-Supply Papers** are comprehensive reports that present significant interpretive results of hydrologic investigations of wide interest to professional geologists, hydrologists, and engineers. The series covers investigations in all phases of hydrology, including hydrogeology, availability of water, quality of water, and use of water.

**Circulars** present administrative information or important scientific information of wide popular interest in a format designed for distribution at no cost to the public. Information is usually of short-term interest.

**Water-Resources Investigations Reports** are papers of an interpretive nature made available to the public outside the formal USGS publications series. Copies are reproduced on request unlike formal USGS publications, and they are also available for public inspection at depositories indicated in USGS catalogs.

**Open-File Reports** include unpublished manuscript reports, maps, and other material that are made available for public consultation at depositories. They are a nonpermanent form of publication that may be cited in other publications as sources of information.

## Maps

**Geologic Quadrangle Maps** are multicolor geologic maps on topographic bases in 7 1/2- or 15-minute quadrangle formats (scales mainly 1:24,000 or 1:62,500) showing bedrock, surficial, or engineering geology. Maps generally include brief texts; some maps include structure and columnar sections only.

**Geophysical Investigations Maps** are on topographic or planimetric bases at various scales; they show results of surveys using geophysical techniques, such as gravity, magnetic, seismic, or radioactivity, which reflect subsurface structures that are of economic or geologic significance. Many maps include correlations with the geology.

**Miscellaneous Investigations Series Maps** are on planimetric or topographic bases of regular and irregular areas at various scales; they present a wide variety of format and subject matter. The series also includes 7 1/2-minute quadrangle photogeologic maps on planimetric bases which show geology as interpreted from aerial photographs. Series also includes maps of Mars and the Moon.

**Coal Investigations Maps** are geologic maps on topographic or planimetric bases at various scales showing bedrock or surficial geology, stratigraphy, and structural relations in certain coal-resource areas.

**Oil and Gas Investigations Charts** show stratigraphic information for certain oil and gas fields and other areas having petroleum potential.

**Miscellaneous Field Studies Maps** are multicolor or black-and-white maps on topographic or planimetric bases on quadrangle or irregular areas at various scales. Pre-1971 maps show bedrock geology in relation to specific mining or mineral-deposit problems; post-1971 maps are primarily black-and-white maps on various subjects such as environmental studies or wilderness mineral investigations.

**Hydrologic Investigations Atlases** are multicolored or black-and-white maps on topographic or planimetric bases presenting a wide range of geohydrologic data of both regular and irregular areas; principal scale is 1:24,000 and regional studies are at 1:250,000 scale or smaller.

## Catalogs

Permanent catalogs, as well as some others, giving comprehensive listings of U.S. Geological Survey publications are available under the conditions indicated below from the U.S. Geological Survey, Books and Open-File Reports Section, Federal Center, Box 25425, Denver, CO 80225. (See latest Price and Availability List.)

**"Publications of the Geological Survey, 1879- 1961"** may be purchased by mail and over the counter in paperback book form and as a set of microfiche.

**"Publications of the Geological Survey, 1962- 1970"** may be purchased by mail and over the counter in paperback book form and as a set of microfiche.

**"Publications of the U.S. Geological Survey, 1971- 1981"** may be purchased by mail and over the counter in paperback book form (two volumes, publications listing and index) and as a set of microfiche.

**Supplements** for 1982, 1983, 1984, 1985, 1986, and for subsequent years since the last permanent catalog may be purchased by mail and over the counter in paperback book form.

**State catalogs,** "List of U.S. Geological Survey Geologic and Water-Supply Reports and Maps For (State)," may be purchased by mail and over the counter in paperback booklet form only.

**"Price and Availability List of U.S. Geological Survey Publications,"** issued annually, is available free of charge in paperback booklet form only.

**Selected copies of a monthly catalog** "New Publications of the U.S. Geological Survey" available free of charge by mail or may be obtained over the counter in paperback booklet form only. Those wishing a free subscription to the monthly catalog "New Publications of the U.S. Geological Survey" should write to the U.S. Geological Survey, 582 National Center, Reston, VA 22092.

**Note.**--Prices of Government publications listed in older catalogs, announcements, and publications may be incorrect. Therefore, the prices charged may differ from the prices in catalogs, announcements, and publications.